

Diagnosing Inflammation in Dry Eye Disease

Assessing the diagnostic utility of clinical tests in detecting inflammation

based on gene quantification studies

Catherine Shon

A thesis submitted in fulfilment of the requirements for the degree of Master of Health Sciences in
Ophthalmology, the University of Auckland 2022.

Abstract

Purpose: Inflammation plays a key role in the development and propagation of dry eye disease (DED). Clinically confirming the presence of inflammation to justify anti-inflammatory therapy remains challenging. This study sought to explore levels of agreement between clinical tests of inflammation and the diagnostic utility of clinical markers of inflammation relative to laboratory markers.

Methods: Participants (n=53), with or without DED, underwent clinical evaluation of inflammation via subjective and automated objective bulbar conjunctival hyperaemia assessment with clinical grading scales and the Oculus Keratograph 5M respectively; the InflammDry® test; and the Tearcheck® Ocular Surface Inflammation Evaluation (OSIE®). Conjunctival impression cytology samples underwent droplet digital PCR to quantify gene copies of MMP-9, IL-8 and IL-1 β . Inter and intra observer agreement in clinical grading was also evaluated, and the diagnostic utility of clinical inflammation tests and DED markers assessed relative to laboratory markers.

Results: Data suitable for laboratory analysis was obtained from 47 participants (79% female, median age 58 (22-82); 37 with DED). MMP-9 levels were positively associated with DED severity. Subjective and objective conjunctival hyperemia grading, and positive InflammDry® outcomes were predictive of elevated MMP-9 levels (all $p < 0.05$). Of the DED diagnostic markers and subclassification tests, tear film stability (with diagnostic cut off of < 5.7 s), symptom scores (with cut offs of > 9 for DEQ-5 and > 33.3 for OSDI), and a thin lipid layer (grade ≤ 2) best predicted elevated MMP-9 ($p < 0.05$). Elevated IL-8 and IL-1 levels could not be predicted from clinical tests. Clinical grading scales were confirmed not to be interchangeable based on the levels of agreement. The VBR-5 grading scale aligned most closely with objective hyperaemia grades.

Conclusion: Clinical ocular surface tests were poorly predictive of IL-8 and IL-1 β levels, however clinical tests of inflammation were found to usefully predict elevated MMP-9 levels as an index of ocular surface inflammation. Results suggest some prediction was possible from clinical testing, but there was limited agreement between test scores which indicates that current clinical tests of inflammation cannot be used interchangeably. More research is required to define diagnostic cut offs for use in guiding treatment in different subtypes of DED.

Acknowledgements

I would like to acknowledge and give my warmest thanks to my supervisor Professor Jennifer P. Craig who provided ongoing support from the beginning to the end of this master's research and thesis completion. Despite the COVID-19 disturbances and the lengthy Auckland lockdown in 2021, her unwavering determination and guidance made completion of this thesis possible.

I would also like to thank my co-supervisor Dr Alex Muntz for his guidance in not only this master's project but also for introducing me to the nuances of the research world as I begin my academic journey.

Special thanks are extended to Salim Ismail, who spent numerous weeks teaching and supervising the entire laboratory component and patiently answered all my lab-based queries to ensure sound scientific evidence could be presented.

I am also very appreciative for the work that Dr Ally Xue has put in to help shape the literary aspect of this thesis. Thank you also to Dr Michael Wang for his excellent statistical knowledge and guidance, and to Dian Zhuang for her support in ensuring both laboratory and clinical aspects could be managed during periods of COVID-related restrictions at the University.

Finally, thank you to my fiancé Jordan, my parents Jennifer and Kevin, and my brother David for your ongoing support in every aspect of my life, allowing me to pursue my passion for research and convincing me to strive high and continue to build my academic career.

Table of Contents

Abstract.....	ii
Acknowledgements.....	iii
List of tables.....	ix
List of figures	xi
Chapter 1. Overview of Dry Eye Disease	13
1.1 Subtypes of Dry Eye Disease	14
1.1.1 Evaporative DED	14
1.1.2 Aqueous deficient Dry Eye Disease	15
1.2 Diagnostic criteria for dry eye disease	15
1.3 Pathophysiology of DED	16
1.3.1 Inflammation in DED	17
1.3.2 Innate immunity of the ocular surface.....	18
1.3.3 Adaptive immunity of the ocular surface.....	19
1.4 Biomarkers of ocular surface inflammation.....	20
1.4.1 Cytokines and chemokines.....	20
1.4.2 Matrix metalloproteinases (MMPs).....	25
1.4.3 Inflammasomes.....	26
1.4.4 Tear collection.....	26
1.4.5 Laboratory analysis.....	27
1.5 Clinical markers of ocular surface inflammation	31
1.5.1 Subjective evaluation of hyperaemia	32
1.5.2 Objective hyperaemia	34

1.5.3 MMP-9 point-of-care testing.....	36
1.5.4 Ocular Surface Staining.....	37
1.6 Anti-inflammatory treatment.....	39
1.6.1 Corticosteroids.....	40
1.6.2 Topical Cyclosporine A.....	40
1.6.3 Lifitegrast.....	41
1.6.4 Tetracycline derivatives.....	41
1.6.5 Macrolides.....	42
1.6.6 Essential fatty acids.....	43
1.7 Aims and hypothesis.....	44
1.7.1 Hypotheses.....	45
Chapter 2. Methods.....	46
2.1 Participants.....	46
2.2 Symptomology.....	47
2.2 Clinical measurements.....	47
2.2.1. Tear meniscus height.....	49
2.2.2. Tear film stability.....	49
2.2.3. Lipid layer evaluation.....	49
2.2.4. Bulbar conjunctival hyperaemia.....	50
2.2.5. Tear osmolarity.....	50
2.2.6 Meibomian gland expressibility.....	51
2.2.7. Ocular surface integrity.....	51
2.2.8 Meibomian gland morphology.....	53
2.2.9 In-office ocular surface MMP-9 assessment.....	54

2.2.10 Laboratory inflammatory marker analysis.....	55
2.3 Laboratory analysis	56
2.3.1 Ribonuclease-free environment.....	56
2.3.2 RNA purification	56
2.3.3 Nanodrop for yield determination.....	58
2.3.4 Tapestation for RNA quality and quantity analysis	58
2.3.5 Spud assay for confirming absence of PCR inhibitors	59
2.3.6 Complementary DNA (cDNA) synthesis	61
2.3.7 β -actin PCR.....	62
2.3.8 β -actin gel electrophoresis.....	64
2.3.9 Droplet Digital PCR.....	65
2.3.10 Controlling for inter-run variability	68
2.3.11 Repeats and losses	68
2.3.12 Normalisation of data	68
2.4 Dry eye diagnosis.....	69
2.5 Statistical analysis	70
Chapter 3. Inter-observer and Intra-observer repeatability of grading scales for conjunctival hyperaemia	72
3.1 Introduction.....	72
3.2 Methods.....	73
3.2.1 Participants and observers	73
3.2.2 Grading systems	73
3.2.3 Data transformation	74
3.2.4 Reproducibility testing.....	74
3.3 Results	75

3.3.1 Inter-observer reproducibility	75
3.3.2 Intra-observer repeatability	77
3.3.3 Inter-instrument agreement.....	79
3.3.4 Subjective grading method comparison.....	79
3.3.4 Subjective vs objective agreement	81
3.4 Discussion	84
3.4.1 Limitations and future directions	86
3.5 Conclusion.....	89
Chapter 4. Results: Diagnostic utility of inflammation markers	90
4.1 Participant characteristics	90
4.2 Correlation Tests	91
4.2.1 Statistical analysis.....	91
4.2.2 Clinical markers of inflammation	91
4.2.3 Laboratory derived markers of inflammation	92
4.2.4 Ocular surface integrity	92
4.3 Association between global dry eye markers and ocular inflammatory biomarkers	95
4.3.1 Global dry eye disease markers and their ability to predict elevated levels of MMP-9 mRNA transcripts.....	95
4.3.2 Global dry eye disease markers and their ability to predict elevated levels of IL-8 mRNA transcripts.....	96
4.3.3 Global dry eye disease markers and their ability to predict elevated levels of IL-1 β mRNA transcripts.....	96
4.4 Predictive ability of clinical biomarkers of inflammation to detect ocular surface inflammation.....	100
4.4.1 Clinical inflammatory markers and their ability to detect elevated levels of MMP-9 mRNA transcripts.....	100

4.4.2 Clinical inflammatory markers and their ability to detect elevated levels of IL-8 mRNA transcripts	101
4.4.3 Clinical inflammatory markers and their ability to detect elevated levels of IL-1 β mRNA transcripts	101
4.5 Ocular Surface Inflammatory Evaluation (OSIE $\text{\textcircled{R}}$) and ocular surface staining correlations and diagnostic utility	105
4.6 Summary	106
Chapter 5. Discussion	107
5.1 Overview	107
5.2 MMP-9 and clinical dry eye disease markers	108
5.3 MMP-9 and clinical markers of inflammation	112
5.4 IL-8 as a biomarker for inflammation	115
5.5 IL-1 β and clinical markers of inflammation	115
5.7 Study limitations and future directions	116
5.8 Seeking to manage inflammation in DED	118
5.8.1 Anti-inflammatory therapies	118
5.8.2 Role of anti-inflammatory therapies in MGD	119
Chapter 6 Conclusion	120
Appendix A: Permission agreement for replication of the Efron hyperaemia grading scale	122
Appendix B. Permission to replicate the Validated Bulbar Redness scale	123
Appendix C: Study participant information sheet	124
Appendix D: Study consent form	125
Appendix E: Table of primer and probe nucleotide sequences	126
References	129

List of tables

Table 1. Reported studies conducted with human participants in the analysis of cytokine biomarkers in DED.	22
Table 2. Testing order of ocular surface characteristics.....	48
Table 3. Korb's grading scale for lid wiper epitheliopathy (206).....	52
Table 4. Pult's Meiboscale grading values and corresponding percentage meibomian gland loss.....	53
Table 5. Constituents and relative proportions of the Purelink™ DNase treatment.....	57
Table 6. Constituents and concentrations of the SPUD assay master mix.....	60
Table 7. PCR cycling conditions for the SPUD assay.....	60
Table 8. Thermal cycling conditions for cDNA synthesis.....	62
Table 9. Constituents for the β -actin PCR reaction.....	63
Table 10. β -actin PCR cycling conditions.....	64
Table 11 Thermal cycler conditions for additional DNase treatment of gDNA* contaminated RNA.....	65
Table 12. Master mix constituents for ddPCR.....	66
Table 13. PCR Cycling conditions for the ddPCR reaction.....	67
Table 14. Dry eye diagnostic criteria as defined by the TFOS DEWS II Diagnostic Methodology report (2). 69	
Table 15. BHVI scale inter-observer reproducibility.....	76
Table 16. Efron scale inter-observer reproducibility.....	76
Table 17. VBR scale inter-observer reproducibility.....	77
Table 18. Participant characteristics.....	90
Table 19. Classification criteria for severity of dry eye disease (1)......	91
Table 20. Grading schemes for evaluating clinical and laboratory inflammation markers and dry eye diagnostic markers.....	93

Table 21. Correlation matrix of all clinical inflammatory tests, dry eye diagnostic tests and laboratory derived inflammation markers.	94
Table 22. Global dry eye markers versus presence of laboratory MMP-9 biomarkers.	97
Table 23. Global dry eye markers versus presence of laboratory IL-8 biomarkers.	98
Table 24. Global dry eye markers versus presence of laboratory IL-1 β biomarkers.	99
Table 25. Clinical measures of inflammation.	100
Table 26. The discriminative ability of clinic-based measures for inflammation in detecting MMP-9 transcripts.	102
Table 27. The discriminative ability of clinical inflammation markers detecting IL-8 transcripts.	103
Table 28. The discriminative ability of clinical inflammation markers detecting IL-1 β transcripts.	104
Table 29. Ocular surface integrity measures and their correlations to the OSIE $^{\text{®}}$ scores.	105
Table 30. Ocular surface integrity measures and their predictive ability to identify positive OSIE $^{\text{®}}$ scores.	105

List of figures

Figure 1. Simplified figure outlining the criteria for diagnosis and subtype classification of DED, adapted from TFOS DEWS II Diagnostic Methodology report (19).....	16
Figure 2. Self-perpetuating vicious circle of DED adapted and simplified from the TFOS DEWS II pathophysiology report (18).....	17
Figure 3. Immunofluorescent image of human corneal limbal cells expressing Vimentin.....	30
Figure 4. Efron bulbar hyperaemia grading scale ranging from normal, trace, mild, moderate and severe. .	33
Figure 5. Validated Bulbar Redness (VBR10) scale consisting of 10 images.....	34
Figure 6. Lipid layer patterns.	50
Figure 7. Tearcheck® device in use.....	52
Figure 8. OSIE® assessment screen.	53
Figure 9. The InflammDry® test.	54
Figure 10. Subcategorisation criteria for evaporative, aqueous deficient or mixed etiology of dry eye disease (2).....	70
Figure 11. Spearman's correlation matrix for inter-observer reproducibility.....	75
Figure 12. Bland-Altman analysis of observer A's intra-observer repeatability.....	78
Figure 13. Bland-Altman analysis of observer B's intra-observer repeatability.....	78
Figure 14. Bland-Altman analysis of the difference between hyperaemia grades on BHVI vs Efron scales plotted against the mean hyperaemia score.	79
Figure 15. Bland-Altman analysis of the differences between hyperaemia grades on BHVI and VBR-5 scales plotted against the mean hyperaemia grade.	80
Figure 16. Bland-Altman analysis of the difference between hyperaemia grades assessed using the Efron and VBR-5 scales plotted against the mean hyperaemia grade from the Efron and VBR-5 scales.	80
Figure 17. Bland-Altman analysis of the difference between BHVI vs JENVIS (R-Scan) scale hyperaemia grades plotted against the average hyperaemia score.	81

Figure 18. Bland-Altman analysis of the difference between Efron vs JENVIS (R-Scan) scale hyperaemia grades plotted against the average hyperaemia score. 82

Figure 19. Bland-Altman analysis of the difference between VBR-5 vs JENVIS (R-Scan) scale hyperaemia grades plotted against the mean hyperaemia score. 82

Chapter 1. Overview of Dry Eye Disease

Dry eye disease (DED) is a complex, multifactorial condition, resulting in the loss of homeostatic mechanisms of tear film maintenance and the ocular surface, as defined by the Tear Film and Ocular Surface Society Dry Eye Workshop II (TFOS DEWS II) (3). Ocular symptoms of DED include chronic irritation, discomfort, grittiness, and visual disturbance (3).

The literature regularly reports the effect of DED on quality of life through ocular discomfort and impediment to visual function. The chronic and progressive nature of DED affects the ability to undertake daily activities such as computer use, reading, driving, smartphone use, and watching the television, and impacts on work productivity are frequently associated with DED (4-10). DED is one of the most commonly encountered eye conditions in clinical practice, affecting between 5 and 50% of the population in different parts of the world (9, 11, 12). The direct economic burden of patients seeking clinic visits, medications, and other treatment interventions, in addition to the indirect costs from decreased work productivity, reduced quality of life and impairment of performing daily living tasks, make DED a significant global public health and financial burden (5, 6, 9, 12). Studies report that the prevalence of dry eye is rising in all age groups (6, 12), with signs and symptoms of DED increasing with age. Extended digital device use is increasingly recognised as a consistent risk factor for DED (6, 13, 14); therefore, the modern world's growing reliance on screens across all age groups is projected to amplify the public health and financial burden of DED in future years (6, 12).

Epidemiological research provides critical prevalence and incidence data across different populations, which can highlight the magnitude of the DED public health burden. Some studies advocate for improved resources in providing public health interventions at the population level, which may potentially be more cost-effective than subsequently providing treatment (6). Identifying modifiable and non-modifiable risk factors for DED can inform the development of public health strategies, including targeted screening, risk factor modification and health promotion interventions, to improve public and practitioner awareness of DED (15).

1.1 Subtypes of Dry Eye Disease

The tear film can be divided into two phases, an mucoaqueous phase and an overlying lipid layer (16, 17). The mucoaqueous phase is located immediately adjacent to the glycocalyx of the epithelial surface of the eye, and possesses a decreasing mucous gradient and increasing aqueous gradient from the epithelium towards the lipid layer. The tear film lipid layer is situated most anteriorly, with its exterior surface exposed to the atmosphere. It is derived from meibum secreted from the orifices of the meibomian glands that open onto the lid margin, and it is spread over the tear film surface with each blink (17). Homeostatic mechanisms tightly control the balance of these layers to provide a lubricated surface for the cornea, ensuring clear vision.

When homeostasis is disrupted, ocular surface diseases such as dry eye can occur. DED can be divided into two subtypes; evaporative dry eye (EDE) and aqueous deficient dry eye (ADDE). EDE is the predominant subtype where excessive tear evaporation occurs in the presence of normal lacrimal gland function. EDE is often caused by meibomian gland dysfunction, resulting from lipid insufficiency that results in an inadequate tear film quality (10, 18). Conversely, ADDE describes a lack of aqueous tear fluid due to dysfunction of the lacrimal gland (3, 18). Regardless of subtype, failure of homeostatic mechanisms at the ocular surface result in tear hyperosmolarity and tear film instability, initiating an inflammatory cascade and subsequent ocular surface damage, described as a self-perpetuating vicious circle of DED (18). Aqueous deficiency can coexist with evaporative dry eye, often resulting in a more severe DED (3, 10, 19).

1.1.1 Evaporative DED

Meibomian gland dysfunction (MGD) is recognised to be the most common cause of evaporative DED (20). It results in decreased functionality of the glands and gland drop-out, with subsequent production of poor quality and quantity of meibum (21). Various factors can cause the ocular surface microbiome to promote commensal bacteria such as *Staphylococcus aureus* that overpopulate the lid margins. *S. aureus* produces lipases that cleave lipid into altered species such as free fatty acids, which can present as foaminess in the tear film due to saponification (22-25). The altered lipid layer results in tear instability and evaporation (26). Risk factors for MGD include increased age, contact lens use,

incomplete blinking, environmental stress, hormonal factors and systemic medications ([12](#), [18](#), [27](#), [28](#)).

Many of these factors have been shown to alter meibomian gland cellular differentiation, and functionality including lipid-producing abilities, believed ultimately to result in meibomian gland atrophy due to loss of function ([29](#)).

1.1.2 Aqueous deficient Dry Eye Disease

ADDE is divided into two subgroups, Sjögren's syndrome dry eye disease (SSDE) and non-Sjögren's syndrome dry eye disease (non-SSDE) ([30](#)). In both cases, there results a lack of aqueous component in the tear film, usually on account of dysfunction in the lacrimal glands, the primary source of the tear aqueous component. Sjögren's syndrome (SS), is an autoimmune condition, characterised by lymphocytic infiltration of the lacrimal and salivary glands. The American-European consensus criteria for SS has six components, that allow a combination of DED signs, DED symptoms, dry mouth signs, dry mouth symptoms, autoantibodies and a minor salivary gland biopsy ([31](#)) to be considered in making a diagnosis. Primary SS is diagnosed where dry eye and dry mouth exist in the absence of any other systemic autoimmune disease ([32](#)) and has been attributed to previous Epstein-Barr virus, hepatitis C virus and human T cell leukaemia virus type I infection, although the pathophysiology is not yet clear ([33](#)). Secondary SS describes manifestation of the ocular and oral features in the presence of autoimmune connective tissue diseases, such as rheumatoid arthritis ([30](#)).

Non-SSDE related aqueous tear deficiency results from non-Sjögren's infiltrative disorders of the lacrimal gland, and cicatricial diseases of the conjunctiva ([32](#)). Another distinguishing factor between the two subcategories is the severity of clinical presentation. SS ADDE typically presents with higher severity of disease signs and symptoms than non-SSDE ([19](#)).

1.2 Diagnostic criteria for dry eye disease

The diagnostic criteria for DED and the ensuing classification of subtypes are outlined in Figure 1, as described by TFOS DEWS II ([2](#)). Triaging questions help differentiate patients with irritation symptoms arising from conditions masquerading as DED, and this is followed by a risk factor assessment.

Diagnostic criteria must include a positive symptomology score based on one of the validated

questionnaires; either the Dry Eye Questionnaire-5 (DEQ-5) or Ocular Surface Disease Index (OSDI), and the presence of at least one sign of ocular surface homeostasis breakdown. Ocular signs include one or more of the following; a decreased non-invasively tested tear break-up time (<10s), increased osmolarity of the tears ≥ 308 mOsm/L or an interocular difference in osmolarity of >8 mOsm/L, or ocular surface staining of one of the following; fluorescein staining of >5 corneal spots, lissamine green staining of >9 conjunctival spots or of the lid wiper portion of the eyelid margin (≥ 2 mm length and $\geq 25\%$ width) (2). Once a DED diagnosis is confirmed, further diagnostic tests are carried out to determine the subtype of DED to help guide management plan for the patient.

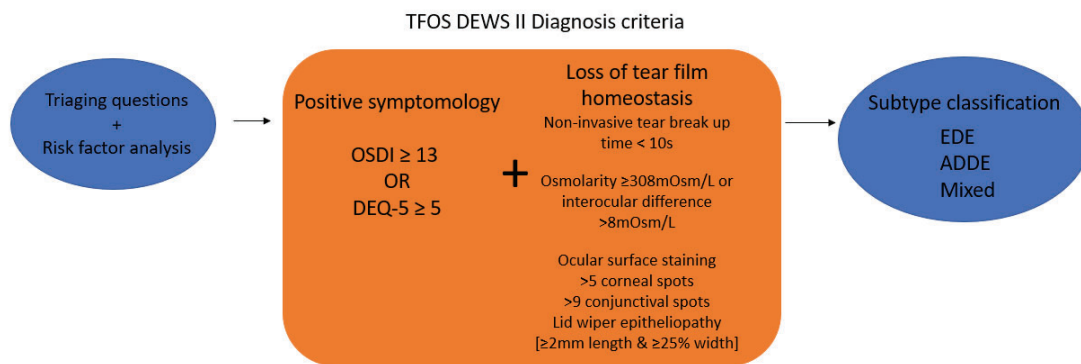


Figure 1. Simplified figure outlining the criteria for diagnosis and subtype classification of DED, adapted from TFOS DEWS II Diagnostic Methodology report (19).¹

1.3 Pathophysiology of DED

Tear film and ocular surface homeostasis is tightly regulated in the healthy eye. Homeostasis is maintained across the lacrimal functional unit, which involves the ocular surface, neuronal interconnectivity, lacrimal glands, eyelids, meibomian glands and the tear film (18, 32, 34). When morphology or functionality of these structures is disrupted, resulting instability of the tear film drives hyperosmolarity, and an inflammatory cascade is initiated, serving as a critical driver of disease progression that leads to self-perpetuating DED (34). According to TFOS DEWS II, the current threshold

¹ Abbreviations. Ocular surface disease index (OSDI), Dry eye questionnaire (DEQ-5), Evaporative dry eye (EDE), Aqueous deficient dry eye (ADDE)

for discriminating between normal and dry eyes is a hyperosmolarity of at least 308 mOsm/L in either eye or an interocular difference of greater than 8 mOsm/L. Values above 316 mOsm/L are considered indicative of moderate-to-severe DED (18). The self-perpetuating vicious circle of inflammation and cellular damage that ensues, leads to the signs and symptoms commonly observed in chronic DED. Any entry point on this circle promotes disruption of tear film homeostasis and propagation of the self-perpetuating vicious circle, as depicted in Figure 2 (18, 34).

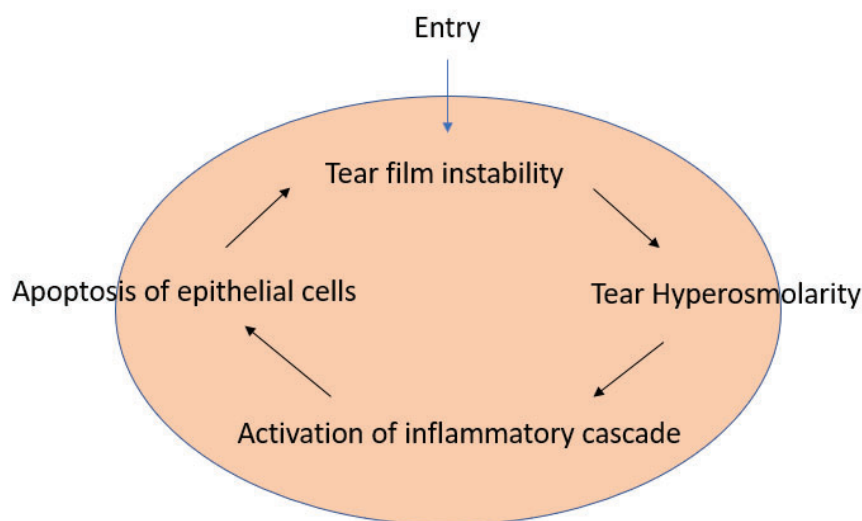


Figure 2. Self-perpetuating vicious circle of DED adapted and simplified from the TFOS DEWS II pathophysiology report (18).

1.3.1 Inflammation in DED

Inflammation is a common feature of DED, regardless of subtype, and has been most researched to date in Sjögren's syndrome due to the high inflammatory involvement in this autoimmune disease (35). The inflammatory drivers in DED differ depending on the subtype pathophysiology. Lacrimal infiltration of inflammatory cells and mediators has been conclusively demonstrated in Sjögren's syndrome (18, 30, 36). On the other hand, evidence suggests that disease aetiology in obstructive MGD centres around hyperkeratinisation of the duct and gland orifice, rather than to immune cell infiltration and cytokine proliferation of the meibomian glands and its structures (18, 37, 38). However, inflammation remains an important downstream feature of EDE, especially in more severe disease forms. It has been proposed

that despite evidence of inflammation in the meibomian glands, ocular surface inflammation can still exist. The lack of meibum due to blocked meibomian glands results in poor tear film instability, thus becoming an entry point to the vicious circle of DED (38), and triggering inflammation. Additionally, the over colonisation of commensal bacteria can result in abnormal meibum production, triggering the vicious circle (18).

The initial inflammatory response arises from the innate immune system, involving epithelial cells, antigen-presenting cells (APC), neutrophils, natural killer cells, and mediators (18). Loss of goblet cells and surface bound mucins that form the glycocalyx, following the upregulation of inflammatory mediators, causes epithelial cell damage by apoptosis, with the resulting poor ocular surface quality leading to further tear film instability and hyperosmolarity, that thus perpetuates the disease state. APCs migrate to local lymph nodes, activating naïve T cells, and initiating the adaptive immune response (39). Continued ocular surface insult leads to chronic disease, typically accompanied by increasing severity of symptoms and signs in DED (32).

1.3.2 Innate immunity of the ocular surface

Our current understanding of the inflammatory cascade events in DED is based on evidence from tissue culture, animal model and human research studies. The self-perpetuating model of the vicious circle is implicated in all subtypes of DED, underlying both upstream and downstream inflammation (18, 40).

Hyperosmolar stress on epithelial cells at the ocular surface initiates the activation of Nuclear Factor kappa-light-chain-enhancer of activated B cells (NFκB) signalling pathways and activation of mitogen-activated protein (MAP) kinases (41). This serves to stimulate the production of interleukin-1 (IL-1), a pro-inflammatory cytokine, and TNF-α, which acts to amplify the immune response downstream to activate further inflammatory mediators and cellular signals (18, 42). IL-1 and TNF-α stimulate the production of matrix metalloproteinase 9 (MMP-9), a protease produced by corneal epithelial cells that disrupts the corneal epithelial barrier by lysing tight junctions (18, 41, 42). Hyperosmolarity directly induces corneal epithelial cell death via apoptosis, resulting in a poor quality ocular surface that cannot support a stable tear film, further perpetuating the inflammatory cascade (18, 42). The complex interaction between upregulated inflammatory mediators results in an amplified response of the inflammatory cascade (42).

Further inflammatory pathways are initiated following desiccation of the ocular surface by pattern recognition receptors such as Toll-like receptors (TLR), nucleotide-binding domain leucine-rich-containing family, pyrin domain-containing-3 (NLRP3) and NOD-like receptors (NLR) to mediate cytosolic, inflammasome pathway inflammation, which together contribute to upregulating IL-1, TNF- α and IL-6 (18, 42).

Generated cytokines, chemokines, and MMPs stimulate migration of neutrophils and natural killer (NK) cells to attack the damaged cells. One defence mechanism of neutrophils against pathogens is to expel their DNA and cellular contents to create neutrophil extracellular traps (NETs). NETs have been shown to be present in higher than normal amounts in patients with severe ADDE (18, 43), possibly as a response to hyperosmolar stress, or due to a lack of availability of regulating tear nucleases which are normally produced by the lacrimal gland (18, 43). NK cells also directly attack damaged epithelial cells and secrete large amount of cytokines, including IFN- γ (44). Dry eye experimental models have shown upregulation of pro-inflammatory cytokines such as IFN- γ , IL-6, IL-17 and IL-23 (45). These cytokines stimulate the activation of macrophages, antigen-presenting cells (APCs) and auto-reactive T cells (18).

1.3.3 Adaptive immunity of the ocular surface

The adaptive CD4+ T-cell autoimmune response occurs following the maturation of dendritic cells that migrate to regional lymph nodes (18). Naïve T cells recognise the presented self-antigens, beginning differentiation and expansion into autoreactive T effector cells types; Th1, Th2, Th17 and T regulatory cells (18, 41, 44). The target autoantigen in this model of DED has not yet been identified (42).

T helper 1 (Th1) and Th17 cells invade the ocular surface after their activation, secreting IFN- γ and IL-17, respectively.

For the adaptive immune response to persist, recruitment of other inflammatory cells specific to the adaptive system is required, mediated through chemokines and adhesion molecules. Chemokines attract macrophages, dendritic cells, neutrophils, and activated T cells that display the respective upregulated chemokine receptors, including CCL3, CCL4, CCL5, CXCL9 CXCL10 and CX3CL1. Conjunctival and corneal epithelial cells express adhesion molecules such as the intercellular adhesion molecule-1 (ICAM-1) to attract and bind inflammatory cells to the ocular surface. ICAM-1 binds to the ligand integrin leukocyte

functional antigen-1 (LFA-1) expressed on the inflammatory cells (18). Dysfunctional regulatory T cells (Tregs) have been induced in desiccation DE models, which have been associated with aging (46, 47). The hypothesis that immune tolerance is disrupted in DED is further demonstrated by the depletion of Treg cells exhibiting the CD4+CD25+Foxp3 phenotype, exacerbating DED (48).

1.4 Biomarkers of ocular surface inflammation

In this context of ocular surface inflammation, a biomarker is a specific, quantifiable protein in the tear fluid. Through its relative presence or absence, it allows insight into pathogenic processes in the ensuing inflammatory cascade. A biomarker can help determine the stage of the disease process and severity and be used to monitor treatment success. Efforts to identify potential biomarkers specific to ocular surface inflammation have so far resulted in variable success, which has been attributed to non-standardised methods of collection and analysis (49). Of the molecules that have been analysed, cytokines, chemokines and MMP-9 are the most studied biomarkers of inflammation (49-52). Panels of biomarkers have been recommended, indicating the complex nature of DED pathophysiology (53, 54).

1.4.1 Cytokines and chemokines

Cytokines are small proteins upregulated in inflammatory processes, serving as potent immunomodulators, and secreted by various cells (53). Chemokines are a type of chemotactic cytokine involved in the recruitment and migration of neutrophils and lymphocytes to the site of inflammation. They are favoured as the diagnostic biomarkers for many ocular surface diseases due to the minimally invasive collection and analysis methods associated with their quantification. A consensus is yet to be reached on the best method for tear collection and subsequent cytokine analysis, resulting in cytokine level norms and cut-off values varying greatly across the literature (55). Discrepancies in outcomes amongst different studies may also reflect the different disease stages and severities of the study cohorts analysed (56).

Various cytokines and chemokines (particularly IL-8) have been reported to be raised in individuals with DED (35, 54, 57). Patients with Sjögren's syndrome typically show higher levels of pro-inflammatory cytokines than other subtypes of DED (35, 57). Throughout the literature, pro-inflammatory cytokines IL-1 β , IL-6, IL-10, IFN- γ , TNF- α and the chemokine IL-8 (or CXCL8) have been reported to be consistently

higher in DED patients compared to normal controls ([54](#), [55](#), [58-66](#)). IFN- γ upregulates production of chemokines, chemokine receptors, human leukocyte antigen (HLA), cell adhesion molecules and inhibits secretion of mucins and promotes goblet cell apoptosis in the long term ([67](#)).

Published studies generally concur that the levels of cytokines and chemokines increase as disease severity progresses ([68](#), [69](#)). Yoon et al. found that IL-6 was significantly increased in tears of patients with SSDE compared to the non-SSDE group, and levels were positively associated with disease severity ([70](#)). Additionally, Tan et al. concluded that the levels of IL-17 and IL-22 were significantly increased in tears of DE patients compared with those of controls and were higher in SSDE patients compared with those of non-SSDE patients ([68](#)). An increase in IL-1 α and mature IL-1 β has also been reported in patients with MGD and SSDE ([71](#)). Significant increases in cytokines IL-1 β , IL-6, IL-8, TNF- α have been found by Boehm et al. for ADDE and mixed-type DED ([72](#)). Recently, Roda et al. conducted a meta-analysis on DED cytokine biomarkers, finding higher levels of IL-1B, IL-6, chemokine IL-8, IL-10, IFN- γ and TNF- α in DED participants compared to non-DED controls across 13 studies ([55](#)). From this study, the evidence for increased IL-2 and IL-17 in DED was reportedly modest ([55](#)). Chan et al. investigated ocular cicatricial pemphigoid and the effect of immunomodulatory treatment. Resolution of IL-8 and MMP-9 were identified as indicators of treatment success, signifying the end of active inflammation ([73](#)). Limitations of the studies comparing cytokine concentrations in DED vs control groups include differing diagnostic criteria for DED and variability in collection and testing methods, as well as the low sample size in some studies ([35](#), [54](#), [61](#), [63-66](#), [68-70](#), [74-79](#)).

Table 1. Reported studies conducted with human participants in the analysis of cytokine biomarkers in DED.²

Reference	Collection method	Testing method	Study groups	n	Increased cytokines in DED vs controls
Acera et al. (64)	Wick cell sponge	Enzyme-linked immunosorbent Assay (ELISA)	DED vs control	95	Pro MMP-9
Akpek et al. (35)	Microcapillary tube (unstimulated*)	Multiplex bead immunoassay (Luminex)	SS vs non-SS vs control	62	SS: IL-8
Enriquez-de-Salamanca et al. (61)	Microcapillary tube (unstimulated)	Multiplex bead immunoassay	EDE vs control	32	IL-1Ra, IL-6, IL-8/CXCL8, EGF
Huang et al. (74)	Microcapillary tube (unstimulated)	Multiplex bead immunoassay (Luminex)	DED vs control	102	IL-1Ra, IL-8
Lam et al. (65)	Microcapillary tube (unstimulated)	Multiplex bead immunoassay	DED vs control	30	IL-6, IL-8, TNF- α

² The literature search was conducted in PubMed, January 2022 using the search query “(cytokine* OR chemokine OR biomarker) AND (ELISA OR multiplex OR Luminex) AND (tear*) AND (dry eye disease)”. Studies were excluded if a direct comparison of cytokines against DED vs control groups were not made.

*Unstimulated tears refers to sample collection that does not induce reflex tears.

Lee et al. (69)	Microcapillary tube (Flush method with 30uL saline)	Multiplex bead immunoassay	SS vs non-SS vs control	70	IL-17, TNF- α , IL-6 SS only: IL-10, IL-4
Luo et al. (76)	Microcapillary tube (unstimulated)	ELISA	SS vs non-SS vs control	90	IL-4, IL-5, IL-33
Massingale et al. (63)	Microcapillary tube (unstimulated) Impression cytology	Multiplex bead immunoassay (Real-time polymerase chain reaction (RT-PCR))	DED vs control	14	IL-2, IL-4, IL-5, IL-6, IL-10, IFN- γ , TNF- α , IL-1 β , IL-8 mRNA: IL-1 β , IL-6, IL-8, TNF- α
Pflugfelder et al. (77)	Wick sponge Impression cytology	ELISA RT-PCR	SS vs control	20	IL-6 mRNA: IL-1 α , IL-6, IL-8, TNF- α , TGF- β
Tan et al. (68)	Microcapillary tube (unstimulated)	ELISA	SS vs non-SS vs control	60	IL-17, IL-22
Tishler et al. (66)	Microcapillary tube (unstimulated)	ELISA	SS vs control	24	IL-6

Wei et al. (78)	Microcapillary tube (unstimulated)	Multiplex bead immunoassay	DED vs control	Pooled [n unknown]	IL-1 β , IL-6, IFN- γ , TNF- α
Willems et al. (79)	Schirmer strip	Multiplex bead immunoassay	SS vs control	25	IL-2, IL-4, IL-6, IL-10, IFN- γ , TNF- α , IL-12p70, IL-5
Yoon et al. (70)	Microcapillary tube (unstimulated)	ELISA	SS vs non-SS vs control	32	IL-6, TNF- α
Zhao et al. (54)	Microcapillary tube (unstimulated)	Multiplex bead immunoassay (Luminex)	SS vs non-SS vs control	70	IL-6, IL-8, TNF- α , IL-12P70

1.4.2 Matrix metalloproteinases (MMPs)

MMP-3 and MMP-9 have been implicated in the innate inflammatory cascade following hyperosmolar damage to the overlying epithelial cells. MMP-9 is a 23-zinc and calcium ion-dependent protease enzyme produced by epithelial cells in the cornea, and by neutrophils that degrade the epithelial basement membrane via degradation of collagen type IV and VII (80-82). MMP-9 has been shown to lyse epithelial tight junctions, breaching the seal of the ocular surface, resulting in increased permeability and further tear film instability due to a compromised epithelium (18, 42).

In DED, the hyperosmolar environment on the corneal surface triggers the stress-activated protein kinase (SAPK) signalling cascade that leads to epithelial cells releasing MMP-9 (18, 51). Furthermore, inflammatory mediators such as IL-1 β prompt local neutrophils to secrete MMP-9 in its proenzyme form, bound to endogenous tissue inhibitors of metalloproteinase (TIMP), which is sequentially activated by other proteinases (83). MMP-9, also known as gelatinase-B, is an important molecule involved in normal physiological tissue remodelling processes such as wound healing and bone development (83).

MMP-9 is present in healthy individuals at a reference range of between 3 to 41 ng/ml; 90% of people within the normal range have MMP-9 levels less than 30ng/ml (64, 71, 82, 84-86). Elevated levels of MMP-9 have been implicated in various ocular surface diseases such as conjunctivochalasis, peripheral ulcerative keratitis, vernal keratoconjunctivitis, corneal erosions, rosacea, pterygium and keratoconus (80, 82, 86-91). Mice with induced evaporative dry eye have shown increases in MMP-9 activity using gel zymography assays on tear fluid to assess active protease activity (92). Levels of MMP-9 mRNA were found to be increased in this same study (92). In humans, MMP-9 levels have also been shown to be elevated in cases of DED (18, 51). MMP-9 is secreted as an inactivated proenzyme, known as a zymogen, then activated by other proteases to its active gelatinase-B form. The mRNA expression of MMP-9, pre-transcription, can be quantified using semi-quantitative real-time PCR from impression cytology samples. The activated form can be quantified by zymography, using electrophoresis and western blotting techniques, immunohistochemistry, enzyme leak immunoassays, and MMP-9 capture activity measurements (93). Chotikavanich et al. demonstrated that both MMP-9 activity and mRNA transcripts were higher in patients with DED than in normal controls (85). MMP-9 levels in tears demonstrate diurnal variation which should be taken into consideration when using MMP-9 as a sole biomarker for ocular surface inflammation in clinical settings (94).

1.4.3 Inflammasomes

Inflammasomes are intracellular, multimeric protein complexes triggered by pathogen-associated molecular patterns (PAMPs) or danger-associated molecular patterns (DAMPs), that form part of the innate immune response ([95](#), [96](#)). Inflammasomes activate procaspase-1, resulting in the cleavage of pro-IL-1 β and pro-IL-18 to become biologically active, further amplifying the ongoing inflammatory cascade ([95](#), [97](#)). Although there are different types of inflammasomes, the most studied inflammasome complex is the Nod-like receptor family pyrin domain-containing 3 (NLRP3), which is a critical contributor to the inflammation process in diseases such as acute graft-versus-host disease, systemic lupus erythematosus, type 2 diabetes, gout and asthma ([98-102](#)). As a relatively newly identified biomarker of inflammation in many inflammatory disease studies, inflammasomes have been proposed as a potential target for novel treatment strategies ([103-105](#)). To date, limited research has been conducted to confirm the presence and role of inflammasomes in DED ([97](#), [106](#), [107](#)). Niu et al. found elevated levels of NLRP3 inflammasome mRNA and protein expression in patients with SS DED. Additionally, increased levels of the associated inflammatory factors, caspase-1, IL-1 β , IL-18 were found. The levels reported were higher in SS-DED than in non-SSDE ([97](#)).

1.4.4 Tear collection

Significant variation in reported cytokine concentration levels has been ascribed, at least in part, to differences in tear collection method and analysis ([49](#)). The most common sampling technique is basal tear collection via a glass micro-capillary tube from the lower lateral canthus. Basal tears are considered to be the most accurate representation of the true protein composition of the tears, however the collection process can be painstaking, with adequate volumes for biomarker analysis difficult to obtain ([108](#)).

Reflex tearing is often a limiting factor, coinciding with participants reporting discomfort during collection and is unavoidable in Schirmer paper and cellulose sponge collection techniques ([109](#)). Reflex tearing occurs when physical or nasal stimulation occurs, and dilutes the sample due to a high flow rate of tears from the lacrimal gland resulting in a correspondingly lower overall concentration of tear proteins being identified ([110](#)). While reflex tearing is, by nature of the disease, reduced in SS patients, reflex tearing is a significant risk in the collection from patients with DED who possess normal lacrimal gland function.

Surprisingly, studies often do not usually disclose the quantity of tears collected from DED study participants(58, 108, 111, 112).

Flush tear collection, also referred to as the 'wash-out' method, has been proposed as a relatively non-invasive method that only minimally stimulates reflex tear production, making it appropriate for the purpose of tear collection for cytokine analysis. This method involves adding a small volume of saline to the lateral canthus via a micropipette, typically between 10uL and 30uL, then immediately collecting the tears via a microcapillary from the lateral canthus much like the collection method for unstimulated tears (69). Flush tear collection facilitates the collection of adequate volumes of sample for analysis, with minimal patient discomfort and with drastically reduced collection time for unstimulated tears (68, 78). Cytokine concentrations in flush tears and unstimulated whole tears have been shown to be comparable (108, 113). However, the potential risks associated with unaccounted dilution must always be considered, especially when analysing molecules that are present in lower concentrations (108). Markoulli et al. validated the flush tear collection using 60µL of saline for cases where it is difficult to yield adequate tear volume for analysis, such as in SS. (108). In 2017, the same group confirmed that flush tear collection using 20µL was more repeatable than 60µL for analysing substance P; however, this study collected samples only from non-dry eye participants, who would be anticipated to possess normal resident tear volumes (113). Recently, Niu et al. collected flush tear samples using 30µL of saline in both types ADDE, as well as healthy controls and successfully obtained cytokine results by ELISA (97). Alternative collection methods include tear adsorption via a polyester wick or cell sponge, and elution of tears from Schirmer strips (58, 64, 71, 72). Schirmer tear collection is straightforward to obtain, however it needs to be recognised that the proteins eluted from these samples arise not only from the resident tear fluid, but also potentially from tissue leakage and cellular sources due to the trauma associated with mechanical rubbing of the strip against the conjunctival epithelium. which will result in a different tear protein profile from that of basal tear fluid (114-116).

1.4.5 Laboratory analysis

A range of immunoassays employing different detection techniques exist for the qualitative and quantitative analysis of a range of inflammatory biomarkers. Most of the methods, such as ELISA and multiplex bead immunoassays, use sandwich antibody capture technology to capture small protein

molecules. RNA expression can also be analysed from conjunctival cell specimens using quantitative real-time polymerase chain reaction (qPCR), and proteins can be identified and distinguished by more robust laboratory methods such as Western blotting and zymography.

1.4.5.1 Cytokine analysis

Current techniques of protein profiling in small volume tear samples include ELISA, membrane antibody microarray and multiplex bead arrays ([54](#), [56](#), [72](#), [117](#), [118](#)). These arrays involve a sandwich technique that involves a primary antibody, designed to identify the molecule in the tear sample, and then a secondary conjugated antibody for identification and quantification. Tear samples are notoriously small in volume, and the composition of proteins present in the samples themselves is heavily susceptible to variation related to environmental ocular exposure, diurnal variation, participant diet and sample evaporation post-tear collection. Therefore, volume considerations and assay sensitivity metrics are key considerations when deciding which assay is the best for study purposes ([56](#)).

Enzyme-linked immunosorbent assays (ELISA) are considered the 'gold standard' in detecting and quantifying tear proteins ([111](#), [118](#)). Their good repeatability, accuracy, precision and lack of cross-reactivity are advantages. However, a disadvantage is their ability to test only a single analyte per assay kit. Another disadvantage is the relatively large sample volume required. ELISAs are often used to retest results obtained using other immunoassays. With technological advances, it is now possible to analyse multiple analytes concurrently, with a smaller sample volume, using multiplex bead analysis techniques.

Multiplex bead arrays, known as bead-based immunoassays, cytometric bead-based assays, or multiplex ELISAs, are assays that utilise sandwich immunoassay techniques from ELISA and combine them with flow cytometry techniques. Unlike traditional ELISAs that are supplied with wells that are pre-coated with the antibody of interest, in multiplex bead arrays, colour-coded microspheres known as beads are coated with the antibodies of interest. The beads provide a larger surface area for analyte binding. Variation in the sensitivities of available commercial kits exists, and protocols for tear cytokine detection and quantification using multiplex assays are yet to be standardised due to the variability in dilution factors between samples and the different buffers used ([56](#)). Despite the risk of cross-reactivity and potentially lowered sensitivity in multiplex bead arrays, researchers have demonstrated good correlation

between multiplex assays and individual ELISAs for detecting cytokines ([53](#), [56](#), [118](#)). The requirement for smaller sample sizes, rapid processing times and the ability to analyse up to 100 analytes in a single sample make multiplex antibody arrays a favoured option for tear cytokine analysis ([56](#)).

Antibody microarrays similarly allow the identification of numerous protein analytes using a small sample volume, making it another valuable tool for tear analysis. Capture antibodies specific to the analyte in question are immobilised on a glass slide as duplicate dots, and samples are directly applied to the membrane and subsequently quantified by fluorescent, chemiluminescent, enzymatic or radiographic detection systems ([56](#)). The main advantages of membrane microarrays are their low relative cost, low sample volume requirement and the absence of a requirement for specialised training, equipment or facilities. The main limitations include lack of standardised protocols, and the semi-quantitative analysis. Additionally, they can be time-consuming, and cross-reactivity between capture/probe antibodies can occur ([119](#)). Cross-reactivity has been demonstrated in a study that analysed plasma ([114](#), [117](#)). The authors concluded that complex protein milieu such as human plasma was not suitable for microarray analysis due to insufficient precision of the technique ([117](#)), and might suggest that tear protein analysis may raise similar challenges due to the complexity of tear fluid.

1.4.5.2 RNA analysis

RNA can be collected via conjunctival cells retrieved from impression cytology using PTFE or cellulose membranes. Cell culture device inserts or circular shapes punched out of sheets of cellulose acetate are also commonly used in research. For clinical application, the Eyeprim™ (Opia Technology, Paris, France) is a purpose-built, bespoke device designed to collect impression cytology from the conjunctival surface ([120](#)). The RNA sample is subsequently analysed using qPCR, a combination of reverse transcriptase (RT) dependent conversion of RNA into complementary DNA (cDNA), the amplification of cDNA using PCR, and the detection and quantification of products in real-time ([121](#)). A fluorescent probe detected by a fluorometer allows quantification of the amplified cDNA during PCR, in the final step. Quantifying gene expression levels using qPCR analysis is considered the gold standard, allowing high sensitivity detection at a lower cost than gene expression microarrays ([121](#)).

Droplet digital PCR (ddPCR) is a novel gene quantification method for target nucleic acids, that has been commercially available since 2011([122](#), [123](#)). Similar to the qPCR technique, a standard PCR reaction is used to amplify the target DNA fragment. However, two distinct differences are the partitioning of the PCR reaction into thousands of individual reaction droplets, prior to amplification, and the acquisition of data at the reaction endpoint ([124](#)). Additionally, ddPCR technology is ideal for low target quantitation due to nucleic acid quantitation being independent of reaction efficiency, resulting in a positive or negative result for each droplet. This confers, for ddPCR, a higher degree of sensitivity, repeatability and less susceptibility to PCR inhibitors than qPCR ([124](#)).

1.4.5.3 Immunofluorescent staining

Immunofluorescent staining has been used to stain cells collected by impression cytology or conjunctival biopsy tissue sections. The treated specimen is observed for fluorescent staining under a microscope and photographed ([71](#)). Yoon et al. demonstrated increased IL-6 expression in conjunctival cells in DED using this method ([70](#)).

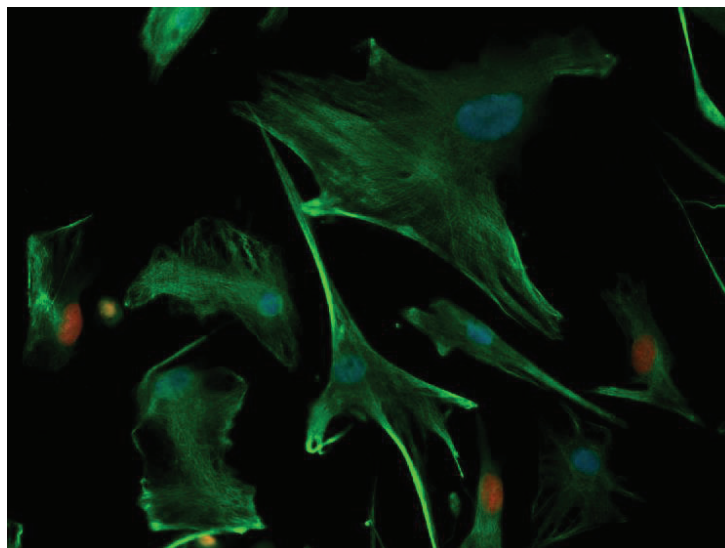


Figure 3. Immunofluorescent image of human corneal limbal cells expressing Vimentin.³

³ Image obtained from the Department of Ophthalmology, University of Auckland with permission.

1.4.5.4 Western Blot

Western blotting of conjunctival impression cytology samples has been performed in the context of dry eye disease. This technique has typically been used for larger protein molecule quantification, such as NLRP3 inflammasome and caspase-1. Proteins are separated by gel electrophoresis and transferred to a membrane which is then incubated with primary and secondary antibodies for subsequent analysis ([97](#)).

1.4.5.5 Zymography

Activity levels of MMP-9, which as previously noted is otherwise known as gelatinase B, can be determined through a technique called gelatin zymography, which measures active gelatinase activity ([87](#), [88](#), [91](#), [92](#)). Diluted tear samples are fractionated by electrophoresis ([92](#)). Further overnight incubation in a digestion buffer allows the gelatinase to digest its substrate, facilitating subsequent quantification using suitable dyes.

1.5 Clinical markers of ocular surface inflammation

Rubor (redness) is one of the five cardinal signs of inflammation and, as such, is considered a hallmark of ocular surface inflammation in clinical examination. The cornea is an avascular tissue, therefore inflammation associated with the surface of the eye is reflected in engorgement of the superficial conjunctival vessels against the white of the sclera, which gives the impression of relative redness ([125](#), [126](#)).

Accordingly, conjunctival hyperaemia is considered the most common index of the severity of inflammation at the ocular surface. Evaluation can be undertaken subjectively, which relies on clinician experience, or objectively, utilising instrumentation and computerised technology.

Bulbar conjunctival redness can result from inflammation arising from a multitude of factors, including allergic and infective conjunctivitis, contact lens wear, ocular irritation, dry eye disease as well as other ocular surface diseases ([125](#), [126](#)). Bulbar redness is inherently variable, as it can be impacted by lack of sleep, environmental factors, eye strain and dehydration ([125](#)). Murphy et al. conducted a study to evaluate the baseline redness of a normal eye in the absence of inflammatory stress or irritation. They

found the highest redness scores for the nasal and temporal quadrants. Additionally, greater redness was observed in males and a linear increase was seen with ten yearly increases in age (125). It has been generally thought that the higher redness values assessed in the horizontal meridian, the nasal and lateral bulbar conjunctiva, relate to the fact that it is the area that is most exposed to the environment, while the superior and inferior bulbar conjunctiva in the vertical meridian are more often protected from exposure by the upper and lower eyelids (127). Schulze et al. conducted a study to assess redness in all meridians before and after application of a topical vasoconstrictor. They found, using a subjective grading scale (Validated Bulbar Redness scale, VBR5), that greater redness was observed for the horizontal meridian than the vertical meridian, as previously reported. However, the investigators found greater differences in the vertical meridian pre and post vasoconstrictor application, which led them to hypothesise that in dry eye disease, the vertical meridian consisting of the superior and inferior bulbar conjunctival redness, may be a more sensitive indicator of ocular surface inflammation (127). Clinically relevant changes in redness values have been defined as any value falling outside of the 95% confidence interval range, as suggested by Bullimore et al., and this approach has been widely adopted by other research groups (128-131).

1.5.1 Subjective evaluation of hyperaemia

Clinically available bulbar redness scales use a mix of verbal descriptors, photographic images and artists' drawings to represent different degrees of redness (129, 131-133). Although objective bulbar conjunctival hyperaemia measurements are superior in terms of sensitivity and specificity (134), subjective grading scales remain commonly applied in everyday practice due to their accessibility, low cost, and practicality for rapid judgment, requiring no additional equipment beyond a regular slit-lamp (132). A clinical judgement of inflammation severity is made, often with the clinician referring back to a pictorial grading scheme. Commonly used subjective grading schemes include the Efron Scale, Brien Holden Vision Institute (BHVI) grading scale and the recently developed VBR10, or its simplified 5-point scale version, the VBR5. In 2004, Wolffsohn et al. used objective methods of colour extraction and edge detection to assess existing printed grading scales assessed, including the Efron scale. The increase in bulbar hyperaemia between the steps was found to be quadratic rather than linear in nature, making the lower end that corresponds to more mild hyperaemia, more sensitive (135). Compared to objective

measurements of bulbar hyperaemia, subjectively graded redness has been shown to be consistently scored higher, supporting the theory that clinicians utilise both blood vessel coverage and colour perception to assess the final hyperaemia grade (136). It has been recommended that interpolation of the scale to 0.1 steps optimises grading sensitivity, and allows clinicians to recognise smaller changes at monitoring visits and facilitate management decisions accordingly (131, 137).

1.5.1.1 Efron scale

The Efron scale (Figure 4) was developed as a tool for grading contact lens-related side effects, including conjunctival hyperaemia. It involves a 5-step scale for both conjunctival and limbal hyperaemia grading, depicted by artistic rendering. A change of 1.0 units has been determined to be a conservative, clinically relevant difference (133, 138)



Figure 4. Efron bulbar hyperaemia grading scale ranging from normal, trace, mild, moderate and severe. ⁴

1.5.1.2 Validated Bulbar Redness scale

The Validated Bulbar Redness scale (Figure 5), also known as the VBR 10, comprises ten pictures that represent a scale of 10 to 100, in 10-unit steps. This scale was developed based on the psychophysical ratings of images reflecting increasing levels of bulbar hyperaemia, by clinicians, optometry students and administrative staff. On analysis, researchers found that practitioners preferred a more limited number of steps and found the abbreviated version (VBR 5) with five pictures (pictures 10, 30, 50, 70 and 90) exhibited a higher level of repeatability and reliability than the VBR 10 scale. The researchers were able to show a statistically significant difference in score between dry eye groups and control groups (127,

⁴ Permission obtained from Elsevier via the Copyright Clearance Centre, Inc. Please see Appendix A for details.

[129](#)). Schulze et al. found a change of +/- 20 units to be the clinically relevant change in grading steps based on the 95% confidence interval for their data ([127](#)).

Validated Bulbar Redness (VBR 10) Scale

© Schulze M, Jones D, Simpson T

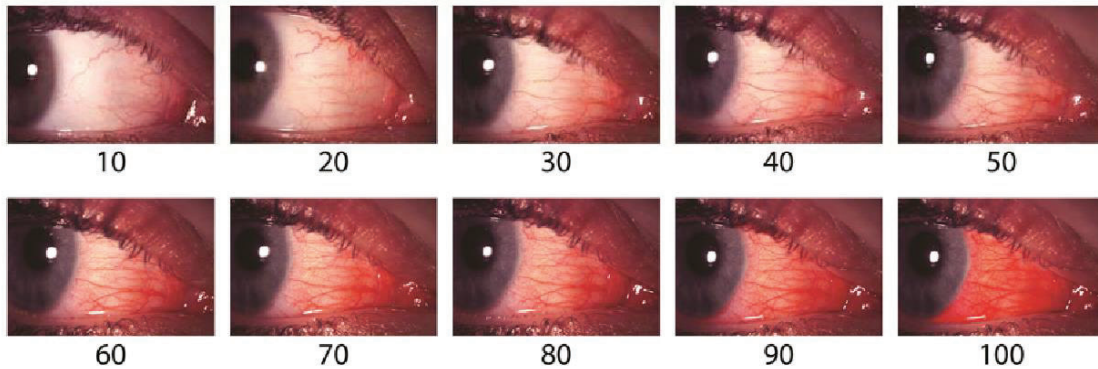


Figure 5. Validated Bulbar Redness (VBR10) scale consisting of 10 images.⁵

1.5.1.3 Brien Holden Vision Institute grading scale

The BHVI grading scale, previously known as the Cornea and Contact Lens Research Unit (CCLRU) scale and the Institute for Eye Research (IER) scale, is a photographic scale comprising four photos. It represents a range of redness from trace (1), through mild (2), and moderate (3), to severe (4). Studies comparing this scale to the Efron scale describe scores with the BHVI scale as consistently 0.6 steps higher on average than those with the Efron scale, which has five steps rather than four, highlighting risks associated with attempting to use different grading scales interchangeably.

1.5.2 Objective hyperaemia

Many studies have explored the benefits of assessing hyperaemia objectively, as automation offers the potential to minimise inter-observer variability ([126](#), [135](#), [136](#), [139](#), [140](#)). Image processing techniques such as thresholding, edge detection, smoothing, colour extraction, morphometry and densitometry have

⁵ The VBR5 scale consists of grades 10, 30, 50, 70 and 90 only. Permission obtained from Wolters Kluwer Health Inc. via the Copyright Clearance Center, Inc. Please see Appendix B.

been utilised in quantifying bulbar redness ([135](#)). The most consistent objective analytical technique has been shown to be edge detection and relative colour extraction, providing 16 times more reliable detection of change in bulbar redness than subjective hyperaemia grading ([134](#), [136](#)).

1.5.2.1 Oculus Keratograph ® 5M

The Oculus Keratograph ® 5M (Oculus K5M) device features proprietary software (R-scan) to quantify bulbar and limbal redness from a captured digital image of the anterior eye and provide a score, relative to the device's JENVIS scale, of between 0.0 and 4.0 in 0.1 steps. The captured digital image is taken *en face*, with the participant looking directly at the camera, and eyes opened widely. The software evaluates the exposed conjunctival areas, and thus considers predominantly the nasal and temporal quadrants. Although it is possible to image the superior and inferior conjunctiva via redirection of patient gaze and/or lid manipulation, the software currently does not offer a means of automatically grading hyperaemia images except those captured in primary gaze. The analytical process underpinning the redness quantification remains unknown, due to the proprietary nature of the software. Computerised grading like the Oculus K5M allows an objective measure of bulbar hyperaemia without the inherent variability associated with clinicians' subjective grading. A change of redness of +/-0.5 units was deemed to be a clinically relevant level of change in a study conducted by Schulze et al. according to the 95% confidence interval ([127](#)). A limitation of computerised grading is evident as the observed redness may be indistinguishable in hue, from the lid margins. Such challenges are more easily overcome in the clinical setting, where a clinician can request altered gaze direction or manually manipulate the conjunctiva to make such a distinction ([126](#)). *En face* measurements within the R-scan feature result in the analysis of a relatively small exposed area of bulbar conjunctiva. This may limit the ability to correctly differentiate redness in dry eye patients vs normal controls, where subjective grading has been shown to be discriminatory in differentiating disease from non-disease in a number of studies ([126](#), [127](#)). This is likely facilitated by the ability to view a larger conjunctival area, consistent with the real life clinical scenario where the clinician can alter patient gaze direction to reveal otherwise concealed areas of bulbar conjunctiva. It has been reported that although repeatable, the Oculus K5M R-scan tends to underestimate redness compared to subjective grading ([126](#), [127](#)).

1.5.2.2 Other objective measures

Downie et al. conducted a study to evaluate a new, simple method of evaluating bulbar hyperaemia ([126](#)). Their method was to take a digital *en face* image of the eye similar to that captured by the K5M, so that comparisons could be made. The group calculated the percentage of red channel activity relative to total channel activity (R+G+B) with image analysis software (Image J, National Institutes of Health, MD, USA). Values similar to the Oculus K5M R-scan values, led to a hypothesis that the R scan software uses a similar calculation method to generate its computerised redness score ([126](#)).

1.5.3 MMP-9 point-of-care testing

A rapidly applied, point-of-care test that evaluates total ocular surface MMP-9 ([93](#)) has been developed for use in clinical practice. The test was developed specifically to aid in the diagnosis of dry eye, following evidence that elevated levels of MMP-9 are found in tears of patients with dry eyes ([64](#), [85](#), [141](#)). The test is based on the principle of a lateral flow immunoassay. It is conducted by dabbing the sampling fleece along the inferior palpebral conjunctiva, then immersing it in the buffer provided, and clipping it into the test cassette. As the solution is absorbed along the test strip, MMP-9 molecules are captured by corresponding antibodies in the test region if present. The result is read after 10 minutes as positive or negative ([141](#)). The cut-off value for the InflammDry® (Rapid Pathogen Screening, Inc, Sarasota, FL, USA), indicating a clinically significant level of ocular surface inflammation, is 40ng/mL of MMP-9 ([83](#), [141](#)).

The ability to identify significant levels of MMP-9 in a clinical setting, avoiding the need for complex laboratory equipment and trained personnel, is convenient for clinicians and may help guide decision-making with regard to offering anti-inflammatory therapy ([93](#)). Contradictory evidence from published clinical studies exists with regard to the diagnostic utility of the InflammDry® point-of-care test for DED. Sambursky et al. conducted two (n=143 and 237) studies that reported positive InflammDry® results in over 80% of patients diagnosed with DED ([142](#), [143](#)). In contrast, Lanza et al. reported only 39% positive MMP-9 results out of those who had been diagnosed with DED (n=143) based on positive signs and symptoms. Similarly, Messmer et al. reported only 40% of their DED cohort displayed positive MMP-9

results with the InflammDry® ([83](#), [144](#)). It is important to note that diagnostic criteria used to classify patients as DED were inconsistent between these studies. A faint positive reading has been reported in individuals with MMP-9 concentrations of 30-40ng/mL, just below the cut-off value. Care is required in ensuring the fleece applicator is sufficiently wetted by tears, as an insufficient sample quantity of less than 5uL can also produce a false negative result ([51](#)). Another disadvantage of relying on MMP-9 as a DED biomarker is that MMP-9 is not specific to DED. It is present in a broad range of inflammatory conditions affecting the ocular surface, such as allergic conjunctivitis, recent ocular surgery or infection ([51](#)), therefore it is critical to differentially diagnose conditions presenting with a positive MMP-9 result.

Inflammation is an important factor in the pathogenesis of DED, however the failure to detect MMP-9 in every patient with DED has lead researchers to believe that either inflammation is not always present in DED or that the initiating pathways are different ([51](#), [83](#), [93](#), [142](#), [144](#), [145](#)). Based on the vicious circle of DED, inflammation contributes to the perpetuation of the disease process, however its prominence and its role may differ, depending on the underlying disease aetiology. For example, in autoimmune disease, a high level of circulating inflammatory mediators could serve as a key trigger of the vicious circle of DED in itself, in contrast to the situation in evaporative dry eye, where inflammation is understood to be a downstream consequence of having triggered the vicious circle via the failure of another homeostatic marker, such as tear instability secondary to lipid deficiency. The levels of inflammation observed in these two scenarios might reasonably be expected to differ, even in diseases of equivalent symptomatic severity. That ocular surface inflammation in severe ADDE from Sjögren's Syndrome would be expected to be more marked than that in severe MGD (EDE) is supported by previous research ([35](#), [54](#), [64](#), [66](#)).

1.5.4 Ocular Surface Staining

Two vital dyes, sodium fluorescein (NaFl) and lissamine green, are commonly used in the clinical setting to highlight damage of the ocular surface tissues. NaFl is an orange-coloured dye that fluoresces green under blue light. Compromised cells and areas of cell loss absorb NaFl more readily, appearing as punctate staining on the cornea. Lissamine green stains dead and devitalised cells that have damaged cell membranes, as well as cells that have damaged or missing glycocalyx. A minimal volume of fluorescein is instilled to avoid quenching and minimise the disruptive effects of fluorescein on the tear

film prior to its assessment. Staining the cornea and conjunctiva are useful in assessing severe DED; however, poor correlation with disease severity has been seen in mild-to-moderate DED (146).

1.5.4.1 Sodium Fluorescein staining

A lack of lubrication at the corneal surface in DED creates shear stress during blinking, which has been shown to worsen with disease severity (18). The loss of tight and adherens junctions in these epithelial cells, coupled with friction from the action of blinking, results in shedding of the epithelial cells. However, it remains difficult to distinguish whether sodium fluorescein staining represents a pool of dye in place of where cells have shed, rather than an increased permeability of an epithelial cell that is close to shedding and has undergone a reduction of its glycocalyx, leading to uptake of dye into the cell (18). A small amount of punctate epithelial staining is considered physiologically normal and occurs in 4-78% of the general population depending on the literature source (147). Staining of corneal punctate epitheliopathy in DED is often found on the inferior cornea, the ocular surface zone with the most prolonged exposure to the external environment. According to TFOS DEWS II diagnostic criteria, detecting >5 corneal spots of NaFl staining indicates homeostatic loss (2). Grading systems such as the Oxford grading scheme are utilised by clinicians to encourage consistency in grading (148). During the slit-lamp exam, visualisation of fluorescence is enhanced with a yellow barrier filter that should band pass at around 500 nm (149). This is recommended particularly when observing fine punctate staining of the cornea and conjunctiva (2).

1.5.4.2 Lissamine green staining

Staining taken up by conjunctival cells indicates damage to the cell membranes, irrespective of the presence of mucin (2). Conjunctival staining scores were evaluated by Yang et al. in 2019 using the Sjögren's International Collaborative Clinical Alliance (SICCA) grading system (150). Conjunctival staining scores were assigned after applying 1% lissamine green, along with grading scores for fluorescein staining of the cornea. Both scores were compared against the measurement of inflammation of the ocular surface, based on inflammatory cytokine gene expressions of IFN- γ , IL-6, IL-17 and MMP-9. All of the gene expressions were strongly correlated for conjunctival staining scores in both the non-SSDE and SSDE groups (150). The Oxford grading scheme (148) can also be used for subjectively grading the level

and distribution of conjunctival staining. The TFOS DEWS II diagnostic criteria includes the presence of at least nine conjunctival spots as a sign of ocular surface homeostasis loss (2).

Lid wiper epitheliopathy (LWE) is epithelial cell damage at the lid margin that can be visualised by staining with lissamine green dye. The staining pattern extends beyond the mucocutaneous junction (Marx's line) onto the palpebral conjunctiva in the 'lid wiper' zone that is in constant immediate contact with the globe. It has been proposed that LWE results from epithelial damage caused by friction between the globe and the upper and lower eyelids during blinking and gaze movements (18). Korb et al. found that 88% of patients who were symptomatic of DED exhibited LWE. Conversely, only 16% of asymptomatic controls showed staining in this region (151). The Korb grading scale is most commonly used to grade the degree of LWE; the cut-off value between normal and abnormal is grade 1 out of a scale range of 0 to 3. This is the equivalent of LWE which measures 2-4 mm in length and has a sagittal width of at least 25%-50%. The final LWE grade is determined from the average between horizontal length and sagittal width staining grades, recorded for the upper and lower eyelids independently. The presence of LWE in dry eye disease has been found to be six times greater than in a non-dry eye control group (151). A recent study by Wang et al. demonstrated that lid wiper epitheliopathy staining scores were a more sensitive discriminative marker of DED than corneal staining (152).

1.6 Anti-inflammatory treatment

As described in Section 2, inflammation is a critical component within the vicious circle and contributes to driving the self-perpetuating cycle of instability, hyperosmolarity, inflammation and ocular surface damage. Topical ophthalmic treatments are available to inhibit inflammatory mediators from activating and initiating further responses. These anti-inflammatory treatments inhibit the inflammatory cascades with the aim of restoring homeostasis of the tear film and ocular surface.

Current anti-inflammatory treatments are classified as either immunosuppressive agents such as corticosteroids, or immunomodulatory agents. Immunomodulatory agents include cyclosporine A, lifitegrast (LFA-1 antagonist) and tacrolimus. The role of essential fatty acids in combating dry eye disease continues to undergo evaluation through research (153-164). Investigations into the potential for targeted treatment involving inflammasomes are currently underway.

1.6.1 Corticosteroids

Topical corticosteroids have potent effects in inhibiting multiple inflammatory mediators and thereby interrupting the inflammatory cascade (165). Activation of acute-phase cytokines such as IL-1, TNF-alpha, MMPs, prostaglandins and phospholipase A is suppressed following the inhibitory action of corticosteroids on NFκB (165-167). Corticosteroids, therefore, inhibit multiple pathways of the inflammatory response mediated by T cells and B cells (168). In long-term use, their effects are predominantly at the genomic level, acting through the cytosolic glucocorticoid receptor (165). The reduction of leukocyte infiltration to the inflamed ocular tissues is another benefit of topical corticosteroids (166, 169). Unfortunately, while effective, corticosteroids have numerous side effects, and clinicians need to be assured that the benefit of treatment will outweigh the risk of side effects, when administering this treatment. The chronic nature of DED makes reliance upon corticosteroids problematic as a treatment of choice, due to the frequent need for long-term treatment.

1.6.2 Topical Cyclosporine A

Molecular effects of the application of topical cyclosporine A (CsA) include increased tear production, increased goblet cell density, inhibition of T cell activation and decreased transcription of IL-2 and IL-6 (170-173). The underlying mechanism of action is inhibition of the calcineurin-phosphatase pathway by intracellular complex formation with cyclophilin, but the subsequent clinical effect in DED is not fully understood (173, 174). A commercial preparation of cyclosporine is not currently available for topical human application in New Zealand. A clinical trial administering topical cyclosporine A to participants with moderate-to-severe dry eye showed a statistically significant improvement in symptoms such as intermittent blurring at four weeks of the trial. Objective signs such as improved Schirmer test values and reduced corneal staining were also consistent with this finding at 4 and 6 months, respectively (175). Ocular burning following instillation was found to be a common side effect in up to 20% of cases, while other issues included blurred vision, itching, conjunctival hyperaemia, foreign body sensation, stinging and discharge (168, 172, 176). Another limitation of topical CsA is that its effects can have a delayed onset of several months (175). A new CsA ophthalmic solution 0.09% has been recently approved in the

United States and was shown to significantly increase tear production following ten weeks of use compared to that in controls (177). The most common side effect was mild pain on instillation.

1.6.3 Lifitegrast

Blocking the binding of the intercellular adhesion molecule 1 (ICAM-1) to the lymphocyte function-associated antigen 1 (LFA-1) that is expressed only on lymphocytes is one proposed mechanism of action of lifitegrast (178). ICAM-1 is expressed on a variety of cells, including APCs and endothelial cells. Lifitegrast was approved by the US Food and Drug Administration (FDA) in 2016 and is available in Canada, the United States, Australia and six other countries, but not yet including New Zealand (165, 178, 179). It is proposed that by blocking the LFA-1:ICAM-1 interaction, activation of the adaptive immune response is prevented by stopping naïve dendritic cells from homing to lymph nodes and preventing activated T cells from migrating back to the conjunctiva (178). Research on dry eye models when exposed to desiccating stress have shown that the application of lifitegrast leads to no increase in pro-inflammatory cytokines such as IFN- γ , IL-1 β , IL-10, indicating that inflammatory cascades have been disrupted (180). Recently, a large multi-site study including 1429 participants concluded that lifitegrast ophthalmic solution 5.0% is favourable for treating moderate-to-severe signs and symptoms of DED (181). However, further research is warranted to investigate the exact mechanism of action of lifitegrast in the treatment of dry eye disease (168).

1.6.4 Tetracycline derivatives

Tetracycline derivatives such as doxycycline and minocycline are antibiotics used as a dry eye disease treatments. In the treatment of DED, they are typically used at a low dose, over an extended period, because they are used not specifically for their antimicrobial action, but more for their immunomodulatory role in suppressing lipases and inflammation (40, 182, 183).

Doxycycline inhibits the expression and production of MMPs 1, 3, 9, and 13 by human corneal epithelial cells (18). In addition it also assists in down-regulating the expression of pro-inflammatory cytokines IL-1 β , TNF- α (184). The mechanism of action for its anti-inflammatory effects involves scavenging reactive oxygen species and inhibiting phospholipase A2 activity (185, 186). No gold standard treatment regime

exists, but the dose concentration of the oral tetracycline derivative typically prescribed is 50-100mg daily, for up to 12 weeks ([182](#), [183](#), [187](#)).

1.6.5 Macrolides

Increasingly, oral azithromycin, a macrolide antibiotic, is used 'off-label' for therapeutic management of DED on the basis of its potent anti-inflammatory effects. Again, there lacks consensus on the optimal dose or dosing regime, but the dosage recommendation typically follows a 3 to 5-day course, for example with 500mg administered on the first day and 250mg per day on the 4 subsequent days. Azithromycin is popular with clinicians due to reduced reliance on patient compliance due to the short term nature of the course, as well as having fewer side effects and contraindications than doxycycline ([188](#)). This modality and standard antibiotic dose (100 mg twice daily, used in this study) doxycycline have been compared in a 1 month clinical trial with both showing significant improvement in symptoms of MGD, although the azithromycin showed a significantly better overall clinical response ([188](#)). An *in vitro* model suggested the mechanism of action relates to increased gland function, stimulation of lipid production and differentiation of meibomian gland epithelial cells ([189](#)).

Tacrolimus ointment, also known as FK506, is a potent immunosuppressant macrolide with a similar mechanism of action to topical cyclosporine A, such that it inhibits the T cell proliferation and activation pathways ([40](#)). As well as inhibiting IL-2 gene transcription by blocking calcineurin activation, tacrolimus also appears to inhibit cytokine receptor expression, reducing the cytokine-stimulated response of the imminent inflammatory cascade ([190](#)). Treatment with tacrolimus ophthalmic ointment has been demonstrated to be beneficial for ocular inflammatory conditions such as atopic conjunctivitis, Thygeson's superficial punctate keratitis, nummular adenoviral keratitis as well as in DED ([191](#)). In a recent investigator-masked, randomised controlled study by Moawad et al., both tacrolimus 0.03% eye drops and cyclosporine 0.05% significantly improved patient symptoms in the SS DED group compared to placebo control ([192](#)). No significant difference was found in efficacy between the two eye drops in this study.

1.6.6 Essential fatty acids

Essential fatty acids are precursors to immunomodulatory molecules naturally present in the body, such as thromboxane, leukotrienes, prostaglandins and prostacyclin. Ingestion of essential fatty acids by diet or dietary supplementation is necessary as the human body cannot synthesise these molecules. The balance of omega-6 and omega-3 is important and their interaction in inflammation remains incompletely understood (193). Omega-3, in all forms, is a precursor for anti-inflammatory mediators, whereas omega-6 is a precursor predominantly for pro-inflammatory lipid mediators (193), although omega-6 from specific, carefully chosen sources can be anti-inflammatory (194). A diet consisting of a high omega-3 to omega-6 ratio is beneficial as the presence of omega-3 inhibits the production of pro-inflammatory cytokines, tumour necrosis factors, prostaglandins and leukotrienes (195). Omega-3 fatty acids are abundant in marine and plant sources. The biologically active eicosapentaenoic acid (20:5 omega-3) and docosahexaenoic acid (22:6 omega-3), are both long-chain fatty acids present in fish oils. Plant omega-3 is a shorter chain fatty acid (alpha-linolenic acid (18:3 omega-3), and the ability of the human body to convert it to eicosapentaenoic acid is inefficient relative to its ability to convert omega-3 from marine sources (196).

Research on the effect of the administration of essential fatty acid supplementation on reducing the signs and symptoms of dry eye disease has shown positive outcomes (197-199). In as little as 30 consecutive days of oral omega-3 supplementation, signs and symptoms of dry eye disease improved, with better tear film stability and increased tear secretion (159). Similarly, a more extended 90-day clinical trial with the administration of oral omega-3 supplementation derived from fish oil and krill oil resulted in reduced tear osmolarity and increased tear stability in patients with mild-to-moderate DED (156). Of interest, the group given krill oil supplementation showed decreased levels of IL-17 in the tear film, suggesting that krill oil has superior anti-inflammatory properties to fish oil (156).

Contradictory evidence regarding omega-3 benefits has arisen from the Dry Eye Assessment and Management Study Research Group (DREAM), a large, multicentre, double-blind, randomised one-year clinical trial comparing omega-3 supplementation at the highest safest dose to humans (3000mg of fish-derived n-3 eicosapentaenoic and docosahexaenoic acid) to refined olive oil as a control. The authors reported no difference in ocular surface parameters and dry eye symptoms and signs in patients with moderate-to-severe dry eye disease relative to the placebo group (161). The DREAM group conducted

an extension study to assess differences in ocular surface parameters related to DED and found the group who discontinued omega-3 supplementation did not have significantly worse outcomes than those who continued omega-3 supplementation for a further 12 months (158). Further research is required to explore the optimal dosage and duration of supplementation required in order to best advise eye care professionals and the public in regard to the anti-inflammatory properties of omega-3 supplementation in treating DED (200).

Omega-6, despite being widely recognised as a precursor for pro-inflammatory mediators, has been shown in specific forms, to improve DED symptoms through the anti-inflammatory properties of gamma-linoleic acid and its precursor linoleic acid. These molecules are found in evening primrose oil and borage oil, and supplementation has been shown to decrease signs of ocular surface inflammation and improve DED symptoms(153, 155, 160, 163).

1.7 Aims and hypothesis

Dry eye disease is a complex condition, with inflammation central to the self-perpetuating, pathophysiological vicious circle. However, dry eye signs and symptoms often do not align, and not all patients with DED present with clinically significant levels of inflammation. This presents challenges for the clinician in deciding when it might be appropriate to initiate anti-inflammatory treatment. While sensitive laboratory-based assays such as PCR have shown MMP-9, IL-8 and IL-1 β to be elevated inflammatory biomarkers in DED, evidence-based recommendations for an accessible method for detecting clinically significant inflammation in everyday clinical settings do not yet exist. In the absence of a gold standard to clinically measure ocular surface inflammation, clinicians typically assess bulbar hyperaemia as a proxy measure of inflammation. A wide variety of subjective and objective scales are in use, yet little is known about the degree to which these can be used interchangeably. More recent developments include point-of-care immunoassays and computerised software that reportedly provide clinically useful assessments of inflammation.

The aims of this observational study were three-fold:

1. To test clinical proxy measures of inflammation relative to laboratory-based measures of inflammation. Specifically, we sought to evaluate one objective measure of hyperaemia (Oculus K5M

R-scan); three subjective hyperaemia grading scales (Efron, BHVI and VBR-5); ocular surface staining (graded using the Oxford scale); the InflammDry® point-of-care immunoassay; and the Ocular Surface Inflammation Evaluation test⁶ (OSIE®, Tearcheck®, ESW-Vision, France), against ex-vivo levels of MMP-9, IL-8 and IL-1 β determined by ddPCR analysis from conjunctival impression cytology samples

2. To explore the predictive ability of clinical tests and dry eye disease markers in identifying ocular surface inflammation according to MMP-9, IL-8 and IL-1 β levels
3. To assess the inter-observer and intra-observer variability of clinical bulbar hyperaemia grading scales and their agreement with objective hyperaemia grading

The primary outcomes were correlation values, predictive values, diagnostic cut off values, as well as sensitivity and specificity values for the various clinical tests.

Exploration of whether a differential inflammatory response according to DED subtype could be demonstrated was proposed as a secondary outcome contingent on the ability to recruit adequate numbers of participants with distinct evaporative and aqueous deficient dry eye phenotypes.

1.7.1 Hypotheses

1. The presence of ocular surface inflammation is associated with DED severity as assessed by TFOS DEWS II diagnostic testing.
2. Subjective clinical grading of hyperaemia can be used to predict levels of ocular surface inflammation as confirmed by laboratory analysis.
3. Subjective clinical grading of hyperaemia correlates with automated objectively graded hyperaemia.
4. A point-of-care immunoassay is an effective screening tool for identifying ocular surface inflammation, as confirmed by laboratory analysis.

⁶ The company ESW Vision have altered the Ocular Surface Inflammation Evaluation Ocular Surface Inflammation Risk Evaluation over the duration of this thesis.

Chapter 2. Methods

2.1 Participants

The study was approved by Auckland Health Research Ethics Committee (reference number 22183) and conducted within the Department of Ophthalmology research rooms in the University of Auckland Eye Clinic. A minimum of 47 participants was required for this study based on power calculations conducted using NCSS PASS version 16 to detect an association of $r \geq 0.40$ between clinical and laboratory markers of inflammation at 80% power ($\beta=0.2$) and a two-sided statistical significance level of 5% ($\alpha=0.05$).

Recruitment of participants was conducted via social media advertisement to volunteers in the Auckland region. Due to the impact of COVID-19 lockdowns, followed by restricted clinic and laboratory access, participants were pre-screened over the phone to check for COVID-19 related symptoms prior to an in-person consultation. During this phone call, the investigators also checked that the patient had read the Participant Information Sheet, and offered the opportunity to discuss any concerns.

Written informed consent was obtained from 53 participants who were allowed sufficient time to thoroughly read the participant information sheet (Appendix C: Study participant information sheet) form that explained the study purpose, outcome measures, data privacy, inclusion/exclusion criteria and study safety. All willing participants over the age of 18, with or without dry eye were included in this study. Participation was excluded in the event individuals were not willing or able to temporarily withhold the use eye drops, or refrain from contact lens wear or warm compress use prior to the study visit. Participants were also excluded if they had a recent history of eye surgery in the past three months, the presence of any ocular disorder or condition which could affect study results, non-normal lid architecture preventing lid closure or the current use of punctal plugs. Any questions were answered, written consent was provided Appendix D: Study consent form. The original signed consent form was retained, independently of the data and a copy was provided for participants.

Participants were required to avoid contact lens wear a minimum of 48 hours prior to the appointment, and refrain from the use of artificial tears and medicated eye drops at least 24 hours prior to the appointment. A dry eye diagnostic workup as informed by TFOS DEWS II (2) and outlined in Table 2 was

conducted on the right eye, along with additional testing to permit subsequent evaluation of ocular surface inflammatory markers.

2.2 Symptomology

The participants were asked to complete two symptom questionnaires, the Ocular Surface Disease Index (OSDI) ([201](#)) and the Dry Eye Questionnaire (DEQ-5) ([202](#)) at the start of the session. It was explained that all quality-of-vision related questions should be answered assuming the use of their personal vision correction spectacles, in order to distinguish dry eye related vision problems from uncorrected vision issues. A score of ≥ 13 was deemed a positive dry eye symptomology score for the OSDI. The DEQ-5 required a score of ≥ 6 to be considered positive.

2.2 Clinical measurements

Ocular surface measurements were performed in order from least to most invasive during the single clinical visit as outlined in Table 2 ([203](#)). The first non-invasive clinical measurements were conducted with the aid of the Keratograph 5M (K5M; Oculus Optikgeräte GmbH, Wetzlar, Germany). Measures included tear meniscus height, non-invasive Keratograph tear break-up time (NIK BUT), lipid layer grade and bulbar hyperaemia grade.

Table 2. Testing order of ocular surface characteristics.⁷

Order	Test name	Instrumentation
1	Tear meniscus height	Keratograph 5M (Oculus, Germany)
2	Non-invasive tear break-up time	Keratograph 5M (Oculus, Germany)
3	Lipid layer grade	Keratograph 5M (Oculus, Germany)
4	Bulbar redness grading (objective automated)	Keratograph 5M (Oculus, Germany)
5	Tear osmolarity (higher value of the two eyes and interocular difference)	TearLab® Osmolarity System, (TearLab, USA)
6	Bulbar redness grading (subjective)	Slit lamp biomicroscope
7	Meibum expressibility and quality	Slit lamp biomicroscope
8	Corneal and conjunctival staining	Slit lamp biomicroscope
9	Ocular surface inflammation evaluation; OSIE®	TearCheck® (ESW-Vision, France)
10	Meibography	Keratograph 5M (Oculus, Germany)
11	In-office MMP-9 measurement	InflammaDry®, (Quidel, USA)
12	Impression cytology	EYEPRIM® (Opia, France)

⁷ Abbreviations: MMP-9=Matrix metalloproteinase

2.2.1. Tear meniscus height

An ocular surface image, encompassing the lower tear meniscus, was captured under infrared illumination to minimise the risk of reflex tearing from a direct bright white light. The height of the tear meniscus relative to the lower eyelid margin was measured with the aid of the digital callipers in the assessment screen (2). Three measurements were taken within ± 1 mm of the pupil centre, and the average calculated.

2.2.2. Tear film stability

Automated first non-invasive Keratograph break-up time (NIK BUT) was measured under infrared illumination using the proprietary Oculus software which detects distortion in the reflected placido mires. The average of three separate NIK BUT measurements was recorded (2).

2.2.3. Lipid layer evaluation

Tear film lipid layer grade was assessed interferometrically. A 10 to 15 second video of the lipid layer of the right eye was recorded using the K5M under 1.4x magnification and white light illumination. The camera was focused on the tear lipid layer, and the participant was requested to blink intermittently to capture the post-blink movement of the lipid pattern. The patterns visible relate to the thickness of the lipid layer, which were graded according to their appearance against the ordinal modified Keeler-Guillon scale from 0 to 5, where 0 is a non-visible (absent) pattern, 1 is open meshwork, 2 is closed meshwork, 3 is a flow pattern, 4 is amorphous and 5 shows coloured fringes. Abnormal coloured fringe patterns are assigned a grade of 0 for statistical purposes to reflect the comparable non-inhibitory nature of such a lipid layer to an absent lipid layer (1, 26).

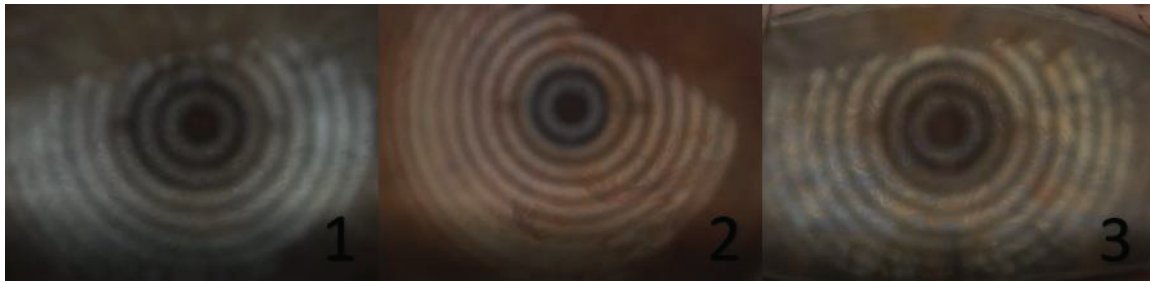


Figure 6. Lipid layer patterns.⁸

2.2.4. Bulbar conjunctival hyperaemia

2.2.4.1 Automated bulbar hyperaemia

Automated bulbar conjunctival redness was assessed using the, proprietary R-scan software of the Oculus K5M which provides an automated quantification of nasal and temporal bulbar conjunctival redness. Nasal and temporal limbal redness, as well as the overall redness of the bulbar conjunctiva were also recorded.

2.2.4.2. Subjective bulbar hyperaemia

A slit lamp biomicroscope (Takagi, Japan) was used to visualise the nasal, temporal, inferior and superior bulbar conjunctiva. The clinician graded the severity of hyperaemia by comparing vascularity and overall eye redness levels to the Efron and VBR5 scales. A clinical impression of hyperaemia, commonly reported in ophthalmic settings where no validated grading scale is in use, was also recorded as 'none', 'mild', 'moderate' or 'severe'.

2.2.5. Tear osmolarity

Tear osmolarity was measured using a clinical osmometer (TearLab, California, USA), the probes for which were calibrated daily, prior to taking measurements, using dedicated calibration cards. For every tear fluid osmolarity measurement, a new disposable test card was used. As a safety precaution,

⁸ Left (1) image is a closed meshwork pattern (grade 2), centre (2) image shows coloured fringes (grade 5) and the right (3) image shows abnormal coloured fringes. Gradings are performed from video recordings on account of the dynamic nature of this tear film characteristic.

participants were requested to gaze supero-nasally, during sample collection from the inferior meniscus. Osmolarity was measured in each eye in turn by dipping the tip of a disposable test card into the lower lateral meniscus without making contact with either the ocular surface or lid margin. The higher value and interocular difference were recorded to enable dry eye diagnosis (2).

2.2.6 Meibomian gland expressibility

The Meibomian Gland Evaluator (MGE) was applied in order to grade the expressibility of five adjacent meibomian glands in each of the temporal, central and nasal regions of the lower eyelid. The total number of glands expressed out of five for each of the three areas (providing a total score out of 15) was recorded using the Meibomian Glands Yielding Liquid Secretion (MGYLS) score (204), and the expressed meibum quality grade was also recorded using the grading scheme described in Bron et al. (205).

2.2.7. Ocular surface integrity

A minimal amount of sodium fluorescein from a strip (BioGlo™, Madhu Instruments, India) wetted with saline, and shaken to remove excess fluid, was applied to the far temporal bulbar conjunctiva (2). Corneal staining, under blue slit lamp illumination and with the aid of a yellow barrier filter, was graded after one to three minutes after instillation (2). Grades between 0 and 5 according to confluence, against the Oxford Grading Scheme for each of five corneal regions (central, superior, inferior, nasal and temporal) were assigned to provide a total score out of 25 corresponding to a score out of 5 for each zone (148).

Lissamine green (LG), was subsequently applied from a wetted strip (GreenGlo™, HUB Pharmaceuticals, USA), by allowing at least 10 seconds for the LG to elute from the strip and then applying a generous amount to the inferior temporal tear meniscus without touching the eye (2). Between 1 and 4 minutes after instillation, conjunctival punctate staining was assessed for confluence under diffuse white light against the Oxford grading scheme (148) to give a score out of 30 for three nasal and three temporal zones. Lid wiper epitheliopathy of the lower and top eyelid margin was also graded according to Korb's grading scale (Table 3) (206). Upper and lower LWE scores were calculated as the average of the corresponding horizontal and sagittal scores.

Table 3. Korb's grading scale for lid wiper epitheliopathy (206).

Grade	Horizontal length of staining (mm)	Sagittal height of staining (%)
0	<2	<25
1	2-4	25-50
2	5-9	50-75
3	>10	>75

2.2.7.1 Ocular Surface Inflammatory Risk Evaluation (OSIE®)

A additional small amount of sodium fluorescein from the BioGlo™ strip was applied to the far temporal bulbar conjunctiva. After two minutes, as recommended by the manufacturer, the Ocular Surface Inflammatory Risk Evaluation (OSIE®) test on the Tearcheck® device was undertaken. An image under blue illumination was obtained and the area of interest manually defined by digitally outlining the interpalpebral zone within the lid margins (Figure 8). Based on this defined area, the proprietary software calculates an inflammatory risk score.

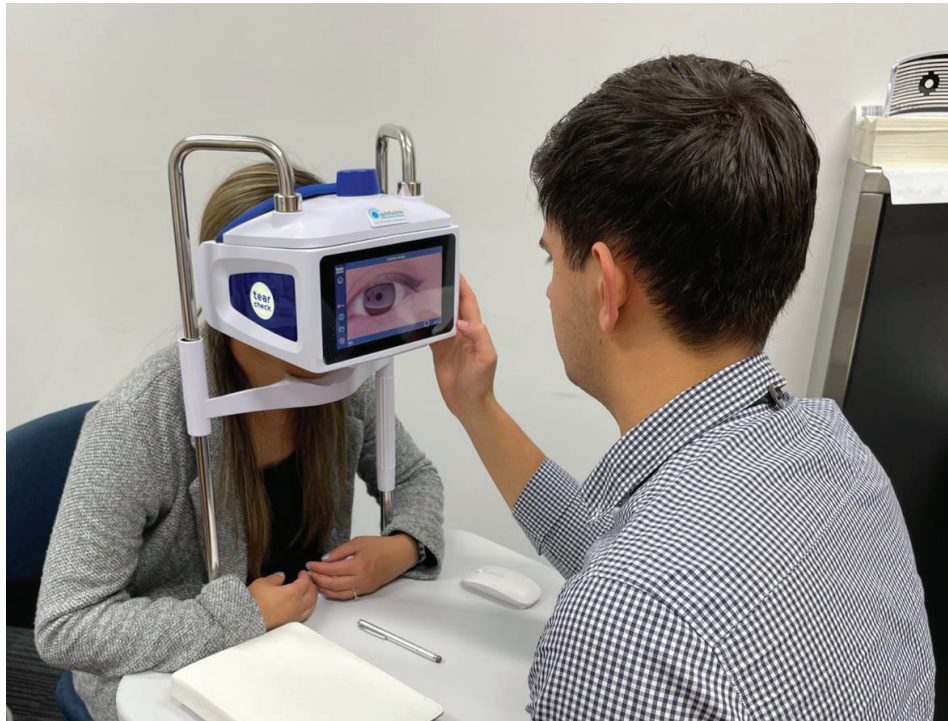


Figure 7. Tearcheck® device in use.

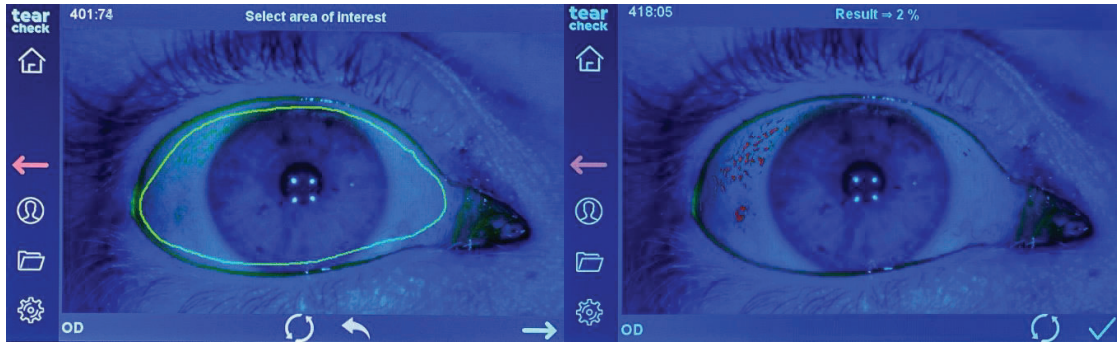


Figure 8. OSIE® assessment screen.⁹

2.2.8 Meibomian gland morphology

Meibomian glands within the upper and lower eyelid were assessed by infrared meibography on the Oculus K5M, and percentage gland dropout was graded by estimating coverage of the everted tarsal areas by meibomian glands (seen as white structures against a dark background) and assigning a grade of between 0 and 4 according to Pult's Meiboscale Table 4 (207). The degree of gland loss is estimated by evaluating the percentage area devoid of meibomian glands (dark areas), relative to the tarsal area that would be expected to house glands.

Table 4. Pult's Meiboscale grading values and corresponding percentage meibomian gland loss

Grade	Degree of gland loss
0	0% (no gland loss)
1	≤25%
2	26%-50%
3	51%-75%
4	>75%

⁹ The left image shows how the area of interest is manually selected within the interpalpebral area of the open eye, avoiding the inferior and superior tear meniscus as per the manufacturer's instructions. The right image shows the result given, and the red areas appear to be the 'inflammation' areas identified and calculated by the proprietary software.

2.2.9 In-office ocular surface MMP-9 assessment

A measure of clinically significant ocular surface inflammation was obtained with the InflammaDry® test (Quidel, USA). The test kit comprises three components: a sample collector, a test cassette, and a buffer vial [0.1% Sodium Azide]. Following the manufacturer's instructions, the lower eyelid of the right eye was everted to expose the tarsal conjunctiva, and the fleece portion of the sample collector applied to the conjunctival surface three times, for 3 - 5 seconds each time, to obtain test samples from the nasal, central and temporal portions. The collection device containing the sample was immediately inserted into the test cassette and the cassette uncapped, to allow the exposed absorbent tip to be submerged into the buffer vial for 20 seconds. The cassette was then re-capped and placed on a flat surface for a timed period of ten minutes. Presence of a 'control line' appearing as a blue line in the control zone, confirmed validity of the test results. In the case of a sample MMP-9 level exceeding 40 ng/mL, a red line would become visible in the test result zone. All complete and incomplete red lines were interpreted as positive as per the manufacturer's recommendation (141). The absence of a red line was interpreted as a negative result, indicating an MMP-9 level below the pre-set cut-off of 40 ng/mL.



Figure 9. The InflammaDry® test.¹⁰

¹⁰ The left image depicts from left to right, the sample collector, the test cassette and the sample buffer. The right image shows sample collection from the inferior palpebral conjunctiva.

2.2.10 Laboratory inflammatory marker analysis

The EYEPRIM™ conjunctival impression device (OPIA Technologies, France) was applied to collect samples by impression cytology [IC], from the superior temporal region of the bulbar conjunctiva. The single-use sterile EYEPRIM™ device was chosen as the preferred collection method due to its ease of use in clinic over other methods such as the Millicell®CM 12 mm diameter, 0.4 µm culture plate insert (Millipore Corp™), which required modification before sample collection ([208](#)).

2.2.10.1 Laboratory preparation

Immediately prior to the clinical appointment, an RNase-free Eppendorf tube containing 1 mL of TRIzol® reagent (ThermoFisher Scientific) was prepared and transported at 4 °C within a chilled polystyrene box, containing an ice block.

2.2.10.2 Clinical area preparation

A designated RNase-free bench area was prepared by wiping it down with RNaseZap™ RNase Decontamination Solution. The clinician wore neoprene gloves (Micro-Touch® Affinity™, Ansell) to protect the skin from contact with TRIzol® as it is a caustic reagent. The rack containing the TRIzol® tube, the packaged EYEPRIM™ device and forceps were wiped down with RNaseZap™ and placed in the designated bench area.

2.2.10.3 Sample collection by impression cytology

The right eye was anaesthetised with one drop of oxybuprocaine hydrochloride 0.4% topical anaesthetic (Benoxinate eyedrop minims, Bausch & Lomb, USA). The participant was instructed to look infero-nasally to expose the superior temporal bulbar conjunctiva of the right eye. The EYEPRIM™ was used to collect the impression cytology sample by depressing the trigger gently and pressing the exposed membrane on the supero-temporal conjunctiva for three to five seconds. The membrane was then slowly removed from the eye and forceps were used to remove the membrane from the device for immediate placement into TRIzol®. The closed tube was immediately returned under refrigerated conditions back to the laboratory. Once in the laboratory, the collection tube was vortexed for 10 s, centrifuged for 15 s then stored in the -80 °C freezer until analysis.

2.3 Laboratory analysis

2.3.1 Ribonuclease-free environment

RNA is easily degradable by ribonucleases (RNase) present in the environment, such as the workbench surfaces and human skin (209). To maintain an RNase-free environment when collecting and analysing the ribonucleic acid (RNA) genetic material extracted from impression cytology (IC) samples, RNaseZap® (Thermo Fisher Scientific) was applied to all work surfaces and the clinician's gloves to limit risk of exposure of the IC samples to RNases in the environment. During laboratory analysis, RNaseZap® was applied to all workbench surfaces, tube racks, and to gloves to mitigate sample contamination and degradation, and thereby maximise RNA yield. Disposable items such as filtered pipette tips and microcentrifuge tubes were certified RNase-free per the manufacturer's guarantee.

2.3.2 RNA purification

The impression cytology samples in TRIzol® were removed from the -80 °C freezer, defrosted, vortexed for 10 seconds, and centrifuged for 15 s to ensure no TRIzol® reagent remained on the lid. These TRIzol® lysates were coupled with the Phasemaker™ tube and PureLink® RNA Mini Kit (Ambion® by Life Technologies™) system to perform an on-column RNA purification. Phasemaker™ tubes were centrifuged at 16,000 x g for 30 s and the contents of the TRIzol® lysates transferred into the Phasemaker™ tubes within a fume hood. A negative control tube containing 1 mL of TRIzol® reagent without an impression cytology sample was used for each RNA purification run to confirm absence of RNA in purification reagents. All tubes were incubated for five minutes at ambient temperature to ensure dissociation of nucleoproteins, then 0.2 mL of chloroform was added to each tube for phase separation to occur. Tubes were vigorously mixed by hand and left to incubate for five minutes before the tubes were centrifuged for five min at 16,000 x g at 4 °C. The upper aqueous phase containing the RNA was then transferred carefully to a new tube in the fume hood. An equal volume of 70% ethanol made with RNase-free water was added to each microtube and mixed via inversion.

The entire volume was sequentially transferred to spin cartridges housed within collection tubes, in two steps of approximately 700 µl each and centrifuged at 12,000 x g for 15 s, discarding the flow-through each time into a beaker and blotting the collection tube on a clean tissue paper before reinserting the spin

cartridge. Following this, 350 μ L of wash buffer I was added to each spin cartridge now containing bound RNA, centrifuged as above, and the flow-through discarded and the collection tube blotted as before.

On column DNase-treatment was performed to remove any residual genomic DNA that may have carried through into the upper aqueous phase during the phase separation step. The PureLink™ DNase (Invitrogen™, Thermo Fisher Scientific) is provided in a lyophilised form requiring reconstitution with 550 μ L of RNase-free water, then frozen, in aliquots, in the -20°C freezer.

A separate preparation of PureLink™ DNase was required for on-column treatment, and was prepared according to the protocol outlined in Table 5.

Table 5. Constituents and relative proportions of the Purelink™ DNase treatment.

Reagent	Volume
10x DNase I Reaction Buffer	8 μ L
Resuspended DNase	10 μ L
RNase Free Water	62 μ L

A 78 μ L volume of PureLink® DNase mixture (Table 5) was pipetted into the centre of each spin cartridge and incubated for 15 min. Again, 350 μ L of wash buffer I was added to the spin cartridge and centrifuged at 12,000 x g for 15 s at room temperature. The collection tube containing the flow-through was discarded, and the spin cartridge inserted into a new collection tube.

Wash buffer II was reconstituted with 60 mL of 100% ethanol before use, then 500 μ L was added to the spin cartridge. This was centrifuged at 12,000 x g for 15 s at room temperature, the flow-through discarded, and the spin cartridge returned to the same collection tube. This step was repeated one more time. The spin cartridge and collection tube were centrifuged at 12,000 x g for one min to dry the RNA-bound membrane. The collection tube was then discarded, and the spin cartridge inserted into a recovery tube. Thirty microlitres of RNase-free water was added to the centre of the spin cartridge and left to incubate for 1 minute at room temperature. The combined tubes were centrifuged for one min at 16,000 x g at room temperature to elute the purified RNA. The spin cartridges were discarded, and the

recovery tubes capped and immediately placed on ice. If no further analysis was to be performed on this day, the purified RNA was stored at -80 °C.

2.3.3 Nanodrop for yield determination

The purified RNA was initially quantified using the NanoDrop™ Nucleic Acid Spectrophotometer (NanoDrop™ 2000C, Thermo Scientific), which measures the absorbance of the sample at a specified wavelength. The sample type was set to 'RNA 40 constant'. Before setting the blank value, the instrument pedestal was wiped on the top and bottom five times with clean tissue paper, and one µL of the same RNase-free water used to elute purified RNA was used for the zero-absorbance measurement. Then, 1 µL of purified RNA was pipetted onto the pedestal and analysed in duplicate, recording the concentration of RNA (ng/µL) for each sample. The averages of two consistent readings were then calculated and recorded.

2.3.4 Tapestation for RNA quality and quantity analysis

The 4150 TapeStation System (Agilent, United States) was used to determine RNA quality and ensure it had not degraded. It was also used to accurately determine quantification of the purified RNA. Unlike the NanoDrop™ which uses spectrophotometry to quantitate the RNA, the TapeStation system uses the principle of automated electrophoresis using the ScreenTape technology (Agilent, United States). The High Sensitivity RNA ScreenTape kit was used, which has a required concentration range between 500 and 10000 pg/µL.

To ensure the RNA concentration fell within this range, the NanoDrop™ data was used to calculate any required dilutions for the RNA where necessary. Checking the RIN value is important as RNA is easily degraded by RNases in the environment, leading to compromised results in sequential analysis ([210](#)). An RNA integrity number (RINe) of seven or above is considered to be undegraded RNA ([211](#)).

A volume of 2 µL of High Sensitivity RNA ScreenTape Ladder (Agilent, United States) was added to tube 1 of an 8-strip of 0.2 ml optical tubes and one µL of High Sensitivity RNA ScreenTape Sample Buffer (Agilent, United States) was added to the remaining tubes. Following this, 2 µL of purified RNA was pipetted into each tube. Tubes were capped, vortexed for one min and centrifuged at 2680 x g for one

min followed by heat-denaturation in a T100™ Thermal Cycler (Bio-Rad, USA) for three min at 72 °C. The heat denatured samples were then placed directly onto ice for two minutes, centrifuged for a further minute and placed into the TapeStation instrument for analysis. Again, a RIN value of over 7.0 ([211](#)) confirmed the RNA was undegraded and suitable for continuation to the SPUD assay. Samples that resulted in a concentration below the quantification threshold of the kit were excluded from further analysis.

2.3.5 Spud assay for confirming absence of PCR inhibitors

Inhibitors of PCR contained within the sample itself or from residual carryover of RNA purification reagents can interfere with accurate PCR-based quantification, justifying the use of the SPUD assay to ensure that RNA samples were free of inhibitors ([212, Vermeulen, 2011 #346](#)), thus minimising the risk of inaccuracies and false negatives in the final analytical stage. The SPUD assay is a quantitative PCR assay designed to amplify the phyB gene from potato (SPUD) template DNA in the presence of SPUD forward and reverse primers. All RNA sample concentrations were standardised to 5 ng/μL where possible by diluting concentrated RNA preparations with RNase-free water. RNA preparations with concentrations below five ng/μL were run without dilution, with the total sample volume containing RNA standardised to 19 μL.

The total reaction volume was 10 μL, and the constituents are outlined in Table 6. Two master mixes were prepared; a SPUD master mix and a no template control (NTC) master mix. The SPUD master mix volume was multiplied according to the number of reactions required; the no template control master mix included 3.52 μL of PCR water, excluding the SPUD template. For controls, a known inhibitor, heparin, was included, and PCR water was used in the case of the no inhibitory controls (NICs).

Table 6. Constituents and concentrations of the SPUD assay master mix.

Name	Stock concentrations	Final concentrations	Volume per 10 μ L reaction
SPUD Forward Primer	10 μ M	0.24 μ M	0.24 μ L
SPUD Reverse primer	10 μ M	0.24 μ M	0.24 μ L
LightCycler® 480 SYBR Green Master Mix (Roche, Switzerland)	2 x	1 x	5 μ L
SPUD template	1 x 10 ⁵ copies/ μ L	10,000 copies per reaction	0.1 μ L
PCR water			3.42 μ L

The reaction mixture was pipetted into a Rotor-Disc® 100 (Qiagen, Germany) tube ring containing 1 μ L of either RNA, water (for NIC), heparin or water (for NTC) and 9 μ L of the appropriate master mix to create a 10 μ L total volume reaction in each tube. All RNA samples were run in triplicate using the Rotor-gene 6000 (Qiagen, Germany). Cycling conditions are outlined in Table 7.

Table 7. PCR cycling conditions for the SPUD assay.

Step	Temperature ($^{\circ}$ C)	Time (min)
Polymerase activation	95	10
DNA denaturation	95	10 s
Primer annealing	55	15 s
Primer extension (acquiring data on green channel this step)	72	20
Repeat steps 2-4, 39 times (40 cycles in total)		
Melt analysis	72-95 (rising by 1 degree each step)	90 s first step 5 s each step afterwards

The melt curves were first examined to ensure a single SPUD amplicon, which is known to have a melt peak at 80 °C (212). Subsequently, a threshold line was set at the exponential amplification phase of the amplification curves to determine a cycle threshold value. The mean cycle threshold (Ct) values of the reactions containing RNA samples were compared to the NICs. If a Ct difference of less than one was observed, the RNA samples were deemed inhibitor free and could proceed to cDNA synthesis (212).

2.3.6 Complementary DNA (cDNA) synthesis

The purified RNA was reverse transcribed into cDNA in this step. The iScript™ gDNA Clear cDNA Synthesis Kit (Bio-Rad) was used due to its convenient preblended iScript Reverse Transcription Supermix included in the kit. The preblended mixture contains Monolevel murine leukaemia virus (MMLV) reverse transcriptase, dNTPs, oligo(dT), random primers and RNase inhibitor, eliminating the need to prepare a master mix, which has the benefit of ensuring consistency of the mixture. The protocol requires the addition of 4 µL of iScript Supermix to 16 µL of sample RNA (remaining from the previous 19 µL aliquoted for the SPUD assay (3 µL used) and 16 µL left for cDNA synthesis). The cDNA synthesis kit has the option of treating RNA samples with DNase prior to the cDNA synthesis, but this option was not used as a DNase-treatment was performed during the RNA purification process.

After adding the iScript Reverse Transcription Supermix to the RNA template, tubes were mixed, centrifuged for 15 s at 2680 x g, then placed in a Bio-Rad T100 thermal cycler for the cDNA synthesis reaction to proceed as described in Table 8.

Table 8. Thermal cycling conditions for cDNA synthesis

Step	Temperature (°C)	Time (min)
Priming	25	5
Reverse transcription	46	20
RT inactivation	95	1
Hold	4	Optional

All cDNA reactions were diluted to standardised RNA equivalent at 1 ng/μL before the β-actin PCR reaction.

2.3.7 β-actin PCR

To ensure the successful synthesis of cDNA, a standard PCR was run using beta-actin as the gene target. All RNA samples were also subjected to the same PCR run to check for genomic DNA contamination that could indicate false-positive results in the synthesised cDNA. The reagents and their concentrations used in this PCR experiment are outlined in Table 9.

Table 9. Constituents for the β -actin PCR reaction.

Reagent	Stock concentration	Final concentration	Volume per 25 μ L reaction
β -actin Forward primer	10 μ M	0.15 μ M	0.375 μ L
β -actin Reverse primer	10 μ M	0.15 μ M	0.375 μ L
dNTP's	10 mMol	0.2 mMol	0.5 μ L
MgCl ₂	25 mMol	1.5 mMol	1.5 μ L
PCR Water			18.45 μ L
Taq polymerase	5 U/ μ L	1.5 U/reaction	0.3 μ L
10x Buffer	10 x	1 x	2.5 μ L

Two master mixes were prepared to minimise the Taq polymerase enzyme activity at sub-optimal temperatures. Master mix 1 included the forward and reverse primers, dNTP's, MgCl₂ and milli-Q water making a total dispensed volume of 21.2 μ L per reaction, which was added first to each PCR tube, followed by 1 μ L of RNA, cDNA, water for no template control or 1 μ L of human corneal cDNA for the positive control. Finally, 2.8 μ L of master mix 2 containing the Taq polymerase enzyme and the 10x buffer was added to each tube to make a total reaction volume of 25 μ L per tube. The PCR reactions were mixed, centrifuged, and placed into the Bio-Rad T100 thermal cycler. The PCR was run using cycling conditions as outlined in Table 10.

Table 10. β -actin PCR cycling conditions.

Step	Temperature (°C)	Time (min:sec)
Initial denaturation	95	1:00
DNA denaturation	95	0:30
Primer annealing	55	0:30
Primer extension	72	0:30
Repeat steps 2-4, 35 times (total 35 cycles)		
Final extension	72	7:00
Hold	12	∞

2.3.8 β -actin gel electrophoresis

All the beta actin PCR reactions from the previous step were resolved on agarose gels by electrophoresis to separate and identify amplified β -actin PCR product. A 2% agarose gel was made by mixing 2 grams of Agarose powder and 100 mL of 1 x TBE (90 mM Tris, 90 mM Boric acid, 1 mM EDTA pH 8.0) in a conical flask, and heating it in a microwave for 30 secs at a time until the agarose was completely dissolved. The conical flask was weighed before and after heating to account for evaporative loss, and the difference in the volume restored with milli-Q water. Additionally, 0.5 μ L of GelRed® Nucleic Acid Gel Stain (Biotum) was pipetted into the dissolved 2% Agarose gel mixture and gently swirled to uniformly distribute the stain. A gel tray was prepared with a 1.5 mm, 20-well comb. The liquid Agarose mixture was poured into the gel tray and left to solidify at room temperature for 15 mins. After solidification, the gel comb was removed, and the gel tray was placed into an electrophoresis tank and filled beyond the top of the gel with 1 x TBE solution, ensuring the gel was fully submerged.

To allow identification of the separated DNA bands, 5 μ L of 1 Kb Plus DNA ladder (ThermoFisher™, USA) was loaded to the first and last well of every row. A strip of Parafilm M® was taped to the bench,

and approximately 1 μ L droplets of 10 x Bromophenol blue loading buffer (1% Sodium-dodecyl sulfate, 50% glycerol, 0.05% Bromophenol blue) was aliquoted onto the surface with even spacing. A volume of 10 μ L of each PCR product was pipetted up and mixed with an individual loading buffer droplet by pipetting up and down, avoiding air bubbles and pipetted into the assigned well of the gel. The electrophoresis tank was connected up to the power supply, set to run at 100 volts for a minimum of 80 min or until the bromophenol blue dye front had migrated two-thirds of the way along the length of the gel. Once the electrophoresis was complete the gel was imaged using the ChemiDoc™ MP Imaging System (Bio-Rad) on the GelRed setting. Any RNA samples that yielded an amplicon with beta-actin PCR, suggesting incomplete removal of genomic DNA and cDNA synthesis was repeated for these RNA samples with an additional DNase-treatment step as described in

Table 11.

Table 11. Thermal cycler conditions for additional DNase treatment of gDNA* contaminated RNA.

Step	Temperature (°C)	Time (min)
DNA digestion	25	5
DNase inactivation	75	5
Storage conditions	4; ice	

*Genomic DNA (gDNA)

2.3.9 Droplet Digital PCR

Droplet digital PCR (ddPCR) was conducted using the QX200 Droplet Digital PCR System (Bio-Rad) on the successful samples that showed adequate RNA quality and quantity, and were negative for inhibitors in the SPUD assay, and absence of B actin amplification in the RNA and positive B actin amplification in the synthesised cDNA ([121](#)). This was chosen as the method of final quantitation analysis for the genes

of interest due to greater precision, smaller sample requirement and the ability to detect smaller differences of one to two-fold with ddPCR, than quantitative PCR (qPCR) can offer (213).

The three genes of interest (MMP-9, IL-8, IL-1 β) along with seven reference genes (POLR2A, PPIA, HPRT1, B2M, TBP, GUSB, RPLP0) were analysed. Where possible, one gene of interest and one reference gene assay were multiplexed, while all remaining reference assays were run individually. The NTC for this assay was PCR water, and the positive control used was DNA from a human corneoscleral rim (NZ Eye Bank, New Zealand). The plate was covered with a silicone seal and centrifuged for 2 minutes at speed 480 x g.

Table 12 shows the single reaction composition. The individual reaction components were multiplied by the number of required reactions to make up the master mixes. In a single-plex reaction, the missing volume for the lack of either a gene of interest assay or reference assay in the reaction, was made up with extra PCR water. The master mixes were prepared for the number of required reactions and 20.9 μ L pipetted into tubes of a 96-well PCR plate using the QIAgility pipetting instrument (QIAGEN) to reduce pipetting error and contamination. This was followed by pipetting of 1.1 μ L of cDNA (or PCR water for the no template controls) to each tube as appropriate. The plate was covered with a silicone seal and centrifuged for 2 minutes at speed 480 x g.

Table 12. Master mix constituents for ddPCR.

Reagent	Per 22 μ L ¹¹ reaction
Gene of interest assay	1.1 μ L
Reference assay	1.1 μ L
ddPCR Supermix for Probes (No dUTP) (Bio-Rad, USA)	11 μ L
PCR water	7.7 μ L

¹¹ Each 22 μ L reaction included 1.1 μ L of cDNA, or PCR water for the NTC in addition to the tabulated components.

Droplet generation was conducted by transferring 20 μ L of each reaction mix and 70 μ L of droplet generation oil to the appropriate wells of disposable DG8™ droplet generation cartridges. The cartridge was covered with a DG8™ Gasket and placed into the QX200 droplet generator. Following this, 40 μ L of generated droplets were then transferred into the appropriate wells of a ddPCR 96-well PCR plate. Once all the samples were processed, the test plate was heat-sealed using a pierceable foil seal and the PCR run on the C1000 Touch™ Thermal Cycler using the programme outlined in Table 13.

Table 13. PCR Cycling conditions for the ddPCR reaction.

Step	Temperature (°C)	Time (min:sec)
Enzyme activation	95	10:00
DNA denaturation	94	0:30
Primer annealing and extension	60	1:00
Repeat steps 2-3, 39 times (total 40 cycles)		
Enzyme deactivation	98	10:00
Hold	12	Infinite

The completed PCR reaction plate was subsequently placed into the QX200™ Droplet Reader to quantify positive and negative droplets; all the wells were programmed with the name of the gene of interest and reference gene to be quantified using the Quantasoft software.

When checking the results, a minimum of 10,000 droplets present for each well and a zero result for the NTC was required for a result to be valid. For each test, a threshold line was manually set between the positive and negative droplets in order to quantify the gene of interest (GOI) or reference gene (REF) present in each reaction. This confirmed the number of gene copies per μ L. The threshold was set at 3000 (units) for uniformity across all measurements.

2.3.10 Controlling for inter-run variability

Inter-run variations were accounted for using an internal calibrator, processed for every gene target in every ddPCR reaction plate, using cDNA synthesised from human corneoscleral rim (NZ Eye Bank, New Zealand). Data were standardised to a cDNA concentration of 1.1 μL in a 22 μL reaction. To account for any inter-run variability, the final gene expression quantities were standardised by dividing by the quantity result of the corneal cDNA. This was to allow for direct comparison of all samples from different reaction plates.

2.3.11 Repeats and losses

There were four reasons why samples might require repeat analysis in this study.

1. The reaction did not meet the minimum 10,000 droplet threshold to give an accurate result.
2. The NTC was positive indicating external contamination.
3. The result was valid but was zero, therefore it was repeated with a greater input of cDNA from 1.1 to 3.3 μL . If 3.3 μL of cDNA did not remain, the total remaining amount was used to repeat the run and the final concentration was calculated accordingly.
4. The upper quantity limit for accuracy is 5000 copies/ μL (as recommended by the manufacturer), so for B2M where there were many reactions producing quantities over 5000, the cDNA was diluted and the analysis repeated in order to obtain a result within the accurate quantitative range of the assay/instrument. These values were then adjusted for the dilution factor in order to compare with the other reactions that were not diluted.

2.3.12 Normalisation of data

NormFinder software (MOMA, Denmark) ([214](#)) was used to identify the most stably expressed and thus optimal normalisation reference genes within Microsoft Excel. The data were grouped into DED and nonDED diagnoses when undergoing NormFinder analysis ([2](#)). Normfinder was used to determine the best combination of two reference genes for normalisation. The geometric means of these two reference

genes for each cDNA sample were used to calculate a normalisation factor. All the results for MMP-9, IL-8, and IL-1 β were divided by the normalisation factor for each cDNA sample to generate calibrated normalised expression values which were used for all subsequent analyses reported within this thesis.

2.4 Dry eye diagnosis

This research project applied the consensus dry eye disease diagnostic criteria published by TFOS DEWS II in making a dry eye diagnosis, thus requiring the presence of signs and symptoms. The TFOS DEWS II Diagnostic Methodology report defined dry eye disease as requiring a positive symptom score combined with at least one positive marker indicating the loss of ocular surface homeostasis (2). Participants were considered positive for symptoms on the basis of their score on one of two validated dry eye questionnaires, the OSDI (score ≥ 13) (202) or the DEQ-5 (score ≥ 6) (201). In addition to positive patient symptomology, a positive marker for loss of homeostasis was also required, as indicated in Table 14.

Table 14. Dry eye diagnostic criteria as defined by the TFOS DEWS II Diagnostic Methodology report (2).¹²

Symptomology (1 of the following)	Homeostasis Markers (1 of the following)
DEQ-5 ≥ 6	Non-invasive tear breakup time <10s
OSDI ≥ 13	Osmolarity; ≥ 308 mOsm/L in either eye or interocular difference > 8 mOsm/L Ocular surface staining; >5 corneal spots, > 9 conjunctival spots or lid margin [≥ 2 mm length & $\geq 25\%$ width]

¹² A positive symptom score and a positive result for at least one homeostatic marker is required to make a dry eye diagnosis.

After a dry eye diagnosis was made, subclassification into aqueous deficiency, evaporative dry eye and mixed aetiology was made. ADDE was deemed to be present if the average TMH measured less than 0.20mm (2) A lipid layer grade of ≤ 3 (1) on the modified Guillon-Keeler grading scheme or expressed meibum quality grade of ≥ 1 (1) were used to guide EDDE subcategorization. Mixed DED was present in cases where both the criteria for ADDE and EDE were met.

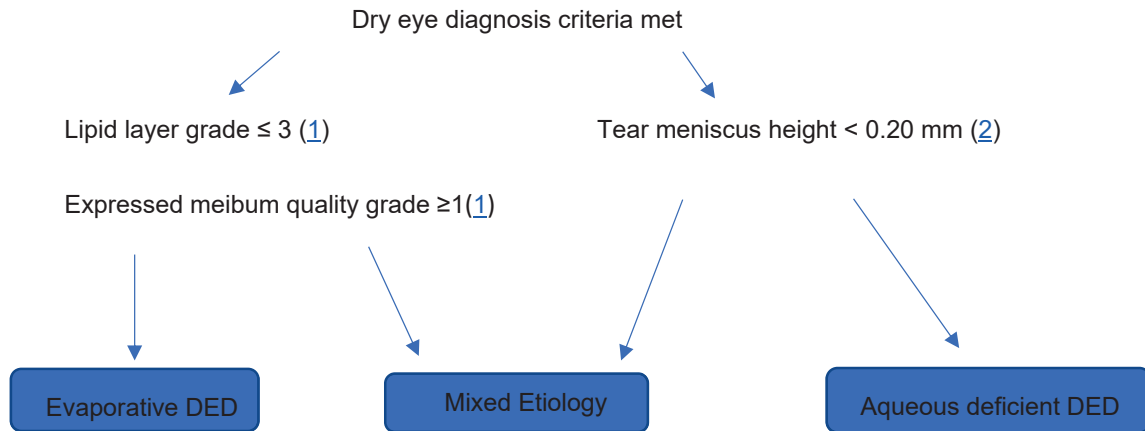


Figure 10. Subclassification criteria for evaporative, aqueous deficient or mixed etiology dry eye disease (2).

2.5 Statistical analysis

Statistical analyses for Chapter 3 were performed using GraphPad Prism 9.3.0 (GraphPad Software, San Diego, California). Inter-observer reproducibility was assessed using grouped column analysis. A normality test for the differences between grading scales confirmed that the data assumed a non-normal distribution ($p < 0.05$) using Kolmogorov-Smirnov normality test. Spearman's rank correlation coefficient testing tested association between the parameters and Bland-Altman analysis was used to assess agreement between testing conditions.

Inter-instrument and inter-grading scale analysis considered grouped column analysis. Spearman's rank correlation coefficient testing was used to confirm association, and Bland-Altman analysis was used to assess the level of agreement between the different instruments.

Statistical analysis for Chapter 4 was performed using MedCalc for Windows, version 19.4 (MedCalc Software, Ostend, Belgium). Normality testing by Kolmogorov-Smirnov indicated the distribution of the data was non-normal ($p < 0.05$), and the need for non-parametric tests in analysis of the data. Receiver operating characteristics (ROC) curve analysis to evaluate diagnostic accuracy, reported in Chapter 4, was performed using the methodology described by DeLong et al. ([215](#)). The C-statistic represents the area under the ROC curve which reflects the discriminative abilities of clinical tests to detect elevated MMP-9 levels. A statistically significant p-value of < 0.05 was used to indicate where the diagnostic performance of clinical tests was greater than random chance.

Chapter 3. Inter-observer and Intra-observer repeatability of grading scales for conjunctival hyperaemia

3.1 Introduction

Ocular surface hyperaemia, commonly referred to as eye redness, is one of the four cardinal signs of inflammation, and its assessment in clinical practice contributes to the management decisions made by eyecare professionals ([125](#)). The subjectivity in judgement, resulting in limited inter-observer reproducibility and intra-observer repeatability amongst clinical grading scales, is recognised and objective grading systems for bulbar conjunctiva have been developed ([126](#), [139](#), [216-218](#)). These are available via software incorporated in diagnostic tools such as the R-scan function within the Keratograph 5M described in Section 2.2.4. Peterson et al. found that automated grading of hyperaemia was up to 51 times more sensitive and 16 times more reliable than subjective grading ([134](#)). Despite this, objective methods of grading bulbar redness are not widely used in clinical practice due to the need for specialised instrumentation and time constraints ([136](#)). Practitioners thus continue to make gross judgments of redness, recorded on a 4-point scale as none, mild, moderate or severe, or rely on matching their clinical impressions against one of a number of image-based grading scales. The current conjunctival hyperaemia grading scales vary in presentation, however, and depict progressive levels of bulbar conjunctival hyperaemia using a mixture of artistic impressions, photographs and computer generated images ([129](#), [131](#)). Understanding how well judgements of the severity of hyperaemia compare using different scales is important for clinicians in ensuring consistent diagnostic messaging for patients.

Whether clinical grading in these ways provides a measure of actual ocular surface inflammation is a question that will be explored more fully in Chapters 4 and 5. In this chapter, a preliminary study is first reported, that sought to determine inter-observer reproducibility and intra-observer repeatability of three subjective grading scales commonly used by eye health professionals, and to compare outcomes to objective measurement of redness using the Oculus K5M. It was hypothesised that subjective grading of bulbar hyperaemia would correlate with objective grading of hyperaemia, and that intra-observer repeatability of hyperaemia grading would be superior to inter-observer reproducibility.

3.2 Methods

3.2.1 Participants and observers

Two bulbar conjunctival images from the nasal and temporal regions of the right eyes of 12 participants were captured on the Oculus K5M under white light illumination to provide a sample of 24 images. Ethical approval for the study was granted by the Auckland Health Research Ethics Committee (AHREC) as described in Chapter 2 and all participants provided written informed consent. The R-scan feature within the K5M software generated automated redness results reported relative to the 0-4 proprietary JENVIS scale.

Five independent observers were asked to grade the series of 24 images that depicted a range of hyperaemia levels, against three different grading scales described in Section 3.2.2. All images were de-identified, numerically labelled, then randomised using a random number generator to minimise any bias associated with grading images from the same eye. The randomised images were collated into a PDF document with a single image per page. The observers were requested to grade the set of randomised images against one grading scale at a time, without referring to their results from the other scales in an attempt to further reduce bias. A recording sheet created in Excel, which listed the image number, the subjective grading scale to be used and the hyperaemia grading in separate columns was provided. In each case, observers were requested to grade each image to the closest 0.1 and were instructed not to extrapolate beyond the given lower and upper limits of each system ([131](#)).

3.2.2 Grading systems

The subjective grading systems used in this study included the Efron grading scale, the BHVI grading scale and the VBR scale ([129](#), [138](#), [219](#)). The Efron and BHVI grading scales are both widely used in clinical practice ([131](#)). The Efron scale is a pictorial scale based on an artist's drawing, ranging from 0 to 4. The BHVI is a photographic scale ranging from 1 to 4. The VBR scale is a more recent psychophysically-developed scale that also is a photographic scale ranging from 0 to 100. The grading scales were described in detail in Section 1.5.1.

3.2.3 Data transformation

The grading scale measurement ranges differ from one another; the Efron and K5M grading scale limits are 0 and 4, VBR-5 provides a measure from 0 to 100, and BHVI score ranges between 1 and 4. To facilitate direct comparison, a 0 to 4 range was chosen for standardisation, for practicality and clinical relevance, and the grading scale scores transformed accordingly. The BHVI grade (y) was transformed using the formula $[y-1*4/3]$, and VBR grade (w), using the formula $[w/100*4]$.

3.2.4 Reproducibility testing

Inter-observer reproducibility for the five observers was confirmed using correlation testing for association, and the level of agreement between observers was evaluated by Bland-Altman analysis.

Two observers repeated the subjective grading exercise on two separate occasions, five weeks apart, to allow assessment of intra-observer repeatability.

Inter-instrument agreement was assessed by comparing the hyperaemia scores from the Efron, VBR-5 and BHVI grading scales, to assess the mean difference and any bias or observable differences between the scales. Subjective grades were then compared to the objective hyperaemia (JENVIS scale) grades generated by the Oculus K5M.

3.3 Results

Reflecting the levels of hyperaemia most commonly observed in clinical practice, the series of 24 images depicted a range of redness levels, with a majority corresponding to mild and moderate degrees of hyperaemia and fewer images depicting marked levels of hyperaemia.

3.3.1 Inter-observer reproducibility

Spearman's rank correlation coefficient testing is presented in Figure 11. Positive correlations with $r > 0.5$ were detected between all observers, indicating moderate-to-high levels of correlation (220). All r values were associated with a p -value < 0.05 confirming statistical significance of all correlations stated in Figure 11.

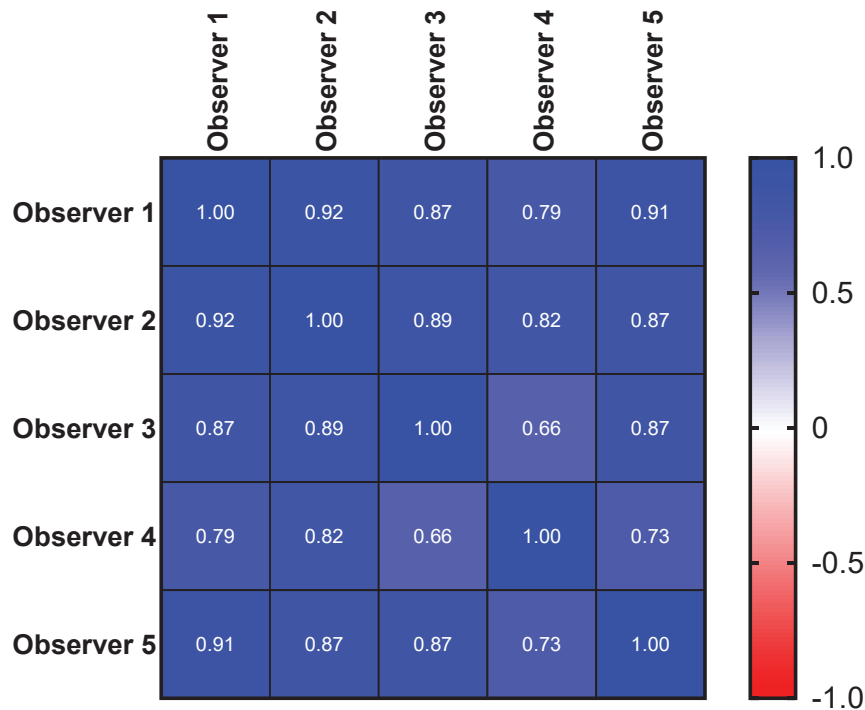


Figure 11. Spearman's correlation matrix for inter-observer reproducibility¹³

Bland-Altman analysis was conducted on the scores to assess the level of agreement between individual observers for each of the subjective grading scales. The mean difference (bias) across all five observers

¹³ Values closer to +1 reflect a strong positive correlation relationship. The bar on the right is the colour legend corresponding to strong through to poor correlation scores. ($p < 0.05$ for all correlations)

for each of the scales was 0.67, 0.29, and 0.21 for the BHVI, Efron, and VBR-5 bulbar hyperaemia grading scales, respectively.

Table 15. BHVI scale inter-observer reproducibility as determined by Bland-Altman analysis.

Observer		1	2	3	4
2	Bias	-1.45			
	95% limits of agreement range	0.71			
3	Bias	-1.53	-0.08		
	95% limits of agreement range	0.53	0.46		
4	Bias	-1.59	-0.14	-0.06	
	95% limits of agreement range	0.87	0.72	0.75	
5	Bias	-1.33	0.11	0.19	0.25
	95% limits of agreement range	0.82	0.67	0.59	0.84

Table 16. Efron scale inter-observer reproducibility as determined by Bland-Altman analysis.

Observer		1	2	3	4
2	Bias	-0.21			
	95% limits of agreement range	0.22			
3	Bias	0.10	0.31		
	95% limits of agreement range	0.25	0.28		
4	Bias	-0.44	-0.23	-0.54	
	95% limits of agreement range	0.49	0.55	0.46	
5	Bias	-0.38	-0.17	-0.48	0.06
	95% limits of agreement range	0.42	0.46	0.50	0.64

Table 17. VBR scale inter-observer reproducibility as determined in Bland-Altman analysis.

Observer		1	2	3	4
2	Bias	0.44			
	95% limits of agreement range	0.23			
3	Bias	0.31	-0.13		
	95% limits of agreement range	0.39	0.31		
4	Bias	0.38	-0.06	0.08	
	95% limits of agreement range	0.31	0.32	0.40	
5	Bias	0.21	-0.23	-0.10	-0.18
	95% limits of agreement range	0.41	0.36	0.37	0.47

3.3.2 Intra-observer repeatability

Repeated sets of grades generated by a single observer at two separate time points, were compared to assess intra-observer repeatability . Intra-observer repeatability assessment was undertaken for two participants, observers A and B.

Bland-Altman: Observer A repeated measures

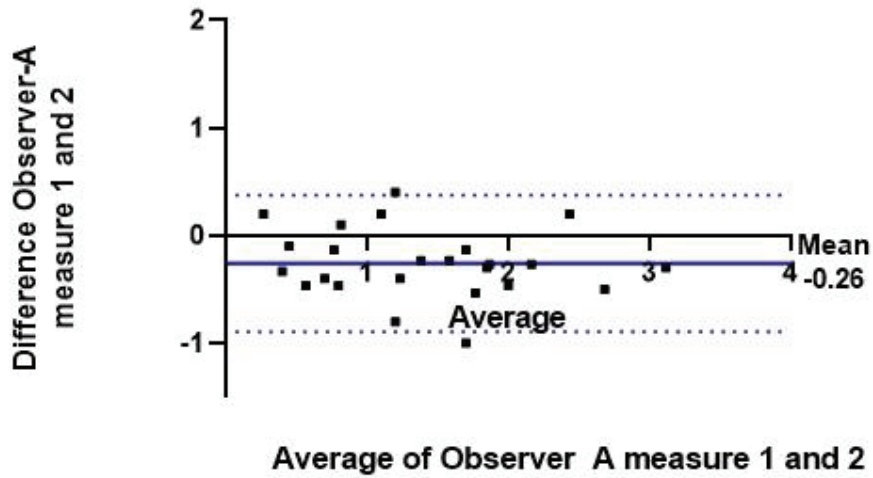


Figure 12. Bland-Altman analysis of observer A's intra-observer repeatability

Bland-Altman of Observer B repeated measures

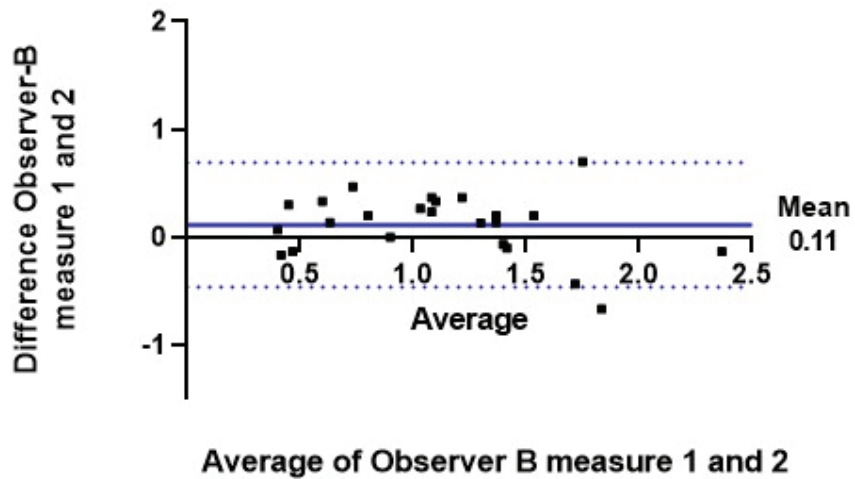


Figure 13. Bland-Altman analysis of observer B's intra-observer repeatability

Observer A displayed an average bias of -0.26 between their first and second grading exercise sessions across all three subjective scales for the same set of 24 randomised bulbar conjunctival pictures. The 95% limits of agreement had an interval of 1.29, ranging from -0.89 to 0.37, and the plot is demonstrated

in Figure 12. Observer B's repeated grading measurements showed a bias of 0.11, with 95% limits of agreement ranging from -0.46 to 0.69, giving a narrow interval of 1.15, as depicted in Figure 13. A small degree of heteroskedasticity is seen in Figure 13.

3.3.3 Inter-instrument agreement

Efron reported that a difference of one grade or more was both clinically relevant and statistically significant, when comparing grades between observers with a range of levels of experience (133). This difference was adopted when assessing the inter-instrument agreement in the current thesis. In addition, the trend of the graph was also evaluated when comparing grading scales to identify systematic differences.

3.3.4 Subjective grading method comparison

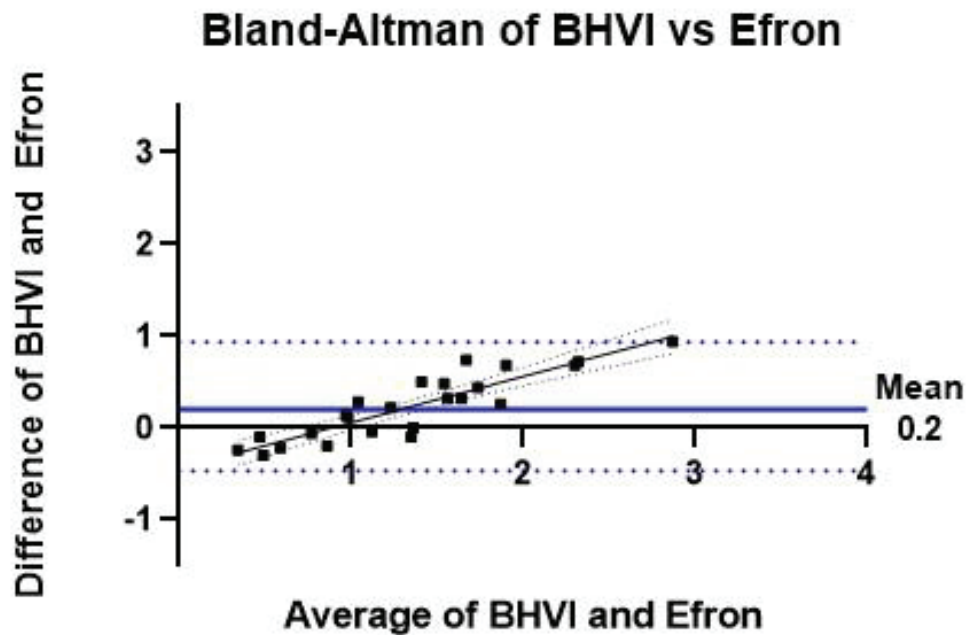


Figure 14. Bland-Altman analysis of the difference between hyperaemia grades on BHVI vs Efron scales plotted against the mean hyperaemia score.

Bland-Altman of BHVI vs VBR-5

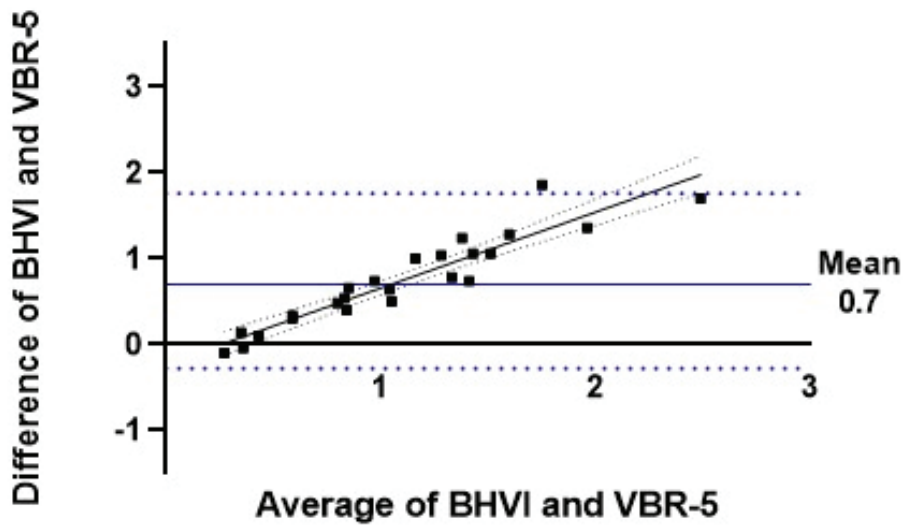


Figure 15. Bland-Altman analysis of the differences between hyperaemia grades on BHVI and VBR-5 scales plotted against the mean hyperaemia grade.

Bland-Altman of Efron vs VBR-5

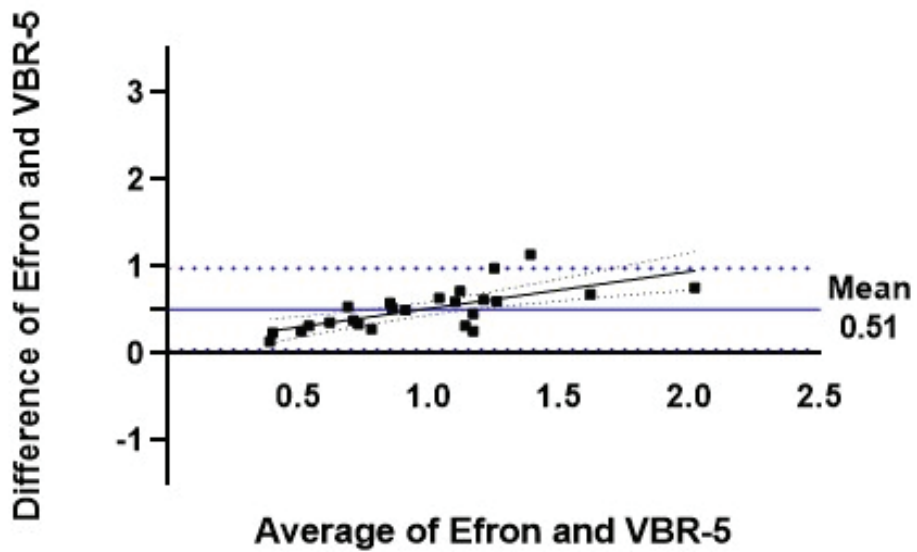


Figure 16. Bland-Altman analysis of the difference between hyperaemia grades assessed using the Efron and VBR-5 scales plotted against the mean hyperaemia grade from the Efron and VBR-5 scales.

The average bias between the BHVI and Efron scales was 0.23, with a standard deviation (SD) of 0.36 as graphically depicted in Figure 14. The 95% limits of agreement extend from -0.47 to 0.93, resulting in a range of 1.4 units. The average bias between the BHVI and VBR-5 scale was 0.74, SD of 0.52 as shown in Figure 15. The total range of the 95% limits of agreement was 2.04, ranging between -0.28 and 1.76. The Efron and VBR-5 scale hyperaemia grades generated an average bias of 0.51, with a SD of 0.24. The 95% limits of agreement range from 0.04 to 0.98, resulting in a 95% confidence interval of 0.94 units as depicted in Figure 16. All three Bland-Altman plots demonstrate a proportional bias, with the difference in measurements between the two methods increasing with the magnitude of the measurements.

3.3.4 Subjective vs objective agreement

To assess agreement between subjective grading and that determined objectively, Bland-Altman analysis was performed for each of the subjective grading scales relative to the automated result obtained from the JENVIS scale (Oculus K5M).

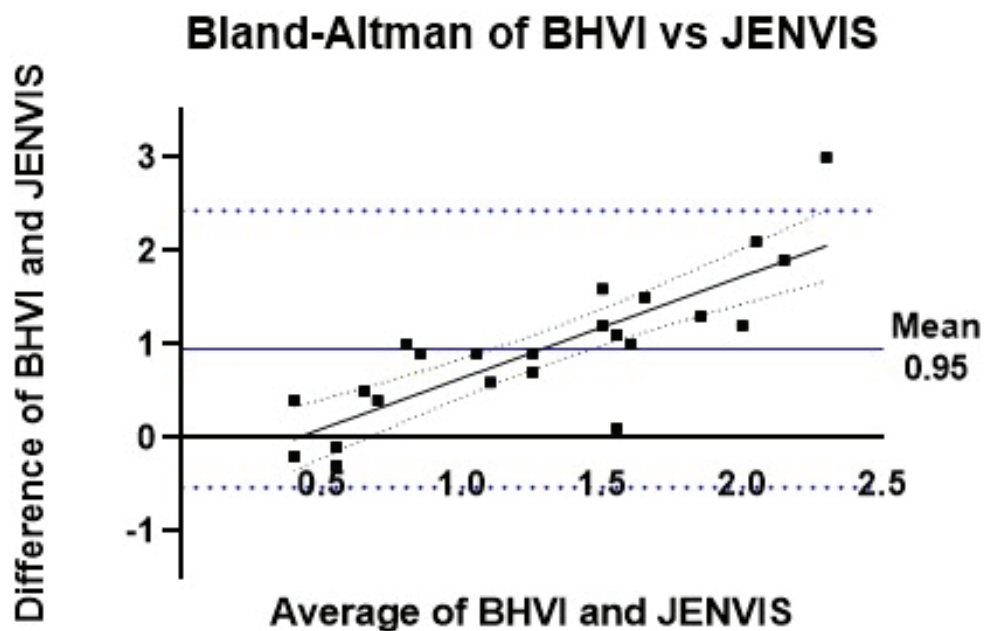


Figure 17. Bland-Altman analysis of the difference between BHVI vs JENVIS (R-Scan) scale hyperaemia grades plotted against the average hyperaemia score.

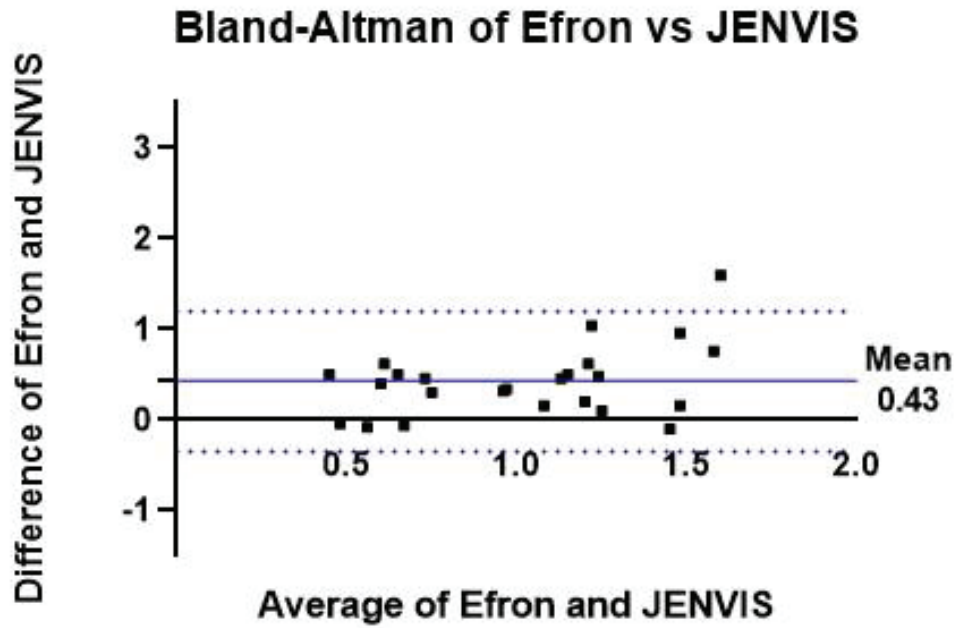


Figure 18. Bland-Altman analysis of the difference between Efron vs JENVIS (R-Scan) scale hyperaemia grades plotted against the average hyperaemia score.

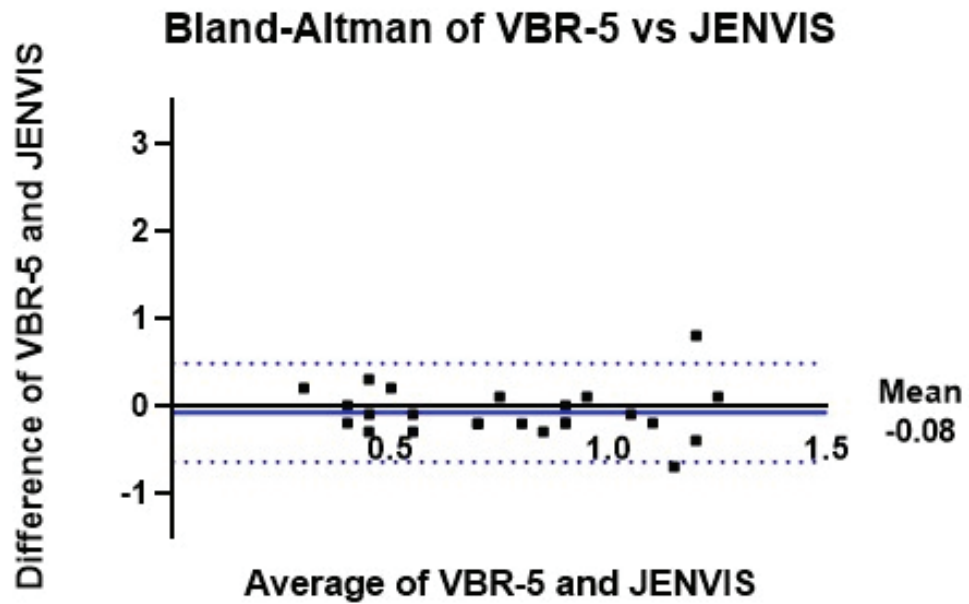


Figure 19. Bland-Altman analysis of the difference between VBR-5 vs JENVIS (R-Scan) scale hyperaemia grades plotted against the mean hyperaemia score.

The mean difference (bias) between the hyperaemia scores assessed using the BHVI and JENVIS scale was 0.95 with an SD of 0.76 as seen in Figure 17. The 95% limits of agreement ranged from -0.53 to 2.43 resulting in a total confidence interval of 2.96 units. Figure 18 depicts the mean bias of 0.43 between the hyperaemia scores graded using the Efron and JENVIS scales, with an SD of 0.39. The 95% limits of agreement ranged from -0.35 to 1.20, resulting in a total range of 1.54 units. The mean bias between the VBR-5 and JENVIS scale hyperaemia scores was -0.08 with an SD of 0.29 (Figure 19). The 95% limits of agreement ranged from -0.65 to 0.49, producing a total range of 1.12 units.

3.4 Discussion

Inter-observer reproducibility of bulbar redness grading is important when different clinicians manage the same patient in practice. Intra-observer repeatability is also important to ensure the individual clinician is able to manage patients consistently and as accurately as possible if anti-inflammatory treatments are to be considered and treatment efficacy to be monitored. Objective methods of grading bulbar hyperaemia have been shown to be more sensitive and reliable than subjective methods of evaluation (134).

However, in general eye care practice, such instrumentation is not widely available, resulting in a majority of clinicians continuing to rely on readily accessible subjective grading scales as their instrument of choice for facilitating clinical recording (129, 138, 219). This chapter set out to explore inter-observer, intra-observer, and inter-instrument agreement to determine the subjective bulbar redness scale with the highest level of agreement with the objective measurement.

The numerical scores resulting from bulbar hyperaemia grading can be useful for clinicians in guiding clinical treatment decisions. If follow-up measures are significantly different from the initial measure, this may prompt alteration of an existing treatment plan or initiation of a different treatment strategy. Efron has described that a clinically significant difference can be reflected mathematically as 1.96x standard deviation of the mean bias between two measures (133). Efron et al. determined that a 95% confidence interval of 1.0 grading scale unit can be considered both statistically significant and clinically meaningful (138). The following discussion will thus consider the 1.0 grade unit as a clinically meaningful difference among observers and instruments. If the mean bias is less than 1.0 and the 95% limits of agreement are narrow, the agreement can be considered to be within acceptable limits.

Based on correlation analysis, the inter-observer agreement in hyperaemia scoring, was fairly high, with a favourable correlation of grading scores noted amongst the observers across each of the subjective grading scales ($p < 0.05$). Bland-Altman analysis demonstrated that grading according to the VBR-5 scale presented the smallest inter-observer variation across the five observers. Between any individual pair of observers, the lowest mean bias produced was 0.06 signifying very close agreement for all images, and the highest was 0.44, which reassuringly fell well within the grade difference of 1.0, beyond which would be deemed clinically significantly different (133). The bulbar hyperaemia scoring assigned by the observers using the Efron scale was similar, with a mean bias of 0.29, and 95% range of agreement being within half a grade. The BHVI scale showed the highest mean bias across the five observers, with

the largest 95% limits of agreement range, indicating the poorest agreement for this scale. One observer when using the BHVI scale was noted to consistently score higher than the others, producing grades with a mean difference of more than 1 unit. When that observer was excluded from the mean difference calculation, the BHVI scale then demonstrated the lowest mean bias of 0.14, suggesting that increasing the observer sample size in testing the agreement between instruments may be advisable to reduce the risk of an individual's results swaying the outcomes. It also raises a potential benefit of promoting consensus training for observers in group practices in an attempt to encourage consistency amongst clinician scoring. The reason why this was observed for the BHVI scale but not the others is unknown, but it was observed that, relative to the Efron and VBR-5 grading scales, the BHVI scale focuses mainly on the redness parameter reflected by the increased number of blood vessels, without changing the background redness hue. This might suggest that the inter-observer variability may be influenced by the different parameters favoured by the different instruments to reflect the severity of bulbar conjunctival hyperaemia.

Two observers independently repeated the subjective grading exercise in order to establish intra-observer repeatability in hyperaemia grading. Both observers demonstrated a high level of repeatability in replicating their initial scores. Observer A showed high levels of repeatability based on fairly narrow limits of agreement, grading approximately quarter of a grade higher on the second grading assessment. Observer B showed even tighter repeatability, with the second grading assessment showing a very slight decrease in the mean grade. In both cases, the variability fell well within a clinically meaningful difference of 1.0 grade (133). A small degree of heteroskedasticity is seen with observer B's repeated measures in Figure 13, indicating decreased consistency when grading more marked hyperaemia with scores above a grade of 1.5.

The inter-instrument comparisons between the Efron and BHVI and between Efron and VBR-5 grading scales showed a good level of agreement, however the BHVI vs VBR-5 grading scales showed poorer agreement. The BHVI and Efron bulbar hyperaemia grading scales had the best agreement with a small mean bias and narrow 95% limits of agreement. The mean bias of 0.74 in hyperaemia scores between the BHVI and VBR-5 suggests only moderate agreement, and the wide 95% confidence limits of 2.04 grading units represents a clinically significant difference between the two methods (± 1.0) confirming that the two instruments are not comparable. Scores obtained using the Efron scale and VBR-5 scale were on

average half a grade apart, as shown in Figure 16. The proportional bias indicated between all the grading scales indicate that the methods are not interchangeable.

The grading results obtained subjectively from the three grading scales were each compared with objective hyperaemia scores from the Red-Scan function on the Oculus K5M, which depicts outcomes relative to the proprietary JENVIS grading scale. Analysis showed that the hyperaemia scores obtained using the VBR-5 scale demonstrated the best agreement with the objective automated grading, with minimal bias that was unaffected by hyperaemia severity, and narrow limits of agreement centred around a mean difference of zero. The VBR-5 vs JENVIS method comparison was also the only plot in this section (Figure 19) that did not demonstrate proportional bias, suggesting the results are not only agreeable but are closest to being considered interchangeable.

A grading score above a difference of 1 was found between the BHVI and JENVIS scores, which is within the range considered clinically significantly different, indicating that there is little agreement between these two instruments. Comparing subjective grading scores from the Efron with the objective JENVIS grading score, shows generally scores assigned via the Efron grading scale are generally higher than those from the automated assessment, but the difference was similar across all severity levels. Additionally, the linear regression trend shown in Figure 17 indicates a proportional bias, where the difference is greater for more marked hyperaemia reflected in scores above 1.5. This suggests that the BHVI and Efron grading scale are not interchangeable with the automated JENVIS scale.

3.4.1 Limitations and future directions

Graders were encouraged to take breaks but it is possible that observer fatigue may have influenced the scoring consistency in this study, based on the somewhat unnatural exercise of being asked to grade many images multiple times. The BHVI scale was the final grading scale of the set, and it is not inconceivable that the higher variability observed with this scale compared to the others could indicate an order effect. Future studies could randomise the order of presentation of the grading scales to mitigate against a possible order effect. The data were transformed to a 0 to 4 scale in each case in order to allow for direct comparisons between different grading scales. Wolffsohn et al. found unequal increments between grading scale images in the Efron and BHVI scales, which followed a quadratic, rather than

linear pattern, as the severity increased (135). Conversely, the VBR-5 scale was developed in a linear pattern with 10 photographs, with increments derived according to chromaticity as determined by a spectrophotometer (129). This irregularity in the step increments within different grading scales lends support to the current study's findings that the scales cannot be used interchangeably. The linear nature of the increments within both the VBR-5 and JENVIS grading scales make them much more likely to compare favourably as supported by the current study findings. In future, refinement of grading scales to use similar, more objectively defined incremental steps would be expected to improve inter-instrument agreement.

A lack of images with marked severity of bulbar hyperaemia was another limitation in this study. As only 2% of the scores given by the five observers were above a grade of 3, the agreement between instruments and observers cannot be extrapolated for higher severities of bulbar redness. This arguably is an important point to address in future research, especially for intra-observer repeatability as the higher levels of bulbar hyperaemia are more likely to be associated with the patient cases requiring consideration for therapeutic intervention.

Previous research has recommended subjectively estimating hyperaemia scores to the closest 0.1 to improve precision in inter-observer reproducibility studies (137, 221), although in clinical practice, eyecare practitioners still tend to grade to the nearest integer (221). A study conducted by Vianya-Estopa et al., to assess precision, had both inexperienced and experienced observers grade to the nearest 0.1 and 0.5. It was found that grading to the nearest 0.5 resulted in closer alignment in scoring between observers in both groups, and it is possible this may have offered greater levels of agreement between observers in the current study had increments of 0.5 been utilised.

The small pool of observers is a limitation of this study, and future studies would benefit from the recruitment of a larger and more broad range of observers, with different levels of experience, in order for results to be most widely applicable in different clinical settings where clinician experience can vary. Furthermore, as alluded to earlier, there may be value in exploring whether inter-observer reproducibility could be improved for hyperaemia grading through consensus training, as was demonstrated in a study seeking to improve inter-observer agreement in manual immune cell quantification (222). Finally, caution is warranted in drawing conclusions from the outcomes of this study where the subjective grading was compared to objective hyperaemia grading based on a single device, in this case the Oculus Keratograph

5M. The proprietary software used to assess bulbar conjunctival redness in each diagnostic instrument will vary according to detection thresholds set by the manufacturer which could impact the results should the same study be conducted with a different automated diagnostic device.

3.5 Conclusion

Intra-observer repeatability and inter-observer reproducibility using three subjective grading scales was found to be similar, and the mean bias was less than the clinically significant difference (1.0 grading scale unit). The mean difference in grading seen in the intra-observer repeatability testing was around 0.1-0.3 which clinically does not have any implications due to the small difference. Inter-observer repeatability tested in this study was also good using the Efron and VBR-5 grading scale. Greater variation of more than 1.0 grading scale units was observed with the BHVI grading scale, although this may have been influenced by a single observer who scored noticeably more highly than the others, highlighting the importance of repeating such studies with a larger number of observers. Nevertheless, similar to other studies, the results suggest that caution should be applied when using clinical grading scales and they cannot be considered interchangeable. It suggests that clinicians should assess patients, where possible, using the same grading scale. The results would further suggest that if different clinicians are managing the same patient base within a clinical practice, that the same grading scale should be adopted by all clinicians within the practice. Objective grading of hyperaemia has been confirmed to offer the best repeatability in a clinical setting, (134) however, where this is not feasible due to resource constraints, the VBR-5 grading scale might be considered the most useful of the clinical tools tested in this study for assessing bulbar hyperaemia, based on its closest alignment with objective testing.

As described in Chapter 1, there remains a lack of scientific evidence confirming which diagnostic tests are optimal for use in the clinical setting for assessing ocular surface inflammation. The following chapter reports the results of the main study of this thesis which explores the relative diagnostic utility of various objective and subjective clinical tools that can be used in clinical practice to identify ocular surface inflammation.

Chapter 4. Results: Diagnostic utility of inflammation markers

This chapter outlines the main outcomes of the statistical analyses described in Section 2.5 in which the primary objective was to evaluate the diagnostic utility of clinical tests in identifying elevated levels of gene expression data for MMP-9, IL-8 and IL-1 β .

4.1 Participant characteristics

A total of 53 subjects satisfied the inclusion criteria as outlined in Section 2.1. Subsequently, six samples were unusable in the laboratory process due to poor RNA integrity and contamination, as described in Section 2.4.11, therefore samples from 47 subjects were included in the overall statistical analysis for this study. The participant characteristics including demographic and clinical test information are shown in Table 18. DED subtype was classified according to the criteria outlined in Figure 10. The severity classification of the disease was made according to Table 19 (1).

Table 18. Participant characteristics including demographic and clinical characteristics.

Characteristics		
Demographic features		
Age (median, range)	53 (22-82)	
Female gender	37 (79%)	
Dry eye diagnosis		
TFOS DEWS II dry eye diagnostic criteria	37 (79%)	
Mild-to-moderate dry eye classification	5 (14%)	
Moderate-to-severe dry eye classification	32 (86%)	
Evaporative dry eye subtype	28 (75%)	
Aqueous dry eye subtype	1 (3%)	
Mixed EDDE and ADDE dry eye	8 (22%)	
	DED ¹⁴	Non-DED
Dry eye symptomology		
Ocular Surface Disease Index score (out of 100)	37 (6-79)	14 (0-37)

¹⁴ DED diagnosis as per the TFOS DEWS II diagnostic methodology report (2)

Dry Eye Questionnaire 5 (out of 22)	12 (5-19)	6.5 (0-14)
Tear film parameters		
Non-invasive tear film break-up time (s)	7 (2-18)	12 (8-20)
Highest tear film osmolarity (mOsm/L)	302 (283-384)	297 (279-315)
Interocular difference in tear film osmolarity (mOsm/L)	10 (1-76)	5 (1-10)
Tear meniscus height (mm)	0.29 (0.11-0.44)	0.35 (0.20-0.37)

Table 19. Classification criteria for severity of dry eye disease (1).

Diagnostic test	Mild to moderate DED	Moderate to Severe DED
Ocular Surface Disease Index (out of 100)	≥ 13	≥ 22
Non-invasive tear film stability (s)	< 10	< 5
Tear film osmolarity (mOsm/L)	≥ 308	≥ 320
Interocular difference in osmolarity (mOsm/L)	> 8	> 12

4.2 Correlation Tests

4.2.1 Statistical analysis

Kolmogorov-Smirnov testing demonstrated that the majority of parameters were non-normally distributed (all $P < 0.05$). Spearman's rank correlation testing was therefore used to test the association between clinical and laboratory markers of inflammation. To assist with understanding correlation directions, the details for the grading schemes used for each test are outlined in Table 20. All significant findings ($p < 0.05$) are highlighted in Table 21.

4.2.2 Clinical markers of inflammation

Of the clinical markers of inflammation listed in Table 21, the subjective bulbar hyperaemia grading scores from the Efron and VBR-5 grading schemes were significantly correlated to each other, to the objective K5M bulbar hyperaemia scores and to the dry eye validated questionnaire scores from the OSDI and DEQ-5.

4.2.3 Laboratory derived markers of inflammation

The laboratory derived marker of inflammation MMP-9 was significantly correlated with the DEQ-5 score, NIKBUT, lipid layer grading but not with subjective or objective hyperaemia grades. IL-8 levels were found to be significantly correlated with IL-1 β levels.

4.2.4 Ocular surface integrity

The Ocular Surface Inflammation Evaluation (OSIE®) test was significantly correlated to the lipid layer grades and IL-1 β concentrations. Ocular surface staining scores, which represent a combination of corneal (NaFI) and conjunctival (lissamine green) scores, did not correlate with any clinical or laboratory markers of inflammation, nor any other individual TFOS DEWS II diagnostic DED marker or subclassification markers.

Table 20. Grading schemes for evaluating clinical and laboratory inflammation markers and dry eye diagnostic markers.¹⁵

Test	Grading scheme	Range	Scale	Clinical/Laboratory marker of inflammation or TFOS DEWS II Dry eye disease diagnostic or subclassification marker
InflammaDry®			0=Positive result 1=Negative result	Clinical
Clinical impression of hyperaemia (ClinicImp)	Gross analysis	Increasing severity	None, mild, moderate, severe	Clinical
Subjective Efron (EFRON)	Efron bulbar hyperaemia	Ascending severity	0-4	Clinical
Objective K5M (K5M)	JENVIS	Ascending severity	0-4	Clinical
Subjective VBR-5 (VBR-5)	VBR-5	Ascending severity	0-100	Clinical
Ocular surface staining (Staining)		Ascending severity	Out of 55	Clinical
Ocular Surface Inflammatory Evaluation (OSIE®)		Ascending severity	0-100%	Clinical
TFOS DEWS II Dry eye diagnosis (Dry eye)		0=Negative 1=Positive	0=TFOS DEWS II diagnostic criteria not met 1=TFOS DEWS II diagnostic criteria met	Dry eye diagnosis
Ocular surface disease index		Ascending severity		Dry eye diagnosis
Dry eye questionnaire-5		Ascending severity		Dry eye diagnosis
Non-invasive keratograph break-up time (NIK BUT)		Descending severity		Dry eye diagnosis
Highest osmolarity (HighOSM)		Ascending severity		Dry eye diagnosis
Difference in osmolarity (DiffOSM)		Ascending severity		Dry eye diagnosis
Tear meniscus height (TMH)		Descending severity		Dry eye subclassification
Lipid layer (Lipid)	Modified Guillon-Keeler	Descending severity		Dry eye subclassification
Matrix metalloproteinase-9 (MMP-9)		Continuous		Laboratory
Interleukin-8 (IL-8)		Continuous		Laboratory
Interleukin-1β (IL-1β)		Continuous		Laboratory

¹⁵ Legend. K5M= Oculus keratograph 5M, VBR-5= Validated bulbar redness 5 grading scale

Table 21. Correlation matrix of all clinical inflammatory tests, dry eye diagnostic tests and laboratory derived inflammation markers.¹⁶

Clinical Hyp	r	EFRON	K5M	VBR-5	Stain-ing	OSIE®	OSDI	DEQ-5	NIK BUT	High OSM	Diff OSM	TMH	Lipid	MMP-9	IL-8	IL-1β
EFRON	r	0.510														
	p	0.000														
K5M	r	0.264	0.611													
	p	0.073	0.000													
VBR-5	r	0.538	0.875	0.555												
	p	0.000	0.000	0.000												
Staining	r	-0.238	0.050	0.048	0.048											
	p	0.107	0.741	0.731	0.751											
OSIE®	r	0.008	0.075	0.137	0.039	-0.116										
	p	0.960	0.634	0.380	0.802	0.459										
OSDI	r	0.102	0.442	0.472	0.351	0.274	-0.264									
	p	0.496	0.002	0.001	0.015	0.063	0.088									
DEQ-5	r	0.029	0.460	0.497	0.360	0.242	-0.114	0.793								
	p	0.847	0.001	0.000	0.013	0.102	0.465	0.000								
NIK BUT	r	0.124	-0.087	-0.218	-0.095	-0.174	-0.051	-0.281	-0.290							
	p	0.404	0.561	0.141	0.527	0.243	0.746	0.055	0.048							
HighOSM	r	0.295	-0.023	0.136	0.051	-0.077	0.012	0.137	0.013	-0.231						
	p	0.044	0.876	0.363	0.735	0.606	0.937	0.358	0.928	0.119						
DiffOSM	r	0.268	0.086	0.142	0.080	-0.097	-0.011	0.091	0.020	-0.231	0.832					
	p	0.068	0.564	0.342	0.595	0.516	0.944	0.541	0.896	0.119	0.000					
TMH	r	0.203	0.163	0.072	0.133	-0.285	-0.120	-0.098	-0.145	0.377	0.003	0.038				
	p	0.170	0.274	0.630	0.373	0.052	0.442	0.514	0.331	0.009	0.986	0.799				
Lipid	r	-0.210	-0.166	-0.065	-0.122	-0.157	0.302	-0.180	0.334	0.113	-0.032	-0.058	0.193			
	p	0.157	0.265	0.666	0.413	0.292	0.049	0.227	0.152	0.448	0.831	0.698	0.193			
MMP-9	r	-0.056	0.075	0.234	-0.009	-0.026	-0.003	0.272	0.334	0.318	0.032	0.071	-0.230	-0.334		
	p	0.707	0.618	0.113	0.955	0.863	0.983	0.064	0.022	0.029	0.831	0.637	0.120	0.022		
IL-8	r	0.017	0.108	0.056	0.070	-0.015	0.296	-0.217	-0.159	-0.026	-0.166	-0.218	0.139	-0.093	-0.097	
	p	0.909	0.468	0.708	0.641	0.919	0.054	0.144	0.285	0.860	0.266	0.142	0.352	0.533	0.517	
IL-1β	r	0.169	0.235	0.271	0.237	0.045	0.316	0.153	0.143	-0.241	-0.065	-0.137	0.014	-0.135	0.235	0.421
	p	0.256	0.112	0.065	0.109	0.762	0.039	0.304	0.336	0.103	0.665	0.358	0.928	0.366	0.112	0.003

¹⁶ All highlighted boxes are statistically significant (p<0.05). Abbreviations: Clinical Hyp= Clinical impression of bulbar hyperaemia, EFRON= Efron grading scale, K5M= JEAVIS grading scale, VBR-5= Validated bulbar redness grading scale, Staining= Ocular surface staining using the Oxford scheme, a combined score of corneal (Nisfi) and conjunctival (Issamite green) staining, OSIE®= Ocular Surface Inflammation Evaluation (tear-locked), Dry Eye= TFOS DEWS II Dry eye diagnosis, OSDI= Ocular surface disease index, DEQ-5= Dry Eye Questionnaire 5, NIK BUT= Non-invasive tear break-up time, HighOSM= Highest osmolarity of two eyes, DiffOSM= Difference in osmolarity between the two eyes, TMH= tear meniscus height, MMP-9= Matrix metalloproteinase-9, IL-8= interleukin 8, IL-1β= interleukin 1β.

4.3 Association between global dry eye markers and ocular inflammatory biomarkers

ROC analysis was performed to assess whether the TFOS DEWS II global dry eye indices that are central to all forms of dry eye, irrespective of subtype (symptomology, tear film stability, tear osmolarity and ocular surface staining), could predict elevated ocular inflammatory biomarker levels (MMP-9, IL-8 and IL-1 β) in the conjunctiva analysed with laboratory techniques described in Section 2.3. In other words, this section was used to identify the risk factors for clinically significant ocular surface inflammation.

4.3.1 Global dry eye disease markers and their ability to predict elevated levels of MMP-9 mRNA transcripts

The dry eye diagnostic marker which demonstrated the highest predictive ability for elevated levels of MMP-9 was non-invasive tear break-up time (NIBUT) [C-statistic 0.747, 95% CI (0.599-0.862), $p=0.0017$, Youden optimal diagnostic cut-off ≤ 5.8 s] as shown in Table 22. In addition, the DEQ-5 score [C-statistic=0.688, 95% CI (0.529-0.808), $p=0.0205$, Youden cut-off >9], OSDI [C-statistic=0.680 95% CI (0.529-0.808), $p= 0.028$, Youden cut-off >33.3] and overall diagnosis of dry eye disease using the TFOS DEWS II criteria [C-statistic=0.652, 95% CI (0.499-0.785), $p=0.0002$] all showed statistically significant predictive accuracy in detecting elevated levels of MMP-9 mRNA transcripts. Among the ADDE and EDE subclassification markers tested, only lipid layer thickness grading demonstrated significant prognostic value for identifying elevated MMP-9 levels [C-statistic=0.685, 95% CI (0.533-0.813), $p=0.033$, Youden optimal diagnostic cut-off ≤ 2].

4.3.2 Global dry eye disease markers and their ability to predict elevated levels of IL-8 mRNA transcripts

Results in

Table 23 highlights that none of the global dry eye disease markers tested in this study demonstrated significant discriminative ability for predicting elevated levels of IL-8 mRNA transcripts (all $p > 0.05$).

4.3.3 Global dry eye disease markers and their ability to predict elevated levels of IL-1 β mRNA transcripts

Results outlined in Table 24 demonstrate that none of the global dry eye indices were able to predict the presence of the IL-1 β biomarker ($p > 0.05$ in all cases).

Table 22. Global dry eye markers versus presence of laboratory MMP-9 biomarkers.¹⁷

	DED Diagnosis		Homeostatic markers			Symptomology			DED Subtype markers	
	TFOS DEWS II criteria – presence/ absence	NIBUT s	HighOSM mOsm/L	DiffOSM mOsm/L	DEQ-5 score	OSDI score	TMH mm	Lipid layer grade		
C-statistic (95% CI)	0.652 (0.499-0.785)	0.747 (0.599-0.862)	0.632 (0.479-0.768)	0.529 (0.378-0.676)	0.688 (0.537-0.815)	0.680 (0.529-0.808)	0.591 (0.438-0.732)	0.685 (0.533-0.813)		
P-value	0.0002*	0.0017*	0.186	0.766	0.021*	0.028*	0.347	0.033*		
Youden optimal diagnostic cut-off		≤5.8	≤298	>12	>9	>33.3	≤0.21	≤2		
Sensitivity, % (95% CI)		79 (49-95)	64 (35-87)	36 (13-65)	93 (66-100)	64 (35-87)	36 (13-65)	57 (29-82)		
Specificity, % (95% CI)		76 (58-89)	70 (61-84)	79 (61-91)	39 (23-58)	67 (48-82)	88 (72-97)	70 (51-84)		
Positive likelihood ratio (95% CI)		3.24 (1.67-6.29)	2.12 (1.11-4.06)	1.68 (0.64-4.41)	1.553 (1.12-2.09)	1.93 (1.04-3.59)	2.95 (0.93-9.37)	1.89 (0.95-3.75)		
Negative likelihood ratio (95% CI)		0.28 (0.10-0.79)	0.51 (0.24-1.07)	0.82 (0.53-1.25)	0.18 (0.026-1.26)	0.54 (0.25-1.13)	0.73 (0.49-1.10)	0.61 (0.32-1.17)		

¹⁷ Asterisks denote statistically significant differences (p<0.05). Abbreviations. NIBUT= Non-invasive break-up time, HighOSM= Highest osmolarity between the two eyes, DiffOSM= Difference in osmolarity between the two eyes, DEQ-5= Dry eye questionnaire-5, OSDI= Ocular surface disease index, TMH= Tear meniscus height

Table 23. Global dry eye markers versus presence of laboratory IL-8 biomarkers.¹⁸

	DED Diagnosis		Homeostatic markers			Symptomology			Subcategorisation markers	
	TFOS DEWS II criteria – presence/ absence	NIKBUS	HighOSM mOsm/L	DiffOSM mOsm/L	DEQ-5 score	OSDI score	TMH mm	Lipid layer grade		
C-statistic (95% CI)	0.581 (0.428-0.723)	0.505 (0.356-0.654)	0.554 (0.402-0.699)	0.620 (0.466-0.757)	0.545 (0.394-0.691)	0.606 (0.453-0.745)	0.505 (0.356-0.654)	0.611 (0.457-0.749)		
P-value	0.175	0.951	0.533	0.153	0.598	0.224	0.951	0.175		
Youden optimal diagnostic cut-off		>11.79	>306	≤4	>15	>47.9	≤0.28	≤2		
Sensitivity, % (95% CI)		25 (10-47)	42 (22-63)	54 (33-74)	25 (10-47)	38 (19-59)	63 (41-81)	46 (26-67)		
Specificity, % (95% CI)		91 (72-99)	78 (56-93)	70 (47-87)	96 (78-100)	100 (85-100)	57 (35-77)	70 (47-87)		
Positive likelihood ratio (95% CI)		2.87 (0.64-12.82)	1.92 (0.77-4.75)	1.78 (0.87-3.65)	5.75 (0.75-44.15)	-	1.44 (0.82-2.52)	1.51 (0.71-3.24)		
Negative likelihood ratio (95% CI)		0.82 (0.63-1.07)	0.75 (0.50-1.11)	0.66 (0.39-1.10)	0.78 (0.61-1.00)	0.63 (0.46-0.85)	0.66 (0.35-1.24)	0.78 (0.49-1.23)		

¹⁸ Asterisks denote statistically significant differences (p<0.05). Abbreviations. NIKBUS= Non-invasive keratograph break-up time, HighOSM= Highest osmolarity between the two eyes, DiffOSM= Difference in osmolarity between the two eyes, DEQ-5= Dry eye questionnaire-5, OSDI= Ocular surface disease index, TMH= Tear meniscus height

Table 24. Global dry eye markers versus presence of laboratory IL-1 β biomarkers.¹⁹

	DED Diagnosis		Homeostatic markers			Symptomology			Subcategorisation markers	
	TFOS DEWS II criteria – presence/absence	NIK BUT s	HighOSM mOsm/L	DiffOSM mOsm/L	DEQ-5 score	OSDI score	TMH mm	Lipid layer grade		
C-statistic (95% CI)	0.538 (0.387-0.684)	0.596 (0.443-0.737)	0.522 (0.371-0.670)	0.544 (0.393-0.690)	0.531 (0.380-0.678)	0.515 (0.365-0.664)	0.569 (0.416-0.712)	0.586 (0.433-0.728)		
P-value	0.530	0.271	0.802	0.607	0.722	0.859	0.427	0.300		
Youden optimal diagnostic cut-off		≤7.90	>313	≤10	>13	≤22.5	> 0.28	≤1		
Sensitivity, % (95% CI)		71 (49-87)	21 (7-42)	75 (53-90)	38 (19-59)	46 (26-67)	67 (45-84)	25 (10-47)		
Specificity, % (95% CI)		57 (35-77)	96 (78-100)	44 (23-66)	78 (56-93)	70 (47-87)	57 (35-77)	91 (72-99)		
Positive likelihood ratio (95% CI)		1.63 (0.96-2.77)	4.79 (0.60-37.95)	1.33 (0.87-2.03)	1.73 (0.68-4.38)	1.51 (0.71-3.21)	1.53 (0.89-2.64)	2.87 (0.64-12.82)		
Negative likelihood ratio (95% CI)		0.52 (0.25-1.06)	0.83 (0.66-1.03)	0.58 (0.25-1.33)	0.80 (0.55-1.16)	0.78 (0.49-1.23)	0.59 (0.30-1.15)	0.82 (0.63-1.07)		

¹⁹ Asterisks denote statistically significant differences (p<0.05). Abbreviations. NIKBUT= Non-invasive keratograph break-up time, HighOSM= Highest osmolarity between the two eyes, DiffOSM= Difference in osmolarity between the two eyes, DEQ-5= Dry eye questionnaire-5, OSDI= Ocular surface disease index, TMH= Tear meniscus height

4.4 Predictive ability of clinical biomarkers of inflammation to detect ocular surface inflammation

A range of clinical tests that are widely considered to be markers of inflammation, or have more recently been proposed to indicate inflammation, were assessed in this study as outlined in Table 25. The markers were tested for their diagnostic utility in detecting laboratory-derived ocular inflammatory biomarker levels (MMP-9, IL-8 and IL-1 β).

Table 25. Clinical measures of inflammation.

Clinical measurement	Grading scheme or instrumentation
In-office MMP-9 measurement	InflammaDry® test
Subjective bulbar hyperaemia score	Efron grading scale
Subjective bulbar hyperaemia score	VBR-5 grading scale
Objective bulbar hyperaemia score	JENVIS scale (Oculus K5M)
Corneal and conjunctival staining	Visualisation via slit lamp biomicroscopy
Ocular surface inflammation evaluation OSIE®	TearCheck® dry eye analysis device

4.4.1 Clinical inflammatory markers and their ability to detect elevated levels of MMP-9 mRNA transcripts

Of all the parameters evaluated, including subjective hyperaemia grading scoring, objective hyperaemia scoring, InflammaDry® test and ocular surface staining, it was found that the objective measure of conjunctival hyperaemia on the JENVIS scale (Oculus K5M) offered the greatest discriminative ability in detecting upregulation of ocular surface MMP-9 RNA transcripts, with a C-statistic of 0.747 [95% CI (0.537-0.815), $p=0.002$] as shown in Table 26. The Youden optimal diagnostic cut-off for this test was ≥ 1.0 , with higher scores corresponding to detectable MMP-9 levels, and scores below this cut off signifying non-detectable MMP-9 levels. The sensitivity of this grading method in identifying clinically significant

inflammation was 86%, and the specificity was 64%. Next most accurate was the InflammaDry® test with a C-statistic of 0.699 [95% CI (0.545-0.822), $p=0.006$], and the Efron hyperaemia grade, with a C-statistic of 0.688 [95% CI (0.537-0.815), $p=0.029$]. These results show that identification of inflammation was significantly greater than chance ($p<0.05$), while the remaining tests ($p>0.05$) failed to offer a predictive ability for inflammation that was better than chance (Table 26).

4.4.2 Clinical inflammatory markers and their ability to detect elevated levels of IL-8 mRNA transcripts

Results outlined in Table 27 suggest that none of the clinical inflammation indices tested in this study were able to predict elevated levels of IL-8 mRNA transcripts. All p values were greater than 0.05.

4.4.3 Clinical inflammatory markers and their ability to detect elevated levels of IL-1 β mRNA transcripts

The ROC analyses for all clinical inflammation indices in predicting increased levels of IL-1 β are listed in Table 28. The VBR-5 scale was the only clinical tool that demonstrated significant discriminative ability in predicting increased levels of IL-1 β mRNA transcripts at the ocular surface [C-statistic=0.661, 95% CI (0.509-0.793), $p=0.047$, Youden optimal diagnostic cut-off >21.5].

Table 26. The discriminative ability of clinic-based measures for inflammation in detecting MMP-9 transcripts.²⁰

	Point of care testing		Bulbar hyperaemia grading			Ocular surface staining		
	InflammaDry® (P or N)	Objective (K5M)	Efron grading scale	VBR-5 grading scale	Clinical impression	Corneal and conjunctival staining (Oxford grading scale)	Ocular Surface Inflammatory Evaluation (Tearcheck®)	
C-statistic (95% CI)	0.699 (0.545-0.822)	0.747 (0.599- 0.862)	0.688 (0.537- 0.815)	0.629 (0.476- 0.765)	0.505 (0.356- 0.654)	0.576 (0.423-0.719)	0.525 (0.367- 0.679)	
P-value	0.006*	0.002*	0.029*	0.193	0.951	0.398	0.847	
Youden optimal diagnostic cut-off	-	>1.0	>1.5	>24	>1	-	-	
Sensitivity, % (95% CI)	64 (35-87)	86 (57-98)	71 (42-92)	57 (29-82)	29 (8-58)	64 (35-87)	100 (77-100)	
Specificity, % (95% CI)	58 (39-75)	64 (45-80)	73 (55-87)	79 (61-91)	76 (58-89)	55 (36-72)	14 (4-32)	
Positive likelihood ratio (95% CI)	1.52 (0.87-2.65)	2.36 (1.43-3.88)	2.62 (1.37-5.01)	2.69 (1.21- 5.99)	1.18 (0.42-3.28)	1.41 (0.82-2.43)	1.16 (1.00-1.34)	
Negative likelihood ratio (95% CI)	0.62 (0.29-1.33)	0.33 (0.06-0.83)	0.39 (0.17-0.92)	0.54 (0.29- 1.02)	0.94 (0.64-1.38)	0.65 (0.30-1.41)	0.00	

²⁰ Asterisks denote statistically significant differences (p<0.05). Abbreviations: K5M= Oculus Keratograph 5M (JENVIS grading scale)

Table 27. The discriminative ability of clinical inflammation markers detecting IL-8 transcripts.²¹

	Bulbar hyperaemia grading				Ocular staining		
	Objective (K5M)	Efron grading scale	VBR-5 grading scale	Clinical impression	Corneal and conjunctival staining (Oxford grading scale)	Ocular Surface Inflammatory Evaluation (Tearcheck®)	
C-statistic (95% CI)	0.747 (0.599-0.862)	0.537 (0.386-0.684)	0.510 (0.360-0.659)	0.520 (0.369-0.668)	0.542 (0.390-0.688)	0.568 (0.408-0.718)	
P-value	0.769	0.670	0.909	0.801	0.603	0.226	
Youden optimal diagnostic cut-off	≤0.7	>2.0	≤43	>1	>4	</0	
Sensitivity, % (95% CI)	29 (13-51)	25 (10-47)	88 (68-97)	33 (16-55)	25 (10-47)	91 (70-99)	
Specificity, % (95% CI)	83 (61-95)	91 (72-99)	0 (0-15)	83 (61-95)	96 (78-100)	23 (8-45)	
Positive likelihood ratio (95% CI)	1.68 (0.57-4.97)	2.87 (0.64-12.82)	0.88 (0.75-1.02)	1.92 (0.67-5.51)	5.75 (0.75-44.15)	1.17 (0.90-1.53)	
Negative likelihood ratio (95% CI)	0.86 (0.62-1.18)	0.82 (0.63-1.07)	0.81 (0.57-1.13)	0.78 (0.61-1.00)	0.42 (0.09-1.93)		

²¹ Asterisks denote statistically significant differences (p<0.05). Abbreviations. K5M= Oculus Keratograph 5M (JENVIS grading scale) VBR = Validated Bulbar Redness CI= confidence interval

Table 28. The discriminative ability of clinical inflammation markers detecting IL-1 β transcripts.²²

	Bulbar hyperaemia grading				Ocular staining		
	Objective (K5M)	Efron grading scale	VBR-5 grading scale	Clinical impression	Corneal and conjunctival staining (Oxford grading scale)	Ocular Surface Inflammatory Evaluation (Tearcheck®)	
C-statistic (95% CI)	0.511 (0.361-0.659)	0.588 (0.435-0.729)	0.661 (0.509-0.793)	0.618 (0.465-0.756)	0.506 (0.357-0.655)	0.516 (0.359-0.671)	
P-value	0.902	0.303	0.047*	0.116	0.937	0.781	
Youden optimal diagnostic cut-off	<0.55	>1.6	>21.5	>1	>2	>1	
Sensitivity, % (95% CI)	25 (10-47)	42 (22-63)	58 (37-78)	38 (19-59)	21 (7-42)	5 (0-24)	
Specificity, % (95% CI)	96 (78-100)	78 (86-93)	83 (61-95)	87 (66-97)	74 (52-90)	86 (65-97)	
Positive likelihood ratio (95% CI)	5.75 (0.75-44.15)	1.92 (0.77-4.75)	3.35 (1.29-8.70)	2.87 (0.89-9.31)	0.80 (0.28-2.26)	0.35 (0.039-3.10)	
Negative likelihood ratio (95% CI)	0.78 (0.61-1.00)	0.75 (0.50-1.11)	0.50 (0.30-0.84)	0.72 (0.51-1.02)	1.07 (0.78-1.47)	1.10 (0.91-1.34)	

²² Asterisks denote statistically significant differences (p<0.05). Abbreviations: K5M= Oculus Keratograph 5M (JENVIS grading scale)

4.5 Ocular Surface Inflammatory Evaluation (OSIE®) and ocular surface staining correlations and diagnostic utility

No significant correlations using Spearman's rank correlation tests were found between ocular surface integrity measures and the proprietary OSIE® test scores (Table 29). On account of the data distribution for this parameter, OSIE® results were dichotomously split where a score >0 was assigned as positive and all scores that were equal to 0 were assigned as negative. The predictive ability of ocular surface integrity measures to identify positive results was analysed using ROC analysis. Conjunctival staining alone, combined conjunctival and corneal staining scores and LWE scores were found to be able to predict positive OSIE® scores but corneal staining alone was not (Table 30).

Table 29. Ocular surface integrity measures and their correlations to the OSIE® scores

	Corneal staining	Conjunctival staining	Combined staining	LWE
r	-0.2403	0.0340	-0.0461	0.1563
P value	0.3169	0.7693	0.1206	0.8284

Table 30. Ocular surface integrity measures and their predictive ability to identify positive OSIE® scores

	Corneal staining (Oxford grading scheme)	Conjunctival staining (Oxford grading scheme)	Combined staining (Oxford grading scheme)	LWE (Korb's grading scheme)
C-statistic	0.5443 (0.4251-0.6635)	0.6450 (0.5312-0.7588)	0.6945 (0.5853-0.8037)	0.7326 (0.6277-0.8374)
P-value	0.4697	0.0179*	0.0015*	0.0001*
Sensitivity	84 (70-92)	84 (70-92)	84 (70-92)	84 (70-92)
Specificity	23 (14-37)	40 (28-55)	49 (35-63)	64 (50-76)

4.6 Summary

Overall, the clinical inflammation tests performed in this study demonstrated better diagnostic utility in detecting gene expression of MMP-9 in bulbar conjunctiva impression cytology samples than in detecting either of the other inflammatory markers of interest. The InflammDry® results, automated hyperaemia grading and the subjective hyperaemia grading using the Efron scale all demonstrated significant predictive ability in detecting elevated levels of MMP-9 transcripts. No clinical inflammation tests were able to predict detection of elevated levels of IL-8 gene expression in this study cohort, and only subjective grading with the VBR-5 scale was able to predict elevated levels of IL-1 β .

Of the global dry eye markers used in the diagnosis and the subclassification of dry eye disease according to the TFOS DEWS II criteria ([2](#)), reduced NIKBUT, elevated DEQ-5 score, elevated OSDI score and lipid layer grading were all predictive markers of elevated MMP-9 gene expression. Again, no parameters were able to predict IL-8 or IL-1B elevation. These results are interpreted within the context of the existing scientific literature on inflammatory processes in DED, and their application in clinical practice is discussed in Chapter 5.

Chapter 5. Discussion

5.1 Overview

Inflammation is implicated in DED, as a contributor to the chronic nature of the condition, either as a primary driver of the disease in auto-immune conditions, or as a downstream impact of triggering the vicious circle of DED ([18](#), [42](#)). Researchers have worked towards identifying biomarkers involved in the inflammatory cascade that commonly arises from tear film instability, and result in tear hyperosmolarity. Such loss of tear film homeostasis further triggers inflammation and ocular surface damage which perpetuates the cycle. However, the exact pathophysiology leading to the expression of inflammation in different subtypes of dry eye disease is yet to be fully understood. No gold standard biomarker of ocular surface inflammation exists, and there continues to be significant research efforts undertaken globally in this area. In the absence of an established gold standard, three laboratory markers (MMP-9, IL-8, IL-1 β) were chosen as being representative of currently identified biomarkers of ocular surface inflammation, for use in the research described in this thesis. These biomarkers were selected on the basis of their increased levels in dry eye disease relative to normal controls, and their varying molecular classifications as a gelatinase enzyme, chemokine and cytokine, respectively ([35](#), [57](#), [74](#), [85](#), [223](#)). Further information about the DED inflammatory cascade was described in Section 1.3.

This analysis of biomarkers was used to help address an identified literature gap – the lack of evidence-based criteria for confirming the presence of ocular surface inflammation using proxy clinical measures of inflammation. Examples of clinical proxies of interest were bulbar hyperaemia grading, the InflammDry®, an inflammation-specific point of care immunoassay and digital screening software for inflammation, and the OSIE® parameter on the Tearcheck® device. Knowledge of the optimal tests for assessing inflammation in dry eye disease could drive future hypothesis driven research to assist clinicians in identifying those patients most likely to benefit from anti-inflammatory therapy. This chapter will discuss the outcomes of this research and its potential implications for diagnosing ocular surface inflammation in DED in clinical practice.

5.2 MMP-9 and clinical dry eye disease markers

Clinical indices of dry eye that feature in the TFOS DEWS II diagnostic criteria include validated DE questionnaires and homeostatic markers such as tear osmolarity, tear film stability and ocular surface integrity. The current study outcomes demonstrate that the TFOS DEWS II diagnostic criteria for dry eye disease can, to some extent, be used to predict elevated levels of MMP-9 transcripts. MMP-9 has been implicated within the inflammatory cascade for its roles in initiation and perpetuation of ocular surface damage as described in Section 1.4.2 ([85](#), [224](#)). Although MMP-9 levels are raised in dry eye disease, it's recognised that raised MMP-9 levels are not specific to dry eye as levels are also elevated in a number of other inflammatory ocular surface conditions such as vernal keratoconjunctivitis and keratoconus ([64](#), [80](#), [82](#), [86](#), [88](#), [89](#)). Inflammation can also occur secondary to ocular surface disruption in conditions such as conjunctivochalasis, where raised MMP-9 levels have been observed ([80](#), [225](#)). Furthermore, it is recognised that dry eye disease does not always present with raised levels of MMP-9, as demonstrated in various studies where the sensitivity of MMP-9 as a marker for DED varies from 39% to 80% ([83](#), [142](#), [143](#), [226](#)).

With regard to the discriminative ability of validated dry eye questionnaires in identifying abnormal MMP-9 levels, positive symptomology scores obtained by DEQ-5 and OSDI were able to significantly predict the presence of MMP-9 transcripts, such that patients with the highest reported levels of symptoms, most often exhibited ocular surface inflammation. The Youden optimal diagnostic cut-off value was found to be >9 for the DEQ-5 test and >33.3 for the OSDI, respectively. These cut-offs are higher than the diagnostic cut-offs recommended by TFOS DEWS II, of ≥ 6 and ≥ 13 , respectively, which delineate the presence vs the absence of symptoms of dry eye disease. This confirms that clinically significant inflammation is not expected to exist in those with mild DED, but rather in those with more severe dry eye since the Youden threshold of 33.3 for the OSDI score falls well within the moderate-to-severe range of dry eye signified by scores of ≥ 22 (Table 19) ([2](#)). This supports the first hypothesis of this thesis that elevated biomarkers such as MMP-9 are present in DED, and shows, most specifically that this is most apparent in moderate-to-severe levels of DED. Other studies also found that clinically significant levels of inflammation are restricted to more severe cases ([83](#), [144](#)) In the current study, the DEQ-5 test showed higher sensitivity than the OSDI at 93%, compared to the OSDI at 64%, but a lower specificity of 39%, compared to the OSDI, with a specificity of 67%. In this context, a positive score on the DEQ-5 is more reliable at detecting ocular surface inflammation; however, the low

specificity indicates the likelihood of a high rate of false positive results, which may make the test unreliable if treatment were to be initiated based solely on this index. It should be noted that the validation of the 5-item dry eye questionnaire (DEQ-5) was performed on a study cohort consisting of a group of asymptomatic controls and a group of SS and non-SS patients with ADDE (202). As inflammation is intrinsic feature in autoimmune related ADDE, it may explain the apparently higher sensitivity of the DEQ-5 in identifying ocular surface inflammation in the previously published study, than in the current study where the cohort comprised predominantly EDE where inflammation when present is presumed to be downstream.

Of the ocular surface homeostasis markers, NIKBUT was the only dry eye index showing promise as a significant predictor of elevated levels of MMP-9 transcripts. The Youden optimal diagnostic cut-off in this case was ≤ 5.8 seconds. This was similar to the NIKBUT cut off of ≤ 5 seconds for moderate-to-severe dry eye disease severity (Table 19). Levels of MMP-9 were significantly negatively correlated with NIKBUT in this study, such that those with poorest tear film stability were found to exhibit the highest levels of inflammation. Chotikavanich et al. similarly found that increased MMP-9 levels were correlated with reduced stability measured with the fluorescein tear break up time test, as well as with increased dry eye symptom severity scores (OSDI) and decreased visual acuity (35).

As outlined in Chapter 1, the vicious circle of DED recognises tear hyperosmolarity as a key trigger of inflammation. This is supported by the work of Li et al. who conducted an experimental dry eye study confirming that exposure to a hyperosmolar medium stimulates the production of MMP-9 in human corneal epithelial cells (227). It might therefore have been expected that hyperosmolarity might correlate with increased levels of MMP-9. However, within the range of severity exhibited by the participants who feature the EDE subtype in the current study, neither tear hyperosmolarity, nor the difference in osmolarity between the two eyes, could discriminate for elevated levels of MMP-9 gene expression, and no significant correlation was found between these parameters. This is in agreement with Schargus and colleagues, who also did not find any correlation between hyperosmolarity and ELISA-derived MMP-9 obtained from Schirmer strip elution or InflammDry® results [n=20] (226). On the contrary, VanDerMeid et al. [n=30] found that MMP-9 levels in samples extracted from a Schirmer strip, subsequently analysed using multiplex immunoassay analysis, positively correlated with tear osmolarity (228). The reason for this contradictory evidence is unknown, although severity in that particular study was based only on symptoms with no other tear film homeostasis

markers being assessed. It is possible therefore that this reflected a group featuring more participants with ADDE in whom more severe DED might be expected to show a stronger relationship with inflammation. Kang et al. [n=24] found a positive correlation between the InflammDry® test results and tear film osmolarity, but only when an ordinal scale was used to assess relative positivity of the InflammDry® results. No correlation was found in the aforementioned study when analysing osmolarity results against the dichotomous InflammDry® results which are limited to a positive or negative outcome (229). Subsequent research on this immunoassay, that considers the prominence of the reaction based on the density of colour of the 'positive' test line, might offer sufficiently greater sensitivity to elicit a correlation. It should be noted that these studies used different methods of MMP-9 analysis from those employed in the current thesis, analysing MMP-9 total protein levels in tears, as opposed to gene expression analysis, which may further contribute to the discrepancy in outcomes. Notably, as explained in Section 1.4.4, eluted tears from Schirmer strips may be more representative of reflex lacrimal secretion than directly reflecting the ocular surface status, as is the case with sampling by impression cytology.

Another point worthy of consideration are the limitations arising from the method by which tear film osmolarity itself is assessed in the clinical setting. While the site of interest is arguably the exposed ocular surface, sampling is limited to taking place at the inferior tear meniscus, where it is possible to collect the required volume in a minimally invasive manner because it is where the bulk of the tear fluid over the exposed ocular surface is located. Unfortunately, peaks of osmolarity occurring across the surface of the eye at sites of tear film breakup, which are thought to exceed 800 to 900 mOsm, are not identifiable with current methods. Instead, investigators have to rely on the extreme tear hyperosmolarity that may be generated in local pockets on the surface, mixing with the remainder of the tears during blinking, and raising the overall tear osmolarity such that it can be detected as hyperosmolar in the meniscus (230). There is an accompanying risk, however, that high osmolarity in localised spots would cause sufficient discomfort due to stimulation of the corneal nerves, to induce reflex tearing as a mechanism to protect the ocular surface tissues. Should such tearing occur prior to collection of the sample from the meniscus, tear osmolarity would not be identified as being high and might even appear low, since tear fluid direct from the lacrimal gland is of slightly lower osmolarity than that on the exposed surface of the eye where it is subject to evaporation. This is an inherent issue with all studies assessing tear osmolarity as no clinical instrumentation currently exists that can assess localised osmolarity changes across the ocular surface.

The differential expression of inflammatory markers based on DED subtype was an exploratory study outcome. Inflammation is believed to play a more central role in the ADDE subtype than in the EDE subtype, most notably in Sjögren's syndrome where various inflammatory biomarkers are known to be raised ([27](#), [28](#), [59](#), [205](#), [211](#)). The proportion of ADDE in the population of DED patients is recognised to be small, and unfortunately, this was reflected in the current study's population, where only one participant qualified as exhibiting solely ADDE and five as mixed DED, with features of both ADDE and EDE. More data to allow the relationship between inflammatory markers and ADDE to be described would have been desirable but unfortunately this subtype did not satisfy sample size requirements for meaningful statistical analysis, and additional targeted recruitment to achieve the necessary sample size was not possible due to pandemic-related constraints. As a result, the thesis remains focused primarily on inflammation in the more common dry eye subtype, EDE.

The pathogenesis of inflammation in the EDE subtype is less clear than it is in ADDE, in the absence of convincing evidence that inflammation occurs within meibomian glands themselves. It is believed that ocular surface inflammation identified in cases of EDE occurs predominantly as a sequela of the ocular surface cellular damage brought about by triggering the vicious circle of DED ([18](#)). On the basis of the large sample of EDE, a low LLG proved to be predictive of elevated MMP-9 transcript levels at the ocular surface. These findings align with current understanding of the vicious circle of DED where tear instability caused by an inadequate lipid layer leads to excessive evaporation ([26](#)). This results in hyperosmolarity of the tears at the ocular surface, triggering the release of inflammatory markers and perpetuating the cycle by driving further tear film instability ([18](#), [231](#)). In this context, clinically relevant levels of inflammation would not be expected to be present in all diagnoses of DED, particularly during an earlier mild stage, but the inflammatory response is recognised to be upregulated with greater disease severity ([61](#)). The Youden optimal diagnostic cut-off value for lipid layer grades associated with inflammation was ≤ 2 , indicating that inflammation was present in those with the thinnest lipid layer grades. Yokoi et al. found evidence that a thin lipid layer significantly correlated to dry eye severity ([232](#)) and a thin lipid layer is known to be associated with reduced tear film stability ([26](#)). Our findings showed that lipid layer thickness was significantly correlated to MMP-9 transcripts, which reflects the presence of inflammation in the current context. This lends further support to the hypothesis that inflammation plays a more significant role in moderate-to-severe dry eye disease ([223](#),

[226](#), [232](#), [233](#)) and aligns with literature describing a negative correlation between symptom severity and lipid layer thickness ([233](#)).

5.3 MMP-9 and clinical markers of inflammation

Six clinical tests purported to provide an index of inflammation in DED, were evaluated for their diagnostic utility. The measures included subjective grading against three bulbar conjunctival hyperaemia grading schemes (broad clinical impression ranging from none to severe); the Efron grading scale; VBR-5 grading scale). as well as, one objective bulbar conjunctival hyperaemia grading device (utilising the JENVIS scale on the Oculus K5M), the presence of inflammation as indicated by the InflammaDry® point-of-care MMP-9 test, and the Ocular Surface Inflammatory Evaluation (OSIE®) score from the Tearcheck® device. Ocular surface staining was included as a fundamental test of ocular surface integrity. Further test details are provided in Chapter 2 and the results of the comparative analyses are outlined in Table 26.

The objective measurement of bulbar hyperaemia using the JENVIS grading scale was determined to be a better clinical test of inflammation than subjective grading, on the basis of its ability to predict increased levels of MMP-9 gene expression. Additionally, a positive, albeit non-statistically significant trend of correlation between MMP-9 and objective hyperaemia grading was noted. The sensitivity of objective bulbar hyperaemia grading was high at 86%. A significant limitation of the objective measurement of hyperaemia arises when highlighted areas do not accurately capture bulbar and limbal areas or mistakenly include the lid margins and the eyelids in the hyperaemia evaluation, considerably skewing the results. This could explain the high false negative rate seen in the specificity value of 64%. Therefore, the reliability of the objective measure of bulbar hyperaemia should be interpreted with caution, and clinicians should review the captured image and bulbar area is free from artefact before proceeding to manage patients based on numerical test scores alone.

Using the Efron grading system, subjective measures of bulbar hyperaemia also demonstrated significant discriminative ability in predicting elevated expression of MMP-9 transcripts in conjunctival cells, satisfying the second hypothesis of this thesis. The result in Chapter 3 demonstrated only modest inter-observer agreement when using the Efron grading system which might suggest that caution should be exercised if relying on subjective grading of bulbar hyperaemia to detect gene expression of inflammatory markers on the

ocular surface, especially where patients may be seen by one of a number of clinicians in a practice. Nonetheless, of the various grading scales tested, the Efron grading scheme was found to work well and should give clinicians confidence in grading hyperaemia in this way.

Based on the findings outlined in Chapter 3, a high level of agreement was found to exist between the scores on the VBR-5 scale and those of objective bulbar hyperaemia grading via the K5M. Surprisingly, though, the VBR scale was less indicative of inflammation than the Efron scale, which might be related to the larger area of ocular surface coverage in the photographic image compared to the Efron artistic representations. The Efron images do not include the lateral canthus, which in the VBR photographs is the area of most pronounced redness, reflecting the concentrated collection of all the visible blood vessels depicted on the image. A significant positive correlation was found between both the subjective grading scale hyperaemia scores (Efron and VBR-5) and the objective K5M scores, confirming the third hypothesis of this study. Furthermore, the overall clinical impression of bulbar hyperaemia as none, mild, moderate or severe performed most poorly, of all the clinical methods tested, as a model for predicting elevated levels of MMP-9 transcripts. Although exhibiting slightly greater specificity than found with objective hyperaemia grading (76% vs 64%), the sensitivity of clinical impression grading was much lower (29% vs 86%). This suggests that relying on a practitioner's clinical approximation of bulbar hyperaemia severity is a poor predictor of cellular levels of inflammation and would support recommendations for the adoption of a clinical grading scale in practice over relying on individual subjective evaluation.

Based on its dichotomous outcomes, the InflammDry® immunoassay was able to predict the presence of MMP-9 mRNA transcripts in this study significantly better than chance, suggesting that both tests are broadly in agreement when identifying patients with elevated levels of inflammation. It is recognised that not all patients with DED return a positive InflammDry® test result and that MMP-9 is more likely to be elevated in higher severity of dry eye disease (83). This was confirmed from the findings of the current study. The sensitivity and specificity of this test in identifying inflammation were found to be 64% and 58% respectively. Although these values show limited confidence in the InflammDry®, sensitivity in this context refers to how accurately the InflammDry® can detect disease relative to the gold-standard, which in this case was taken for the purpose of this study to be the gene copy number of mRNA transcripts of MMP-9 in the conjunctival

cell sample. However as mentioned in the introduction of this thesis, there is no globally agreed gold-standard biomarker of DED-related inflammation. The positive likelihood ratio (1.52) confirmed the screening utility of the InflammDry® in its ability to identify increased levels of MMP-9 (234). The negative likelihood ratio was reported as 0.62, indicating that the InflammDry® is not as good at identifying true negatives as it is identifying true positives from this cohort. In conclusion, confirming the fourth and last hypothesis of this study, the InflammDry® test has value as a screening test for inflammation, but should the test outcome be negative, the presence of clinically significant inflammation should not be dismissed without considering other parameters indicative of ocular surface inflammation.

MMP-9 causes disruption of the corneal epithelium leading to ocular staining due to increased permeability, and this has been found to increase in animal models when desiccating stress is applied (224, 235). Given this, and knowing the established direct role of MMP-9 in promoting corneal epithelial disruption (224, 236), it might be anticipated that corneal staining and inflammation would be directly related. However, the data did not support any such hypothesis, with the severity of ocular surface staining failing to show a significant ability to discriminate increased levels of MMP-9 gene expression on the ocular surface in the present study. Ocular staining has been identified by Wang et al. as a very late stage clinical marker to emerge in the natural history of dry eye disease, possibly indicating that an association between ocular surface disruption and inflammation might become more apparent in later stages of DED than those exhibited by the participants in the current study (11).

The proprietary test termed the Ocular Surface Inflammatory Evaluation (OSIE®) did not significantly correlate with the conjunctival or corneal staining scores, either alone or in combination, nor with lid wiper epitheliopathy scores. No significant correlation was found between the OSIE® test and MMP-9, IL-8 or IL-1 β gene copy numbers. In addition, the OSIE® results were unable to predict elevation of MMP-9, IL-8 or IL-1 β . An attempt was made to uncover the staining measure to which the OSIE® was most closely aligned. The conjunctival staining scores, combined conjunctival and corneal staining scores and the LWE scores were able to predict the presence of a positive vs negative OSIE® result. However, no significant correlations could be found between the severity of these staining parameters and severity of the OSIE® result. This emphasises the need for novel metrics built into dedicated software in new technology. to be

scientifically validated before making clinical decisions relating to patient management. More research is required to confirm the utility of the OSIE® parameter in diagnosing and helping direct management of DED. The range of severity of DED in this study cohort was relatively limited and it is possible that different outcomes would have arisen if evaluations were conducted on a broader range of DED severities and subtypes.

5.4 IL-8 as a biomarker for inflammation

In this study of predominantly EDE secondary to MGD, no clinical markers of inflammation were found to be predictive of elevated levels of IL-8 mRNA transcripts. Whether a relationship between clinical tear film or inflammatory measures and IL-8 might have been demonstrated with ADDE is not known, although this may have been more likely. As a chemokine, IL-8 is involved in the pathogenesis of dry eye disease showing raised levels in the disease, especially among patients with Sjögren's syndrome relative to normal controls ([35](#), [57](#), [63](#), [77](#)). The chemokine is a neutrophil-specific chemoattractant that is secreted by epithelial cells and neutrophils ([237](#)). In addition, IL-8 is known to be secreted by neutrophils which are activated by SS-associated auto-antigen Sjögren syndrome type B or lupus La ([238](#)).

The clinical dry eye disease and subtype markers also showed no significant discriminative ability to predict elevated levels of IL-8 transcripts, however once again the lack of number of ADDE participants means no definitive conclusion can be drawn from this study in terms of differences in inflammatory presentation of DED subtypes, and further research in this dry eye subtype is warranted.

5.5 IL-1 β and clinical markers of inflammation

Subjective grading of bulbar hyperaemia using the VBR-5 scale was able to predict elevated levels of IL-1 β better than chance. The Youden optimal diagnostic cut-off value was >21.5, based on its scale that ranges from 0 to 100. As a single index, this result should be interpreted with caution as no other subjective or objective hyperaemia grading method, ocular staining scores or dry eye diagnostic marker had diagnostic utility to predict elevated levels of IL-1 β .

IL-1 β has been implicated in the inflammatory cascade, with direct relation to MMP-9 in that it is an activator of pro-MMP-9 in the extracellular space. It has also been shown to be raised in tear fluid and mRNA by

Massingale et al. (63). IL-1 β , along with IL-1 α , are the proinflammatory forms of IL-1, which have been implicated in several other inflammatory diseases such as rheumatoid arthritis, periodontitis and septic shock (239, 240). Plugfelder et al. reported that IL-1, 6, 8 and TNF- α were elevated in SS compared to normal subjects (77). Conversely, Enríquez-de-Salamanca et al. and Narayanan et al. reported that symptomatic, moderate severity dry eye patients showed no increase in IL-8 or IL-1 β compared to normal controls (61, 241). Interestingly, there was a significant positive correlation observed between the number of IL-8 and IL-1 β gene copies in the current study. This evidence suggests that IL-1 β is still implicated in the inflammatory cascade of DED, however its upregulation could be further upstream as an activator of pro-MMP-9, existing as more of an intermediary mediator. Its concentration could also follow nonlinear kinetics, which was not considered in the ROC analysis, where the median gene copy number was used as the cut off to determine upregulation of the gene.

5.7 Study limitations and future directions

As described in the aims of this thesis, there is no agreed gold standard inflammatory biomarker specific to dry eye disease. MMP-9, IL-8 and IL-1 β were chosen to represent different classes of inflammatory markers to try and capture different stages of the inflammatory cascade that ensues in dry eye pathogenesis. The laboratory test chosen to analyse these biomarkers was the highly sensitive dd-PCR, however a limitation is the restriction on the number of inflammatory markers it was possible to analyse in this study. Future studies might consider comparing clinical measures of inflammation against other molecules such as IL-6, TNF- α and IFN- γ to further identify strengthen the correlation and diagnostic utility of clinical tests that are readily available to eye care practitioners.

As identified in this chapter, the objective measurement of hyperaemia shows promising results in its ability to predict MMP-9 gene copy elevations, however its algorithm can be subject to inaccuracies in defining the area of interest. This in turn could result in subjective measures of bulbar hyperaemia proving more accurate at times and thus clinicians should be cautious in relying upon the objective outcome as a stand-alone numerical value to guide patient management. To improve this objective measure, an option to manually select the area of interest, or override that estimated by the device algorithm, could be designed into the proprietary software as a back-up option for users of this device. As Peterson et al. proved, the adoption of

objective methods of identifying ocular surface inflammation offer more sensitivity and greater reliability than subjective techniques, however this would only apply if the inaccuracies relating to the area selected for assessment can be mitigated ([136](#)).

Due to participant recruitment being severely restricted in the duration of this thesis, participants with EDE and the association of inflammation tests remained the primary focus. In the future, further investigations could usefully be conducted with ADDE participants, particularly autoimmune-related ADDE such as Sjögren's syndrome to help understand relative levels of inflammation between ADDE and EDE subtypes which could contribute to our knowledge about the inflammatory pathways involved in different subtypes of DED.

Despite MMP-9 levels showing diurnal variation in a paper produced by Markoulli et al., it is unlikely that these fluctuations would have affected our study ([94](#)). The study found that healthy individuals had elevated MMP-9 levels of 200-fold on awakening, but these levels were fully inhibited by TIMP-1 by midday ([94](#)). Although none of our study participants had conjunctival samples collected immediately after awakening, the study could have been strengthened by collecting all specimens within a limited time period after midday, to minimise any impact of diurnal variation.

Future research directions could involve assessing how study participants, identified to have in-clinic markers of inflammation that suggest elevated MMP-9 gene expression, respond to different anti-inflammatory treatments. In this study design, inflammation-proxy measures such as subjective and objective hyperaemia grading scores, InflammDry® results could be recorded pre- and post- administration of various anti-inflammatory therapies and conventional dry eye therapies, to refine treatment protocols, and offer a more targeted treatment plan based on the baseline characteristics of the patient. This could be of prognostic value, providing clinicians with more accurate, evidence-based information regarding anticipated responses to different therapeutic strategies. The ability to make informed decisions would encourage optimal engagement of patients in working with their clinician to select their treatment.

5.8 Seeking to manage inflammation in DED

Inflammation is a key feature in the vicious circle of dry eye disease. Loss of homeostasis in tear film mechanisms leads to a hyperosmolarity-triggered inflammatory cascade, provoking and helping perpetuate the vicious circle (18). A range of inflammatory molecules are escalated in dry eye disease; however, more research is required to establish variations that might exist in the inflammatory processes between different dry eye subtypes. Currently, inflammation is accepted to be a fundamental contributor to dry eye disease pathophysiology in aqueous deficient dry eye, especially in autoimmune disease such as Sjogren's syndrome where there is already an underlying systemic inflammatory condition prior to the triggering of the vicious cycle in the ocular surface (242). In contrast, meibomian gland dysfunction allows excess tear evaporation due to a poorly functioning lipid layer secondary to inadequate production and/or quality of meibum and, in this case, the inflammation of the ocular surface is thought to occur as a downstream consequence of the resultant tear hyperosmolarity (18, 242) in contrast to being driven by underlying local or systemic inflammation.

5.8.1 Anti-inflammatory therapies

Increasingly, contemporary dry eye treatments are being developed to target the underlying inflammation when the DED severity is moderate or severe, in preference to more palliative options such as artificial lubricants. Topical treatments available in some parts of the world include anti-inflammatories such as lifitegrast, corticosteroids of varying potency and penetration potential, immunomodulators such as cyclosporin (5) and oral antibiotics including tetracyclines such as doxycycline and azithromycin (40). Their use is not risk free, however, therefore it is important that clinicians ensure the benefits from use of such therapies outweighs their potential to generate unwanted side effects, particularly since it is recognised that underlying inflammation is not the source of dry eye disease in all patients (83). Topical steroid use is associated with the increased risk of cataracts, elevated IOP and infection development (243, 244). This was reflected in the outcomes of a study by Prabhasawat and Tseng (245) [n=70] where despite managing the dry eye symptoms, one patient had intraocular pressure (IOP) elevation and two had developed cataracts by the 6-month follow up in a cohort of 70 patients. On reporting the efficacy of using cyclosporin A, an immunomodulator used in the treatment of DED, Perry et al. [n=158] reported 72.1% of participants showing improvement in signs and symptoms, however no placebo group was utilised (246).

Pflugfelder et al. reported that cyclosporin and Lifitegrast both inhibit T cell activation and cytokine production; however, both treatments are not effective in all patients with DED, further emphasising the need to improve diagnostic ability to detect clinically significant inflammation in an attempt to identify the baseline characteristics of the patients most likely to respond favourably ([42](#), [175](#), [246](#), [247](#)).

5.8.2 Role of anti-inflammatory therapies in MGD

MGD-related EDE is associated with downstream rather than intrinsic inflammation such as in Sjögren's syndrome related ADDE. Where the source of the DED is identified as MGD, there is the potential for a wide range of therapies such as intense pulsed light therapy (IPL) and warm compress therapy to resolve the source problem. This can improve tear film instability, thereby restoring homeostasis to the ocular surface. Management with corticosteroids or other anti-inflammatories fails to resolve the underlying source of the DED that is triggering inflammation in the majority of EDE cases. Although some signs and symptoms may temporarily improve during the course of corticosteroid treatment, problems associated with MGD will return on cessation of the drops, which serves to encourage patient reliance on the anti-inflammatory. This is an issue because of the side effects associated with long term corticosteroid use ([244](#)). Immunomodulators are indicated in SS-DED to reduce circulating T cells, thereby increasing lacrimal gland function. This is distinct from the pathophysiology of MGD and therefore treatment for the dry eye subtypes can differ. First line conventional therapies to treat MGD include the regular use of artificial tears and warm compresses followed by eyelid massage ([248](#), [249](#)). Craig et al. suggested that regular lipid-containing eyedrop use four times a day has the potential to break the vicious circle and over a number of months can result in improvements in tear quality, as well as the more immediate symptomatic relief that is observed within a month of commencing topical drops ([248](#)). If patient-applied therapies are unsuccessful in resolving the effects of MGD, in-clinic treatments such as IPL and LipiFlow may be recommended. IPL has been shown to reduce MMP-9 levels, reduce inflammatory cells around the glandular structures and reduce conjunctival and limbal injection in patients with MGD ([145](#), [250](#), [251](#)).

Chapter 6 Conclusion

The research reported in this thesis demonstrated potential indicators in a clinical examination that could predict the presence of clinically significant inflammation in evaporative dry eye patients. With regards to the inflammatory markers chosen in this study, optimal diagnostic utility was demonstrated by the presence of MMP-9 gene expression, compared to IL-8 and IL-1 β . This could indicate that IL-8 and IL-1 β have further upstream implications, at least in the EDE subtype. It is possible that outcomes for ADDE may differ but could not be confirmed in the current study due to pandemic impacts on participant recruitment within the time constraints of this thesis.

Of the TFOS DEWS II diagnostic dry eye disease markers, NIBUT and lipid layer grading showed the best ability to discriminate elevated levels of MMP-9 transcripts. The cut off values of ≤ 5.8 seconds and ≤ 2 respectively fall within the moderate-to-severe range of DED. In addition, the OSDI and DEQ-5 symptomatology questionnaires predicted elevated levels of MMP-9 transcripts, with diagnostic cut-off values set at higher values than the TFOS DEWS II requirement for diagnosis, similarly indicating that the presence of inflammation is limited to the more severe cases of EDE. The current study has provided a useful starting point for future research to determine the level of inflammation that might optimally benefit from anti-inflammatory therapy or, indeed, whether the inflammation present will resolve adequately if the MGD itself is managed. Successful MGD management with lid warming and hygiene has the potential to restore homeostasis by improving the lipid layer and tear film stability, breaking the vicious circle of DED which may avoid the need for anti-inflammatory therapy and its attendant risks. Determining thresholds for instigating treatment will be valuable, as it is not inconceivable that patients with more severe DED might benefit from a short course of topical steroid therapy in combination with long term MGD management for optimal disease resolution.

The clinical inflammatory markers that best predicted elevated levels of MMP-9 were found to be objective bulbar conjunctival hyperaemia grading (Oculus K5M), subjective bulbar conjunctival hyperaemia grading (Efron scale), and the InflammDry® test result.

The InflammaDry® test could be a useful screening tool for the presence of clinically significant inflammation, however clinicians should not dismiss the diagnosis of ocular surface inflammation in the event the result is negative.

In Chapter 3, it was established that existing subjective and objective grading scales used to assess bulbar hyperaemia cannot be used interchangeably. The results of Chapter 3 suggest that a single grading scale per practice should be used to assess bulbar hyperaemia, and where possible the same clinician should manage the same patient. However, in clinical practice, this is not always feasible, in which care should be taken that the same grading scale is utilised by different clinicians. The Efron scale provided the best predictability of MMP-9 elevation along with smaller inter-observer repeatability than that of the VBR-5 scale. If available, an objective measure of hyperaemia is preferable as this can better predict the presence of inflammation over subjective measures which has also been found to reduce inter and intra observer variation. However, the results should be accepted with caution, ensuring the intended area of the eye is being measured.

The sensitivity of PCR testing is generally 30-40% higher than a point-of-care immunoassays as seen in the SARS-CoV-2 infection testing, despite their relative convenience of use ([252](#)). However, dd-PCR is expensive and time-consuming, and is thus out of reach of the clinical optometrist. This study presented an opportunity to test a range of clinical tests against a laboratory measure that would normally be inaccessible to the clinician, in an attempt to contribute to the evidence-based recommendations to clinicians about which of the routine clinical tests might offer the greatest amount of information about the 'true' inflammatory status in EDE. This information could ultimately assist clinicians in making treatment decisions. Similarly to the need for a wide battery of clinical tests to diagnose and subclassify DED, it appears that no single clinical marker can yet be used exclusively to reliably characterise a process as complex as the inflammatory cascade in ocular surface disease. The findings of this thesis suggest various tests such as the Efron grading system for bulbar hyperaemia along with validated questionnaire results and lipid layer grade results might be useful in helping guide DED management for clinicians.

Appendix A: Permission agreement for replication of the Efron hyperaemia grading scale

RightsLink Printable License

ELSEVIER LICENSE TERMS AND CONDITIONS

Jun 20, 2022

This Agreement between Miss. Catherine Shon ("You") and Elsevier ("Elsevier") consists of your license details and the terms and conditions provided by Elsevier and Copyright Clearance Center.

License Number	5306241232555
License date	May 11, 2022
Licensed Content Publisher	Elsevier
Licensed Content Publication	Elsevier Books
Licensed Content Title	Contact Lens Practice
Licensed Content Author	Richard G. Lindsay
Licensed Content Date	Jan 1, 2018
Licensed Content Pages	3
Start Page	453
End Page	455
Type of Use	reuse in a thesis/dissertation
Portion	figures/tables/illustrations
Number of figures/tables/illustrations	1

<https://s100.copyright.com/CustomAdmin/PLF.jsp?ref=021f923d-56b3-491a-b385-a6e54ac44254>[20/06/2022 4:23:25 pm]

Appendix B. Permission to replicate the Validated Bulbar Redness scale

RightsLink Printable License

WOLTERS KLUWER HEALTH, INC. LICENSE TERMS AND CONDITIONS

Jun 20, 2022

This Agreement between Miss. Catherine Shon ("You") and Wolters Kluwer Health, Inc. ("Wolters Kluwer Health, Inc.") consists of your license details and the terms and conditions provided by Wolters Kluwer Health, Inc. and Copyright Clearance Center.

License Number	5306831210656
License date	May 12, 2022
Licensed Content Publisher	Wolters Kluwer Health, Inc.
Licensed Content Publication	Optometry and Vision Science
Licensed Content Title	The Development of Validated Bulbar Redness Grading Scales
Licensed Content Author	MARC SCHULZE, DEBORAH JONES, and TREFFORD SIMPSON
Licensed Content Date	Oct 1, 2007
Licensed Content Volume	84
Licensed Content Issue	10
Type of Use	Dissertation/Thesis
Requestor type	University/College
Sponsorship	No Sponsorship

[https://s100.copyright.com/CustomAdmin/PLF.jsp?ref=393e4ab7-9f18-45ba-82da-8fba72784dd\[20/06/2022 4:26:37 pm\]](https://s100.copyright.com/CustomAdmin/PLF.jsp?ref=393e4ab7-9f18-45ba-82da-8fba72784dd[20/06/2022 4:26:37 pm])

Appendix C: Study participant information sheet

DEPARTMENT OF OPHTHALMOLOGY

Faculty of Medical and Health Sciences

Prof. Jennifer P. Craig
BSc (Hons) MSc (Cataract & Refractive Surgery) PhD FCOptom FAAO FBCLA FRCLSA
Associate Professor



**MEDICAL AND
HEALTH SCIENCES**

Building 504, 4th Floor
85 Park Road, Grafton
Auckland 1023, New Zealand
Telephone 64 9 923 8173
Facsimile 64 9 367 7173
Email: jp.craig@auckland.ac.nz
www.ophtalmology.auckland.ac.nz

The University of Auckland
Private Bag 92019
Auckland 1142,
New Zealand

PARTICIPANT INFORMATION SHEET

Project Title: Diagnosing Inflammation in Dry Eye Disease

M

Researcher(s): Prof. Jennifer P. Craig, Ms Catherine Shon, Mr Isaac Samuels, Dr Alex Muntz

Researcher Introduction and Project Background:

Thank you for taking the time to read this information sheet. This information sheet covers many study details so please feel free to contact us if you have any further questions. You are welcome to share and discuss this information sheet with friends and/or whānau, before deciding to participate in this study.

I am **Catherine Shon**, an NZ registered therapeutic optometrist pursuing a Masters of Health Science under the supervision of **Professor Jennifer Craig**, an NZ registered therapeutic optometrist. This study is conducted in the Ocular Surface Laboratory at the Grafton site at the University of Auckland, where I may be assisted by 5th year MBChB student, **Isaac Samuels**.

Dry eye disease is a common eye disorder. Patients typically experience gritty, irritated, sometimes watery eyes and poor vision. The complex disease mechanism may involve inflammation, however, there is no agreed method for measuring inflammation in a clinical setting. If clinicians could assess inflammation more easily and consistently, treatment and management decisions may be better guided to improve patient outcomes.

In this study, we are evaluating different ways of diagnosing inflammation in dry eye disease. We will be using standard non-invasive clinical imaging devices [Keratograph 5M (Oculus), Tearcheck (E-Swin)], and a common in-office point of care test [Inflammadry (Quidel)] and comparing these methods to laboratory analysis of inflammation. We hope that at the conclusion of this research we will be able to recommend an optimal technique for diagnosing inflammation in dry eye disease to clinicians so that patients can be offered the most appropriate treatment.

Study Description:

In the first instance, contact will be made over phone or email where you will be asked questions to determine your eligibility for the study. If eligible, we will schedule a single study visit (lasting up to 1 hour) at the Grafton Eye Clinic, to undergo clinical assessment, at your convenience.

**Approved by the Auckland Health Research Ethics Committee on 27 July 2021 for three years.
Reference number AH22183.**

Appendix E: Table of primer and probe nucleotide sequences

Gene Target	Assay	Forward and Reverse Primers and Probes	Catalogue number
INHIBITION ASSAY			
SPUD		(F) 5'- AAC TTG GCT TTA ATG GAC CTC CA -3'	99726095
		(R) 5'- ACA TTC ATC CTT ACA TGG CAC CA -3'	99726096
BETA-ACTIN ASSAY			
Beta-Actin		(F) 5'- AAC TCC ATC ATG AAG TGT GAC G -3'	783462
		(R) 5'- GAT CCA CAT CTG CTG GAA GG -3'	783463
DROPLET DIGITAL PCR			
MMP-9	Gene of interest	(F) 5'-CHTCGAAATGGGCGTCT-3' (R) 5'-ACATCGTCATCCAGTTTGGTG-3' (P) 5'-/56-FAM/CCAGGAGGA/ZEN/AAGGCGTGTGC/3IABkFQ/-3'	10092307 6
Interleukin 8 (IL-8)	Gene of interest	(F) 5'-AATTTTCATTGCCACAAAGTTGATG-3' (R) 5'-CAGACCTTCCAGATCGCTTC-3' (P) 5'-56-FAM/TGTCTTCTA/ZEN/CTGGTTCAGCAGCCATC/3IABkFQ/-3'	

Interleukin 1 beta (IL-1 β)	Gene of interest	(F) 5'-GAACAAGTCATCCTCATTGCC-3' (R) 5'-CAGCCAATCTTCATTGCTCAAG-3' (p) 5'-/56-FAM/AGAAGTACC/ZEN/TGAGCTCGCCAGTGA/3IABkFQ/-3'	
PPIA	Reference gene	(F) 5'-CAAGACTGAGATGCACAAGTG-3' (R) 5'-GTGGCGGATTTGATCATTGG-3' (P) 5'-/5HEX/AATTCCGC/ZEN/AGAAGGAACCAGACAGT/3IABkFQ/-3'	101136876
RPLP0	Reference Gene	(F) 5'-TGTCTGCTCCCACAATGAAAC-3' (R) 5'-TCGTCTTTAAACCCTGCGTG-3' (P) 5'-5HEX/CCTGTCTT/ZEN/CCCTGGGCATCAC/3IABkFQ/-3'	101136872
POLR2A	Reference Gene	(F) 5'-TCGTCTCTGGGTATTTGATGC-3' (R) 5'-CAGTTCGGAGTCCTGAGTC-3' (P) 5'-/5HEX/ACTGAAGCG/ZEB/AATHTCTHTHACHHAH/3IABkFQ/-3'	101136868
TBP	Reference Gene	(F) 5'-CAGCAACTTCCTCAATTCCTTG-3' (R) 5'-GCTGTTAACTTCGCTTCCG-3' (P) 5'-/5HEX/TGATCTTTG/ZEN/CAGTGACCCAGCATCA/3IABkFQ/-3'	1136860
B2M		(F) 5'-CAGCAACTTCCTCAATTCCTTG-3' (R) 5'-GCTGTTAACTTCGCTTCCG-3' (P) 5'-/5HEX/TGATCTTTG/ZEN/CAGTGACCCAGCATCA/3IABkFQ/-3'	101136860

GUSB		(F) 5'-GTTTTTGATCCAGACCCAGATG-3' (R) 5'-GCCATTATTCAGAGCGAGTA-3' (P) 5'- /5HEX/TGCAGGGTT/ZEN/TCACCAGGATCCAC/3IABkFQ/-3'	10113686 4
HPRT1		(F) 5'-TTGTTGTAGGATATGCCCTTGA-3' (R) 5'-GCGATGTCAATAGGACTCCAG-3' (P) 5'- /5HEX/AGCCTAAGA/ZEN/TGAGAGTTCAAGTTGAGTTTGG/3IA BkFQ/-3'	10500808 0

References

1. Wang MTM, Dean SJ, Muntz A, Craig JP. Evaluating the diagnostic utility of evaporative dry eye disease markers. *Clinical and Experimental Ophthalmology*. 2020;48(2):267-70.
2. Wolffsohn JS, Arita R, Chalmers R, Djalilian A, Dogru M, Dumbleton K, et al. TFOS DEWS II Diagnostic Methodology report. *Ocular Surface*. 2017;15(3):539-74.
3. Craig JP, Nichols KK, Akpek EK, Caffery B, Dua HS, Joo CK, et al. TFOS DEWS II Definition and Classification Report. *Ocular Surface*. 2017;15(3):276-83.
4. Wang MTM, Vidal-Rohr M, Muntz A, Diprose WK, Ormonde SE, Wolffsohn JS, et al. Systemic risk factors of dry eye disease subtypes: A New Zealand cross-sectional study. *Ocular Surface*. 2020;18(3):374-80.
5. Anderson DKLJW, Catherine L. Advances in Dry Eye Disease Treatment. *Physiology and Behavior*. 2017;176(5):139-48.
6. Wolffsohn JS, Wang MTM, Vidal-Rohr M, Menduni F, Dhallu S, Ipek T, et al. Demographic and lifestyle risk factors of dry eye disease subtypes: A cross-sectional study. *Ocul Surf*. 2021;21:58-63.
7. Bakkar MM, Shihadeh WA, Haddad MF, Khader YS. Epidemiology of symptoms of dry eye disease (DED) in Jordan: A cross-sectional non-clinical population-based study. *Contact Lens and Anterior Eye*. 2016;39(3):197-202.
8. Uchino M. What We Know About the Epidemiology of Dry Eye Disease in Japan. *Invest Ophthalmol Vis Sci*. 2018;59(14):DES1-DES6.
9. Kuo YK, Lin IC, Chien LN, Lin TY, How YT, Chen KH, et al. Dry Eye Disease: A Review of Epidemiology in Taiwan, and its Clinical Treatment and Merits. *J Clin Med*. 2019;8(8):1227.
10. Lemp MA, Crews LA, Bron AJ, Foulks GN, Sullivan BD. Distribution of aqueous-deficient and evaporative dry eye in a clinic-based patient cohort: A retrospective study. *Cornea*. 2012;31(5):472-8.
11. Wang MTM, Muntz A, Lim J, Kim JS, Lacerda L, Arora A, et al. Ageing and the natural history of dry eye disease: A prospective registry-based cross-sectional study. *Ocul Surf*. 2020;18(4):736-41.
12. Stapleton F, Alves M, Bunya VY, Jalbert I, Lekhanont K, Malet F, et al. TFOS DEWS II Epidemiology Report. *Ocul Surf*. 2017;15(3):334-65.
13. Portello JK, Rosenfield M, Chu CA. Blink rate, incomplete blinks and computer vision syndrome. *Optometry and Vision Science*. 2013;90(5):482-7.
14. Wang MT, Chan E, Ea L, Kam C, Lu Y, Misra SL, et al. Randomized trial of desktop humidifier for dry eye relief in computer users. *Optometry and Vision Science*. 2017;94(11):1052-7.

15. Uchino M, Nishiwaki Y, Michikawa T, Shirakawa K, Kuwahara E, Yamada M, et al. Prevalence and risk factors of dry eye disease in Japan: Koumi study. *Ophthalmology*. 2011;118(12):2361-7.
16. Cher I. A New Look at Lubrication of the Ocular Surface: Fluid Mechanics Behind the Blinking Eyelids. *The Ocular Surface*. 2008;6(2):79-86.
17. Willcox MDP, Argüeso P, Georgiev GA, Holopainen JM, Laurie GW, Millar TJ, et al. TFOS DEWS II Tear Film Report. *Ocular Surface*. 2017;15(3):366-403.
18. Bron AJ, de Paiva CS, Chauhan SK, Bonini S, Gabison EE, Jain S, et al. TFOS DEWS II pathophysiology report. *Ocular Surface*. 2017;15(3):438-510.
19. Foulks GN, Forstot SL, Donshik PC, Forstot JZ, Goldstein MH, Lemp MA, et al. Clinical guidelines for management of dry eye associated with Sjögren disease. *Ocular Surface*. 2015;13(2):118-32.
20. Nichols KK, Foulks GN, Bron AJ, Glasgow BJ, Dogru M, Tsubota K, et al. The international workshop on meibomian gland dysfunction: executive summary. *Investigative Ophthalmology and Visual Science*. 2011;52(4):1922-9.
21. Arita R, Itoh K, Inoue K, Amano S. Noncontact infrared meibography to document age-related changes of the meibomian glands in a normal population. *Ophthalmology*. 2008;115(5):911-5.
22. Dougherty JM, McCulley JP. Bacterial lipases and chronic blepharitis. *Investigative Ophthalmology and Visual Science*. 1986;27(4):486-91.
23. Dougherty JM, McCulley JP. Comparative bacteriology of chronic blepharitis. *British journal of ophthalmology*. 1984;68(8):524-8.
24. McCulley JP, Dougherty J. Bacterial aspects of chronic blepharitis. *Transactions of the ophthalmological societies of the United Kingdom*. 1986;105:314-8.
25. Driver PJ, Lemp MA. Meibomian gland dysfunction. *Survey of ophthalmology*. 1996;40(5):343-67.
26. Craig JP, Tomlinson A. Importance of the lipid layer in human tear film stability and evaporation. *Optometry and Vision Science*. 1997;74(1):8-13.
27. Craig JP, Wang MT, Kim D, Lee JM. Exploring the Predisposition of the Asian Eye to Development of Dry Eye. *Ocul Surf*. 2016;14(3):385-92.
28. Wang MTM, Tien L, Han A, Lee JM, Kim D, Markoulli M, et al. Impact of blinking on ocular surface and tear film parameters. *Ocular Surface*. 2018;16(4):424-9.
29. Arita R, Itoh K, Inoue K, Kuchiba A, Yamaguchi T, Amano S. Contact lens wear is associated with decrease of meibomian glands. *Ophthalmology*. 2009;116(3):379-84.
30. Akpek EK, Klimava A, Thorne JE, Martin D, Lekhanont K, Ostrovsky A. Evaluation of patients with dry eye for presence of underlying Sjögren syndrome. *Cornea*. 2010; 28(5):493-7.
31. Vitali C, Del Papa N. Chapter 4 - Classification Criteria for Sjögren's Syndrome. In: Gerli R, Bartoloni E, Alunno A, editors. *Sjögren's Syndrome*: Academic Press; 2016. p. 47-60.
32. Yagci A, Gurdal C. The role and treatment of inflammation in dry eye disease. *International Ophthalmology*. 2014;34(6):1291-301.

33. Barabino S, Chen Y, Chauhan S, Dana R. Ocular surface immunity: Homeostatic mechanisms and their disruption in dry eye disease. *Progress in Retinal and Eye Research*. 2012;31(3):271-85.
34. Rhee MK, Mah FS. Inflammation in Dry Eye Disease: How Do We Break the Cycle? *Ophthalmology*. 2017;124(11):S14-S9.
35. Akpek EK, Wu HY, Karakus S, Zhang Q, Masli S. Differential Diagnosis of Sjögren Versus Non-Sjögren Dry Eye Through Tear Film Biomarkers. *Cornea*. 2020;39(8):991-7.
36. Fernandez Castro M, Sánchez-Piedra C, Andreu JL, Martínez Taboada V, Olivé A, Rosas J. Factors associated with severe dry eye in primary Sjögren's syndrome diagnosed patients. *Rheumatology International*. 2018;38(6):1075-82.
37. Knop E, Knop N, Millar T, Obata H, Sullivan DA. The international workshop on meibomian gland dysfunction: Report of the subcommittee on anatomy, physiology, and pathophysiology of the meibomian gland. *Investigative Ophthalmology and Visual Science*. 2011;52(4):1938-78.
38. Suzuki T. Inflamed Obstructive Meibomian Gland Dysfunction Causes Ocular Surface Inflammation. *Investigative Ophthalmology and Visual Science*. 2018;59(14):DES94-DES101.
39. Stern M, Schaumburg C, Dana R, Calonge M, Niederkorn J, Pflugfelder S. Autoimmunity at the ocular surface: pathogenesis and regulation. *Mucosal Immunology*. 2010;3(5):425-42.
40. Ganesalingam K, Ismail S, Sherwin T, Craig JP. Molecular evidence for the role of inflammation in dry eye disease. *Clinical and Experimental Optometry*. 2019;102(5):446-54.
41. Yamaguchi T. Inflammatory response in dry eye. *Investigative Ophthalmology and Visual Science*. 2018;59(14 Special Issue):DES192-DES199.
42. Pflugfelder SC, de Paiva CS. The Pathophysiology of Dry Eye Disease: What We Know and Future Directions for Research. *Ophthalmology*. 2017;124(11):S4-S13.
43. Estúa-Acosta GA, Zamora-Ortiz R, Buentello-Volante B, García-Mejía M, Garfias Y. Neutrophil Extracellular Traps: Current Perspectives in the Eye. *Cells*. 2019 Aug 27;8(9):979..
44. Perez VL, Stern ME, Pflugfelder SC. Inflammatory basis for dry eye disease flares. *Experimental Eye Research*. 2020;201(October):108294-.
45. Springer TA. Adhesion receptors of the immune system. *Nature*. 1990;346(6283):425-34.
46. Chauhan SK, El Annan J, Ecoiffier T, Goyal S, Zhang Q, Saban DR, et al. Autoimmunity in dry eye is due to resistance of Th17 to Treg suppression. *The Journal of Immunology*. 2009;182(3):1247-52.
47. Coursey TG, Bian F, Zaheer M, Pflugfelder SC, Volpe EA, de Paiva CS. Age-related spontaneous lacrimal keratoconjunctivitis is accompanied by dysfunctional T regulatory cells. *Mucosal Immunology*. 2017;10(3):743-56.
48. Niederkorn JY, Stern ME, Pflugfelder SC, De Paiva CS, Corrales RM, Gao J, et al. Desiccating stress induces T cell-mediated Sjögren's syndrome-like lacrimal keratoconjunctivitis. *The Journal of Immunology*. 2006;176(7):3950-7.

49. Di Zazzo A, Micera A, De Piano M, Cortes M, Bonini S. Tears and ocular surface disorders: Usefulness of biomarkers. *Journal of Cellular Physiology*. 2019;234(7):9982-93.
50. Hagan S, Martin E, Enríquez-de-Salamanca A. Tear fluid biomarkers in ocular and systemic disease: Potential use for predictive, preventive and personalised medicine. *EPMA Journal*. 2016;7(1):1-20.
51. Lanza NL, McClellan AL, Batawi H, Felix ER, Sarantopoulos KD, Levitt RC, et al. Dry Eye Profiles in Patients with a Positive Elevated Surface Matrix Metalloproteinase 9 Point-of-Care Test Versus Negative Patients. *Ocular Surface*. 2016;14(2):216-23.
52. Wei Y, Asbell PA. The core mechanism of dry eye disease is inflammation. *Eye and Contact Lens*. 2014;40(4):248-56.
53. Balne PK, Au VB, Tong L, Ghosh A, Agrawal M, Connolly J, et al. Bead Based Multiplex Assay for Analysis of Tear Cytokine Profiles. *Journal of Visualized Experiments*. 2017(128).
54. Zhao H, Li Q, Ye M, Yu J. Tear Luminex Analysis in Dry Eye Patients. *Medical Science Monitor*. 2018;24:7595-602.
55. Roda M, Corazza I, Reggiani MLB, Pellegrini M, Taroni L, Giannaccare G, et al. Dry eye disease and tear cytokine levels— a meta-analysis. *International Journal of Molecular Sciences*. 2020;21(9):3111.
56. Hagan S, Tomlinson A. Tear fluid biomarker profiling: a review of multiplex bead analysis. *Ocular Surface*. 2013;11(4):219-35.
57. Chen X, Aqrabi LA, Utheim TP, Tashbayev B, Utheim ØA, Reppe S, et al. Elevated cytokine levels in tears and saliva of patients with primary Sjögren's syndrome correlate with clinical ocular and oral manifestations. *Scientific Reports*. 2019;9(1):7319.
58. Nair S, Vanathi M, Mahapatra M, Seth T, Kaur J, Velpandian T, et al. Tear inflammatory mediators and protein in eyes of post allogeneic hematopoietic stem cell transplant patients. *Ocular Surface*. 2018;16(3):352-67.
59. Guyette N, Williams L, Tran MT, Than T, Bradley J, Kehinde L, et al. Comparison of low-abundance biomarker levels in capillary-collected nonstimulated tears and washout tears of aqueous-deficient and normal patients. *Investigative Ophthalmology and Visual Science*. 2013;54(5):3729-37.
60. Na K, Chun Y, Mok J, Joo C. Inflammatory Cytokines Analysis In The Tears In Sjogren And Non-Sjogren Dry Eye Patients. *Journal of Allergy and Clinical Immunology*. 2011;127(2):AB130.
61. Enríquez-de-Salamanca A, Castellanos E, Stern ME, Fernández I, Carreño E, García-Vázquez C, et al. Tear cytokine and chemokine analysis and clinical correlations in evaporative-type dry eye disease. *Molecular Vision*. 2010;16:862-73.
62. Cocho L, Fernández I, Calonge M, Martínez V, González-García MJ, Caballero D, et al. Biomarkers in ocular chronic graft versus host disease: Tear cytokine- and chemokine-based predictive model. *Investigative Ophthalmology and Visual Science*. 2016;57(2):746-58.
63. Massingale ML, Li X, Vallabhajosyula M, Chen D, Wei Y, Asbell PA. Analysis of inflammatory cytokines in the tears of dry eye patients. *Cornea*. 2009;28(9):1023-7.

64. Acera A, Rocha G, Vecino E, Lema I, Durán JA. Inflammatory markers in the tears of patients with ocular surface disease. *Ophthalmic Research*. 2008;40(6):315-21.
65. Lam H, Bleiden L, de Paiva CS, Farley W, Stern ME, Pflugfelder SC. Tear cytokine profiles in dysfunctional tear syndrome. *American Journal of Ophthalmology*. 2009;147(2):198-205. e1.
66. Tishler M, Yaron I, Geyer O, Shirazi I, Naftaliev E, Yaron M. Elevated tear interleukin-6 levels in patients with Sjögren syndrome. *Ophthalmology*. 1998;105(12):2327-9.
67. García-Posadas L, Hodges RR, Li D, Shatos MA, Storr-Paulsen T, Diebold Y, et al. Interaction of IFN- γ with cholinergic agonists to modulate rat and human goblet cell function. *Mucosal Immunology*. 2016;9(1):206-17.
68. Tan X, Sun S, Liu Y, Zhu T, Wang K, Ren T, et al. Analysis of Th17-associated cytokines in tears of patients with dry eye syndrome. *Eye (Lond)*. 2014;28(5):608-13.
69. Lee SY, Han SJ, Nam SM, Yoon SC, Ahn JM, Kim TI, et al. Analysis of tear cytokines and clinical correlations in Sjögren syndrome dry eye patients and non-Sjögren syndrome dry eye patients. *American Journal of Ophthalmology*. 2013;156(2):247-53.e1.
70. Yoon KC, Jeong IY, Park YG, Yang SY. Interleukin-6 and tumor necrosis factor- α levels in tears of patients with dry eye syndrome. *Cornea*. 2007;26(4):431-7.
71. Solomon A, Dursun D, Liu Z, Xie Y, Macri A, Pflugfelder SC. Pro- and anti-inflammatory forms of interleukin-1 in the tear fluid and conjunctiva of patients with dry-eye disease. *Investigative Ophthalmology and Visual Science*. 2001;42(10):2283-92.
72. Boehm N, Riechardt AI, Wiegand M, Pfeiffer N, Grus FH. Proinflammatory cytokine profiling of tears from dry eye patients by means of antibody microarrays. *Investigative Ophthalmology and Visual Science*. 2011;52(10):7725-30.
73. Chan MF, Sack R, Quigley DA, Sathe S, Vijmasi T, Li S, et al. Membrane array analysis of tear proteins in ocular cicatricial pemphigoid. *Optometry and Vision Science*. 2011;88(8):1005-9.
74. Huang JF, Zhang Y, Rittenhouse KD, Pickering EH, McDowell MT. Evaluations of tear protein markers in dry eye disease: repeatability of measurement and correlation with disease. *Investigative Ophthalmology and Visual Science*. 2012;53(8):4556-64.
75. Jackson DC, Zeng W, Wong CY, Mifsud EJ, Williamson NA, Ang CS, et al. Tear Interferon-Gamma as a Biomarker for Evaporative Dry Eye Disease. *Investigative Ophthalmology and Visual Science*. 2016;57(11):4824-30.
76. Luo G, Xin Y, Qin D, Yan A, Zhou Z, Liu Z. Correlation of interleukin-33 with Th cytokines and clinical severity of dry eye disease. *Indian Journal of Ophthalmology*. 2018;66(1):39-43.
77. Pflugfelder SC, Jones D, Ji Z, Afonso A, Monroy D. Altered cytokine balance in the tear fluid and conjunctiva of patients with Sjögren's syndrome keratoconjunctivitis sicca. *Current Eye Research*. 1999;19(3):201-11.
78. Wei Y, Gadaria-Rathod N, Epstein S, Asbell P. Tear cytokine profile as a noninvasive biomarker of inflammation for ocular surface diseases: standard operating procedures. *Investigative Ophthalmology and Visual Science*. 2013;54(13):8327-36.

79. Willems B, Tong L, Minh TDT, Pham ND, Nguyen XH, Zumbansen M. Novel Cytokine Multiplex Assay for Tear Fluid Analysis in Sjogren's Syndrome. *Ocul Immunol Inflamm.* 2021 Nov 17;29(7-8):1639-1644.
80. Acera A, Vecino E, Duran JA. Tear MMP-9 levels as a marker of ocular surface inflammation in conjunctivochalasis. *Investigative Ophthalmology and Visual Science.* 2013;54(13):8285-91.
81. Collier IE, Wilhelm SM, Eisen AZ, Marmer BL, Grant GA, Seltzer JL, et al. H-ras oncogene-transformed human bronchial epithelial cells (TBE-1) secrete a single metalloprotease capable of degrading basement membrane collagen. *Journal of Biological Chemistry.* 1988;263(14):6579-87.
82. Leonardi A, Brun P, Abatangelo G, Plebani M, Secchi AG. Tear levels and activity of matrix metalloproteinase (MMP)-1 and MMP-9 in vernal keratoconjunctivitis. *Investigative Ophthalmology and Visual Science.* 2003;44(7):3052-8.
83. Lanza NL, Valenzuela F, Perez VL, Galor A. The Matrix Metalloproteinase 9 Point-of-Care Test in Dry Eye. *Ocular Surface.* 2016;14(2):189-95.
84. Sambursky R, O'Brien TP. MMP-9 and the perioperative management of LASIK surgery. *Current Opinion in Ophthalmology.* 2011;22(4):294-303.
85. Chotikavanich S, de Paiva CS, Li DQ, Chen JJ, Bian F, Farley W, et al. Production and Activity of Matrix Metalloproteinase-9 on the Ocular Surface Increase in Dysfunctional Tear Syndrome. *Bone.* 2009;50(7):3203-9.
86. Lema I, Durán JA. Inflammatory molecules in the tears of patients with keratoconus. *Ophthalmology.* 2005;112(4):654-9.
87. Afonso AA, Sobrin L, Monroy DC, Selzer M, Lokeshwar B, Pflugfelder SC. Tear fluid gelatinase B activity correlates with IL-1 α concentration and fluorescein clearance in ocular rosacea. *Investigative Ophthalmology and Visual Science.* 1999;40(11):2506-12.
88. Di Girolamo N, Wakefield D, Coroneo MT. Differential expression of matrix metalloproteinases and their tissue inhibitors at the advancing pterygium head. *Investigative Ophthalmology and Visual Science.* 2000;41(13):4142-9.
89. Garrana RMR, Zieske JD, Assouline M, Gipson IK. Matrix metalloproteinases in epithelia from human recurrent corneal erosion. *Investigative Ophthalmology and Visual Science.* 1999;40(6):1266-70.
90. Smith VA, Hoh HB, Easty DL. Role of ocular matrix metalloproteinases in peripheral ulcerative keratitis. *British Journal of Ophthalmology.* 1999;83:1376-83.
91. Smith VA, Rishmawi H, Hussein H, Easty DL. Tear film MMP accumulation and corneal disease. *Br J Ophthalmol.* 2001;85:147-53.
92. Luo L, Li DQ, Doshi A, Farley W, Corrales RM, Pflugfelder SC. Experimental dry eye stimulates production of inflammatory cytokines and MMP-9 and activates MAPK signaling pathways on the ocular surface. *Investigative Ophthalmology and Visual Science.* 2004;45(12):4293-301.
93. Kaufman HE. The practical detection of MMP-9 diagnoses ocular surface disease and may help prevent its complications. *Cornea.* 2013;32(2):211-6.

94. Markoulli M, Papas E, Cole N, Holden BA. The diurnal variation of matrix metalloproteinase-9 and its associated factors in human tears. *Investigative Ophthalmology and Visual Science*. 2012;53(3):1479-84.
95. Kelley N, Jeltema D, Duan Y, He Y. The NLRP3 inflammasome: An overview of mechanisms of activation and regulation. *International Journal of Molecular Sciences*. 2019;20(13).
96. Shao BZ, Xu ZQ, Han BZ, Su DF, Liu C. NLRP3 inflammasome and its inhibitors: A review. *Frontiers in Pharmacology*. 2015;6(NOV):1-9.
97. Niu L, Zhang S, Wu J, Chen L, Wang Y. Upregulation of NLRP3 inflammasome in the tears and ocular surface of dry eye patients. *PLoS ONE*. 2015;10(5):1-14.
98. Im H, Ammit AJ. The NLRP3 inflammasome: Role in airway inflammation. *Clinical and Experimental Allergy*. 2014;44(2):160-72.
99. Kahlenberg JM, Kaplan MJ. The inflammasome and lupus: Another innate immune mechanism contributing to disease pathogenesis? *Current Opinion in Rheumatology*. 2014;26(5):475-81.
100. Jankovic D, Ganesan J, Bscheider M, Stickel N, Weber FC, Guarda G, et al. The Nlrp3 inflammasome regulates acute graft-versus-host disease. *Journal of Experimental Medicine*. 2013;210(10):1899-910.
101. Rock KL, Kataoka H, Lai JJ. Uric acid as a danger signal in gout and its comorbidities. *Nature Reviews Rheumatology*. 2013;9(1):13-23.
102. Benetti E, Chiazza F, Patel NSA, Collino M. The NLRP3 Inflammasome as a Novel Player of the Intercellular Crosstalk in Metabolic Disorders. *Mediators of Inflammation*. 2013;2013(678627):9-.
103. Zhang X, Xu A, Lv J, Zhang Q, Ran Y, Wei C, et al. Development of small molecule inhibitors targeting NLRP3 inflammasome pathway for inflammatory diseases. *European Journal of Medicinal Chemistry*. 2020;185:111822.
104. Seok JK, Kang HC, Cho YY, Lee HS, Lee JY. Therapeutic regulation of the NLRP3 inflammasome in chronic inflammatory diseases. *Archives of Pharmacal Research*. 2021;44(1):16-35.
105. Marchetti C. The NLRP3 Inflammasome as a Pharmacological Target. *Journal of Cardiovascular Pharmacology*. 2019;74(4):285-96.
106. Zheng Q, Ren Y, Reinach PS, Xiao B, Lu H, Zhu Y, et al. Reactive oxygen species activated NLRP3 inflammasomes initiate inflammation in hyperosmolarity stressed human corneal epithelial cells and environment-induced dry eye patients. *Experimental Eye Research*. 2015;134:133-40.
107. Yerramothu P, Vijay AK, Willcox MDP. Inflammasomes, the eye and anti-inflammasome therapy. *Eye*. 2018;32(3):491-505.
108. Markoulli M, Papas E, Petznick A, Holden B. Validation of the flush method as an alternative to basal or reflex tear collection. *Current Eye Research*. 2011;36(3):198-207.
109. Thakur A, Willcox MDP. Detection of Cytokines in Tears. *Interleukin Protocols*. 2003;60(3):345-53.

110. Fullard RJ, Tucker DL. Changes in human tear protein levels with progressively increasing stimulus. *Investigative Ophthalmology and Visual Science*. 1991;32(8):2290-301.
111. Benitez-Del-Castillo JM, Soria J, Acera A, Muñoz AM, Rodríguez S, Suárez T. Quantification of a panel for dry-eye protein biomarkers in tears: A comparative pilot study using standard ELISA and customized microarrays. *Molecular Vision*. 2021;27:243-61.
112. Yoon KC, Jeong IY, Park YG, Yang SY. Interleukin-6 and tumor necrosis factor- α levels in tears of patients with dry eye syndrome. *Cornea*. 2007;26(4):431-7.
113. Markoulli M, Gokhale M, You J. Substance p in flush tears and schirmer strips of healthy participants. *Optometry and Vision Science*. 2017;94(4):527-33.
114. Choy CKM, Cho P, Chung W-Y, Benzie IFF. Water-Soluble Antioxidants in Human Tears: Effect of the Collection Method. *Investigative Ophthalmology and Visual Science*. 2001;42(13):3130-4.
115. van Haeringen NJ, Glasius E. The origin of some enzymes in tear fluid, determined by comparative investigation with two collection methods. *Experimental Eye Research*. 1976;22(3):267-72.
116. Van Setten GB, Stephens R, Tervo T, Salonen EM, Tarkkanen A, Vaheri A. Effects of the Schirmer test on the fibrinolytic system in the tear fluid. *Experimental Eye Research*. 1990;50(2):135-41.
117. Copeland S, Siddiqui J, Remick D. Direct comparison of traditional ELISAs and membrane protein arrays for detection and quantification of human cytokines. *Journal of Immunological Methods*. 2004;284(1-2):99-106.
118. Elshal MF, McCoy JP. Multiplex bead array assays: Performance evaluation and comparison of sensitivity to ELISA. *Methods*. 2006;38(4):317-23.
119. Dionne K, Redfern RL, Nichols JJ, Nichols KK. Analysis of tear inflammatory mediators: A comparison between the microarray and Luminex methods. *Molecular Vision*. 2016;22:177-88.
120. Ganesalingam K, Ismail S, Craig JP, Sherwin T. Use of a purpose-built impression cytology device for gene expression quantification at the ocular surface using quantitative PCR and droplet digital PCR. *Cornea*. 2019;38(1):127-33.
121. Nolan T, Hands RE, Bustin SA. Quantification of mRNA using real-time RT-PCR. *Nature Protocols*. 2006;1(3):1559-82.
122. Hindson BJ, Ness KD, Masquelier DA, Belgrader P, Heredia NJ, Makarewicz AJ, et al. High-throughput droplet digital PCR system for absolute quantitation of DNA copy number. *Analytical Chemistry*. 2011;83(22):8604-10.
123. Hindson CM, Chevillet JR, Briggs HA, Gallichotte EN, Ruf IK, Hindson BJ, et al. Absolute quantification by droplet digital PCR versus analog real-time PCR. *Nature Methods*. 2013;10(10):1003-5.
124. Taylor SC, Laperriere G, Germain H. Droplet Digital PCR versus qPCR for gene expression analysis with low abundant targets: from variable nonsense to publication quality data. *Scientific Reports*. 2017;7(1):2409.
125. Murphy PJ, Lau JSC, Sim MML, Woods RL. How red is a white eye? Clinical grading of normal conjunctival hyperaemia. *Eye*. 2007;21(5):633-8.

126. Downie LE, Keller PR, Vingrys AJ. Assessing ocular bulbar redness: A comparison of methods. *Ophthalmic and Physiological Optics*. 2016;36(2):132-9.
127. Schulze MM, Ng A, Yang M, Panjwani F, Srinivasan S, Jones LW, et al. Bulbar Redness and Dry Eye Disease: Comparison of a Validated Subjective Grading Scale and an Objective Automated Method. *Optometry and vision science : official publication of the American Academy of Optometry*. 2021;98(2):113-20.
128. Bullimore MA, Bailey IL. Considerations in the Subjective Assessment of Cataract. *Optometry and Vision Science*. 1993;70(11):880-5.
129. Schulze MM, Jones DA, Simpson TL. The development of validated bulbar redness grading scales. *Optometry and Vision Science*. 2007;84(10):976-83.
130. Chong T, Simpson T, Fonn D. The repeatability of discrete and continuous anterior segment grading scales. *Optometry and Vision Science*. 2000;77(5):244-51.
131. Efron N, Morgan PB, Katsara SS. Validation of grading scales for contact lens complications. *Ophthalmic and Physiological Optics*. 2001;21(1):17-29.
132. Schulze MM, Hutchings N, Simpson TL. The perceived bulbar redness of clinical grading scales. *Optometry and Vision Science*. 2009;86(11):E1250-E8.
133. Efron N. Contact lens complications. 3rd ed. Boston: Edinburgh: Elsevier Saunders; 2012.
134. Peterson RC, Wolffsohn JS. Sensitivity and reliability of objective image analysis compared to subjective grading of bulbar hyperaemia. *British Journal of Ophthalmology*. 2007;91(11):1464-6.
135. Wolffsohn JS. Incremental nature of anterior eye grading scales determined by objective image analysis. *British Journal of Ophthalmology*. 2004;88(11):1434-8.
136. Peterson RC, Wolffsohn JS. Objective grading of the anterior eye. *Optometry and Vision Science*. 2009;86(3):273-8.
137. Bailey IL, Bullimore MA, Raasch TW, Taylor HR. Clinical grading and the effects of scaling. *Investigative Ophthalmology and Visual Science*. 1991;32(2):422-32.
138. Efron N. Grading scales for contact lens complications. *Ophthalmic and Physiological Optics*. 1998;18(2):182-6.
139. Huntjens B, Basi M, Nagra M. Evaluating a new objective grading software for conjunctival hyperaemia. *Contact Lens and Anterior Eye*. 2020;43(2):137-43.
140. Amparo F, Wang H, Emami-Naeini P, Karimian P, Dana R. The ocular redness index: A novel automated method for measuring ocular injection. *Investigative Ophthalmology and Visual Science*. 2013;54(7):4821-6.
141. InflammDry(R) [package insert]. San Diego, USA: Quidel Corporation; 2013.
142. Sambursky R, Davitt WF, Friedberg M, Tauber S. Prospective, multicenter, clinical evaluation of point-of-care matrix metalloproteinase-9 test for confirming dry eye disease. *Cornea*. 2014;33(8):812-8.
143. Sambursky R, Davitt WF, Latkany R, Tauber S, Starr C, Friedberg M, et al. Sensitivity and specificity of a point-of-care matrix metalloproteinase 9 immunoassay for diagnosing inflammation related to dry eye. *Archives of Ophthalmology*. 2013;131(1):24-8.

144. Messmer EM, von Lindenfels V, Garbe A, Kampik A. Matrix Metalloproteinase 9 Testing in Dry Eye Disease Using a Commercially Available Point-of-Care Immunoassay. *Ophthalmology*. 2016;123(11):2300-8.
145. Lee H, Han YE, Park SY, Lee JH, Chung HS, Moon SY, et al. Changes in the expression of matrix metalloproteinase-9 after intense pulsed light therapy combined with meibomian gland expression in moderate and severe meibomian gland dysfunction. *Contact Lens and Anterior Eye*. 2021;44(3).
146. Tomlinson A, Khanal S, Ramaesh K, Diaper C, McFadyen A. Tear film osmolarity: determination of a referent for dry eye diagnosis. *Investigative Ophthalmology and Visual Science*. 2006;47(10):4309-15.
147. Caffery BE, Josephson JE. Corneal staining after sequential instillations of fluorescein over 30 days. *Optometry and Vision Science*. 1991;68(6):467-9.
148. Bron AJ, Evans VE, Smith JA. Grading of corneal and conjunctival staining in the context of other dry eye tests. *Cornea*. 2003;22(7):640-50.
149. Peterson RC, Wolffsohn JS, Fowler CW. Optimization of anterior eye fluorescein viewing. *American Journal of Ophthalmology*. 2006;142(4):572-5. e2.
150. Yang S, Lee HJ, Kim DY, Shin S, Barabino S, Chung SH. The Use of Conjunctival Staining to Measure Ocular Surface Inflammation in Patients with Dry Eye. *Cornea*. 2019;38(6):698-705.
151. Korb DR, Herman JP, Blackie CA, Scaffidi RC, Greiner JV, Exford JM, et al. Prevalence of lid wiper epitheliopathy in subjects with dry eye signs and symptoms. *Cornea*. 2010;29(4):377-83.
152. Wang MTM, Dean SJ, Xue AL, Craig JP. Comparative performance of lid wiper epitheliopathy and corneal staining in detecting dry eye disease. *Clinical and Experimental Ophthalmology*. 2019;47(4):546-8.
153. Aragona P, Bucolo C, Spinella R, Giuffrida S, Ferreri G. Systemic omega-6 essential fatty acid treatment and PGE1 tear content in Sjögren's syndrome patients. *Investigative Ophthalmology and Visual Science*. 2005;46(12):4474-9.
154. Asbell PA, Maguire MG, Peskin E, Bunya VY, Kuklinski EJ. Dry Eye Assessment and Management (DREAM©) Study: Study design and baseline characteristics. *Contemporary Clinical Trials*. 2018;71(May 2018):70-9.
155. Belch JJF, Hill A. Evening primrose oil and borage oil in rheumatologic conditions. *American Journal of Clinical Nutrition*. 2000;71(1 SUPPL.):352-6.
156. Deinema LA, Vingrys AJ, Wong CY, Jackson DC, Chinnery HR, Downie LE. A Randomized, Double-Masked, Placebo-Controlled Clinical Trial of Two Forms of Omega-3 Supplements for Treating Dry Eye Disease. *Ophthalmology*. 2017;124(1):43-52.
157. Giannaccare G, Pellegrini M, Sebastiani S, Bernabei F, Roda M, Taroni L, et al. Efficacy of Omega-3 Fatty Acid Supplementation for Treatment of Dry Eye Disease: A Meta-Analysis of Randomized Clinical Trials. *Cornea*. 2019;38(5):565-73.
158. Hussain M, Shtein RM, Pistilli M, Maguire MG, Oydanich M, Asbell PA. The Dry Eye Assessment and Management (DREAM) extension study – A randomized clinical trial of withdrawal of supplementation with omega-3 fatty acid in patients with dry eye disease. *Ocular Surface*. 2020;18(1):47-55.

159. Kangari H, Eftekhari MH, Sardari S, Hashemi H, Salamzadeh J, Ghassemi-Broumand M, et al. Short-term consumption of oral omega-3 and dry eye syndrome. *Ophthalmology*. 2013;120(11):2191-6.
160. Kokke KH, Morris JA, Lawrenson JG. Oral omega-6 essential fatty acid treatment in contact lens associated dry eye. *Contact Lens and Anterior Eye*. 2008;31(3):141-6.
161. Maguire G, Pistilli M, Ying G-S, Lin MC, Shtein RM, Quintana M, et al. n-3 Fatty Acid Supplementation for the Treatment of Dry Eye Disease. *New England Journal of Medicine*. 2018;378(18):1681-90.
162. Miljanović B, Trivedi KA, Dana MR, Gilbard JP, Buring JE, Schaumberg DA. Relation between dietary n-3 and n-6 fatty acids and clinically diagnosed dry eye syndrome in women. *American Journal of Clinical Nutrition*. 2005;82(4):887-93.
163. Sheppard JD, Singh R, McClellan AJ, Weikert MP, et al. Long-term Supplementation With n-6 and n-3 PUFAs Improves Moderate-to-Severe Keratoconjunctivitis Sicca: A Randomized Double-Blind Clinical Trial. *Cornea* 2013;32(10):1297-304.
164. Wojtowicz JC, Butovich I, Uchiyama E, Aronowicz J, Agee S, McCulley JP, et al. Placebo-controlled Clinical Trial of an Omega-3. *Cornea*. 2011;30(3):308-14.
165. Barnes PJ. How corticosteroids control inflammation: Quintiles Prize Lecture 2005. *British Journal of Pharmacology*. 2006;148(3):245-54.
166. Periman LM, Perez VL, Saban DR, Lin MC, Neri P. The Immunological Basis of Dry Eye Disease and Current Topical Treatment Options. *Journal of Ocular Pharmacology and Therapeutics*. 2020;36(3):137-46.
167. Min J-K, Kim Y-M, Kim SW, Kwon M-C, Kong Y-Y, Hwang IK, et al. TNF-Related Activation-Induced Cytokine Enhances Leukocyte Adhesiveness: Induction of ICAM-1 and VCAM-1 via TNF Receptor-Associated Factor and Protein Kinase C-Dependent NF- κ B Activation in Endothelial Cells. *The Journal of Immunology*. 2005;175(1):531-40.
168. Cutolo CA, Barabino S, Bonzano C, Traverso CE. The Use of Topical Corticosteroids for Treatment of Dry Eye Syndrome. *Ocular Immunology and Inflammation*. 2019;27(2):266-75.
169. Marsh P, Pflugfelder SC. Therapy for Keratoconjunctivitis Sicca in Sjögren Syndrome. 1998:811-6.
170. Kunert KS, Tisdale S. A, Gipson IK. Goblet cell numbers and epithelial proliferation in the conjunctiva of patients with dry eye syndrome treated with cyclosporine. *Archives of Ophthalmology*. 2002;120(3):330-7.
171. Stern ME, Schaumburg CS, Dana R, Calonge M, Niederkorn JY, Pflugfelder SC. Autoimmunity at the ocular surface: Pathogenesis and regulation. *Mucosal Immunology*. 2010;3(5):425-42.
172. Allergan. Restasis® (cyclosporine ophthalmic emulsion) 0.05%. 1983:0-5.
173. Kunert KS, Tisdale AS, Stern ME, Smith JA, Gipson IK. Analysis of topical cyclosporine treatment of patients with dry eye syndrome: Effect on conjunctival lymphocytes. *Archives of Ophthalmology*. 2000;118(11):1489-96.

174. Periman LM, Mah FS, Karpecki PM. A review of the mechanism of action of cyclosporine a: The role of cyclosporine a in dry eye disease and recent formulation developments. *Clinical Ophthalmology*. 2020;14:4187-200.
175. Sall K, Stevenson OD, Mundorf TK, Reis BL. Two multicenter randomized studies of the efficacy and safety of cyclosporine ophthalmic emulsion in moderate to severe dry eye disease. *Ophthalmology*. 2000;107(4):631-9.
176. Mah F, Milner M, Yiu S, Donnenfeld E, Conway TM, Hollander DA. PERSIST: Physician's Evaluation of Restasis® Satisfaction in Second Trial of topical cyclosporine ophthalmic emulsion 0.05% for dry eye: a retrospective review. *Clinical Ophthalmology*. 2012;6:1971-6.
177. Luchs J. Phase 3 Clinical Results of Cyclosporine 0.09% in a New Nanomicellar Ophthalmic Solution to Treatment Keratoconjunctivitis Sicca. 2018:45230.
178. Perez VL, Pflugfelder SC, Zhang S, Shojaei A, Haque R. Lifitegrast, a Novel Integrin Antagonist for Treatment of Dry Eye Disease. *Ocular Surface*. 2016;14(2):207-15.
179. Eyewire N. Novartis Withdraws Marketing Application of Dry Eye Drug Xiidra in Europe. 2020. <https://eyewire.news/articles/novartis-pulls-eu-filing-seeking-approval-of-xiidra-for-dry-eye-disease/>
180. Murphy CJ, Bentley E, Miller PE, McIntyre K, Leatherberry G, Dubielzig R, et al. The pharmacologic assessment of a novel lymphocyte function-associated antigen-1 antagonist (SAR 1118) for the treatment of keratoconjunctivitis sicca in dogs. *Investigative Ophthalmology and Visual Science*. 2011;52(6):3174-80.
181. Holland EJ, Jackson MA, Donnenfeld E, Piccolo R, Cohen A, Barabino S, et al. Efficacy of Lifitegrast Ophthalmic Solution, 5.0%, in Patients With Moderate to Severe Dry Eye Disease A Post Hoc Analysis of 2 Randomized Clinical Trials. *JAMA Ophthalmology*. 2021:1-9.
182. Yoo SE, Lee DC, Chang MH. The effect of low-dose doxycycline therapy in chronic meibomian gland dysfunction. *Korean journal of ophthalmology : KJO*. 2005;19(4):258-63.
183. Del Rosso JQ, Webster GF, Jackson M, Rendon M, Rich P, Torok H, et al. Two randomized phase III clinical trials evaluating anti-inflammatory dose doxycycline (40-mg doxycycline, USP capsules) administered once daily for treatment of rosacea. *Journal of the American Academy of Dermatology*. 2007;56(5):791-802.
184. Solomon A, Rosenblatt M, Li DQ, Liu Z, Monroy D, Ji Z, et al. Doxycycline inhibition of interleukin-1 in the corneal epithelium. *Investigative Ophthalmology and Visual Science*. 2000;41(9):2544-57.
185. Jean-F T, White O, Kerlavage AR, Clayton RA, Sutton GG, Fleischmann RD, et al. Effect of Doxycycline on the Generation of Reactive Oxygen Species: A Possible Mechanism of Action of Acne Therapy with Doxycycline. 1997. p. 539-47.
186. Pruzanski W, Greenwald RA, Street LP, Lauberte F, Stefanski E, Vadas P. Inhibition of enzymatic activity of phospholipases A2 by minocycline and doxycycline. *Biochemical Pharmacology*. 1992;44(6):1165-70.
187. Aronowicz JD, Shine WE, Oral D, Vargas JM, McCulley JP. Short term oral minocycline treatment of meibomianitis. *British Journal of Ophthalmology*. 2006;90(7):856-60.

188. Kashkouli MB, Fazel AJ, Kiavash V, Nojomi M, Ghiasian L. Oral azithromycin versus doxycycline in meibomian gland dysfunction: A randomised double-masked open-label clinical trial. *British Journal of Ophthalmology*. 2015;99(2):199-204.
189. Liu Y, Kam WR, Ding J, Sullivan DA. Effect of azithromycin on lipid accumulation in immortalized human meibomian gland epithelial cells. *JAMA Ophthalmology*. 2014;132(2):226-8.
190. Mori A, Suko M, Kaminuma O, Inoue S, Ohmura T, Hoshino A, et al. IL-2-Induced IL-5 Synthesis, but Not Proliferation, of Human CD4+ T Cells Is Suppressed by FK506. *The Journal of Immunology*. 1997;158(8):3659-65.
191. Vedovato M, Do Carmo TM, Rios L, Corrêa V, Oliveira F, Capelanes N, et al. Use of topical tacrolimus in ophthalmology: Nonsystematic review. *The Pan-American Journal of Ophthalmology*. 2020;2(1):36.
192. Moawad P, Shamma R, Hassanein D, Ragab G, El Zawahry O. Evaluation of the effect of topical tacrolimus 0.03% versus cyclosporine 0.05% in the treatment of dry eye secondary to Sjogren syndrome. *European Journal of Ophthalmology*. 2022;Jan;32(1):673-679.
193. Innes JK, Calder PC. Omega-6 fatty acids and inflammation. *Prostaglandins, Leukotrienes and Essential Fatty Acids*. 2018;132:41-8.
194. Kelley DS, Taylor PC, Nelson GJ, Mackey BE. Arachidonic acid supplementation enhances synthesis of eicosanoids without suppressing immune functions in young healthy men. *Lipids*. 1998;33(2):125-30.
195. James MJ, Gibson RA, Cleland LG. Dietary polyunsaturated fatty acids and inflammatory mediator production. *American Journal of Clinical Nutrition*. 2000;71(1 SUPPL.):1-6.
196. Nettleton JA. ω -3 fatty acids: comparison of plant and seafood sources in human nutrition. *Journal of the American Dietetic Association*. 1991;91(3):331-7.
197. Wojtowicz JC, Butovich I, Uchiyama E, Aronowicz J, Agee S, McCulley JP. Pilot, prospective, randomized, double-masked, placebo-controlled clinical trial of an omega-3 supplement for dry eye. *Cornea*. 2011;30(3):308-14.
198. Barabino S, Rolando M, Camicione P, Ravera G, Zanardi S, Giuffrida S, et al. Systemic linoleic and γ -linolenic acid therapy in dry eye syndrome with an inflammatory component. *Cornea*. 2003;22(2):97-101.
199. Miljanovic B, Trivedi KA, Dana MR, Gilbard JP, Buring JE, Schaumberg DA. Relation between dietary n-3 and n-6 fatty acids and clinically diagnosed dry eye syndrome in women. *The American Journal of Clinical Nutrition*. 2005;82(4):887-93.
200. Downie LE, Ng SM, Lindsley KB, Akpek EK. Omega-3 and omega-6 polyunsaturated fatty acids for dry eye disease. *Cochrane Database of Systematic Reviews*. 2019(12): CD011016.
201. Schiffman RM, Christianson MD, Jacobsen G, Hirsch JD, Reis BL. Reliability and Validity of the Ocular Surface Disease Index. *Archives of Ophthalmology*. 2000;118(5):615-21.

202. Chalmers RL, Begley CG, Caffery B. Validation of the 5-Item Dry Eye Questionnaire (DEQ-5): Discrimination across self-assessed severity and aqueous tear deficient dry eye diagnoses. *Contact Lens and Anterior Eye*. 2010;33(2):55-60.
203. Wolffsohn JS, Travé Huarte S, Jones L, Craig JP, Wang MTM. Clinical practice patterns in the management of dry eye disease: A TFOS international survey. *Ocular Surface*. 2021;21(March):78-86.
204. Tomlinson A, Bron AJ, Korb DR, Amano S, Paugh JR, Pearce EI, et al. The International Workshop on Meibomian Gland Dysfunction: Report of the Diagnosis Subcommittee. *Investigative Ophthalmology and Visual Science*. 2011;52(4):2006-49.
205. Bron A, Benjamin L, Snibson G. Meibomian gland disease. Classification and grading of lid changes. *Eye*. 1991;5(4):395-411.
206. Korb DR, Herman JP, Greiner JV, Scaffidi RC, Finnemore VM, Exford JM, et al. Lid wiper epitheliopathy and dry eye symptoms. *Eye and Contact Lens*. 2005;31(1):2-8.
207. Pult H, Riede-Pult B. Comparison of subjective grading and objective assessment in meibography. *Contact Lens and Anterior Eye*. 2013;36(1):22-7.
208. Ganesalingam K. Tolerability of Mānuka Honey with CycloPower™ in Microemulsion on the ocular surface: MHS thesis. University of Auckland; 2016.
209. Chomczynski P. Solubilization in formamide protects RNA from degradation. *Nucleic Acids Research*. 1992;20(14):3791-2.
210. Schroeder A, Mueller O, Stocker S, Salowsky R, Leiber M, Gassmann M, et al. The RIN: an RNA integrity number for assigning integrity values to RNA measurements. *BMC Molecular Biology*. 2006;7(1):3.
211. Fleige S, Pfaffl MW. RNA integrity and the effect on the real-time qRT-PCR performance. *Molecular Aspects of Medicine*. 2006;27(2):126-39.
212. Nolan T, Hands RE, Ogunkolade W, Bustin SA. SPUD: A quantitative PCR assay for the detection of inhibitors in nucleic acid preparations. *Analytical Biochemistry*. 2006;351(2):308-10.
213. dMIQE, Huggett JF. The Digital MIQE Guidelines Update: Minimum Information for Publication of Quantitative Digital PCR Experiments for 2020. *Clinical Chemistry*. 2020;66(8):1012-29.
214. Andersen CL, Jensen JL, Ørntoft TF. Normalization of real-time quantitative reverse transcription-PCR data: a model-based variance estimation approach to identify genes suited for normalization, applied to bladder and colon cancer data sets. *Cancer research*. 2004;64(15):5245-50.
215. DeLong ER, DeLong DM, Clarke-Pearson DL. Comparing the areas under two or more correlated receiver operating characteristic curves: a nonparametric approach. *Biometrics*. 1988:837-45.
216. Sorbara L, Simpson T, Duench S, Schulze M, Fonn D. Comparison of an objective method of measuring bulbar redness to the use of traditional grading scales. *Contact Lens and Anterior Eye*. 2007;30(1):53-9.
217. Walker MK, Tomiyama ES, Skidmore KV, Assaad JR, Ticak A, Richdale K. A comparison of subjective and objective conjunctival hyperaemia grading with AOS® Anterior software. *Clinical and Experimental Optometry*. 2021:1-6.

218. Yoneda T, Sumi T, Hoshikawa Y, Kobayashi M, Fukushima A. Hyperemia Analysis Software for Assessment of Conjunctival Hyperemia Severity. *Current Eye Research*. 2019;44(4):376-80.
219. Phillips AJ, Speedwell L. Contact lenses. 4th ed. Oxford England Boston: Butterworth-Heinemann 1997.; 1997.
220. Mukaka MM. Statistics corner: A guide to appropriate use of correlation coefficient in medical research. *Malawi Med J*. 2012;24(3):69-71.
221. Wolffsohn JS, Naroo SA, Christie C, Morris J, Conway R, Maldonado-Codina C. Anterior eye health recording. *Contact Lens and Anterior Eye*. 2015;38(4):266-71.
222. Britten-Jones AC, Rajan R, Craig JP, Downie LE. Quantifying corneal immune cells from human in vivo confocal microscopy images: Can manual quantification be improved with observer training? *Experimental Eye Research*. 2022;216:108950.
223. Aragona P, Aguenouz MH, Rania L, Postorino E, Sommario MS, Roszkowska AM, et al. Matrix metalloproteinase 9 and transglutaminase 2 expression at the ocular surface in patients with different forms of dry eye disease. *Ophthalmology*. 2015;122(1):62-71.
224. Pflugfelder SC, Farley W, Luo L, Chen LZ, de Paiva CS, Olmos LC, et al. Matrix Metalloproteinase-9 Knockout Confers Resistance to Corneal Epithelial Barrier Disruption in Experimental Dry Eye. *The American Journal of Pathology*. 2005;166(1):61-71.
225. Fodor E, Barabino S, Montaldo E, Mingari MC, Rolando M. Quantitative evaluation of ocular surface inflammation in patients with different grade of conjunctivochalasis. *Current Eye Research*. 2010;35(8):665-9.
226. Schargus M, Ivanova S, Kakkassery V, Dick HB, Joachim S. Correlation of tear film osmolarity and 2 different MMP-9 tests with common dry eye tests in a cohort of non-dry eye patients. *Cornea*. 2015;34(7):739-44.
227. Li D-Q, Chen Z, Song XJ, Luo L, Pflugfelder SC. Stimulation of Matrix Metalloproteinases by Hyperosmolarity via a JNK Pathway in Human Corneal Epithelial Cells. *Investigative Ophthalmology and Visual Science*. 2004;45(12):4302.
228. VanDerMeid KR, Su SP, Ward KW, Zhang JZ. Correlation of tear inflammatory cytokines and matrix metalloproteinases with four dry eye diagnostic tests. *Invest Ophthalmol Vis Sci*. 2012;53(3):1512-8.
229. Kang M-J, Kim HS, Kim MS, Kim EC. The Correlation between Matrix Metalloproteinase-9 Point-of-Care Immunoassay, Tear Film Osmolarity, and Ocular Surface Parameters. *Journal of Ophthalmology*. 2022;2022:1-7.
230. Liu H, Begley C, Chen M, Bradley A, Bonanno J, McNamara NA, et al. A Link between Tear Instability and Hyperosmolarity in Dry Eye. *Investigative Ophthalmology and Visual Science*. 2009;50(3671).
231. Baudouin C, Messmer EM, Aragona P, Geerling G, Akova YA, Benítez-del-Castillo J, et al. Revisiting the vicious circle of dry eye disease: a focus on the pathophysiology of meibomian gland dysfunction. *British Journal of Ophthalmology*. 2016;100(3):300-6.
232. Yokoi N, Takehisa Y, Kinoshita S. Correlation of Tear Lipid Layer Interference Patterns With the Diagnosis and Severity of Dry Eye. *American Journal of Ophthalmology*. 1996;122(6):818-24.

233. Blackie CA, Solomon JD, Scaffidi RC, Greiner JV, Lemp MA, Korb DR. The relationship between dry eye symptoms and lipid layer thickness. *Cornea*. 2009;28(7):789-94.
234. Trevethan R. Sensitivity, Specificity, and Predictive Values: Foundations, Pliabilities, and Pitfalls in Research and Practice. *Front Public Health*. 2017;5:307.
235. Corrales RM, Stern ME, De Paiva CS, Welch J, Li D-Q, Pflugfelder SC. Desiccating Stress Stimulates Expression of Matrix Metalloproteinases by the Corneal Epithelium. *Investigative Ophthalmology and Visual Science*. 2006;47(8):3293.
236. Li D-Q, Pflugfelder SC. Matrix Metalloproteinases in Corneal Inflammation. *The Ocular Surface*. 2005;3(4, Supplement):S-198-S-202.
237. Ryu J-S, Kang J-H, Jung S-Y, Shin M-H, Kim J-M, Park H, et al. Production of interleukin-8 by human neutrophils stimulated with *Trichomonas vaginalis*. *Infection and Immunity*. 2004;72(3):1326-32.
238. Wu C-H, Li K-J, Yu C-L, Tsai C-Y, Hsieh S-C. Sjögren's syndrome antigen B acts as an endogenous danger molecule to induce interleukin-8 gene expression in polymorphonuclear neutrophils. *PLoS One*. 2015;10(4):e0125501.
239. Okusawa S, Gelfand JA, Ikejima T, Connolly RJ, Dinarello CA. Interleukin 1 induces a shock-like state in rabbits. Synergism with tumor necrosis factor and the effect of cyclooxygenase inhibition. *Journal of Clinical Investigation*. 1988;81(4):1162-72.
240. McDevitt MJ, Wang H-Y, Knobelman C, Newman MG, di Giovine FS, Timms J, et al. Interleukin-1 Genetic Association With Periodontitis in Clinical Practice. *Journal of Periodontology*. 2000;71(2):156-63.
241. Narayanan S, Miller WL, McDermott AM. Conjunctival Cytokine Expression in Symptomatic Moderate Dry Eye Subjects. *Investigative Ophthalmology and Visual Science*. 2006;47(6):2445.
242. Pflugfelder SC, Stern ME. *Dry Eye: Inflammation of the Lacrimal Functional Unit*. Springer-Verlag; 2005. p. 11-24.
243. Pflugfelder SC. Antiinflammatory therapy for dry eye. *American Journal of Ophthalmology*. 2004;137(2):337-42.
244. McGhee CNJ, Dean S, Danesh-Meyer H. Locally Administered Ocular Corticosteroids. *Drug Safety*. 2002;25(1):33-55.
245. Prabhasawat P, Tseng SCG. Frequent association of delayed tear clearance in ocular irritation. *British Journal of Ophthalmology*. 1998;82(6):666-75.
246. Perry HD, Solomon R, Donnenfeld ED, Perry AR, Wittpenn JR, Greenman HE, et al. Evaluation of Topical Cyclosporine for the Treatment of Dry Eye Disease. *Archives of Ophthalmology*. 2008;126(8):1046-50.
247. Semba CP, Torkildsen GL, Lonsdale JD, McLaurin EB, Geffin JA, Mundorf TK, et al. A Phase 2 Randomized, Double-Masked, Placebo-Controlled Study of a Novel Integrin Antagonist (SAR 1118) for the Treatment of Dry Eye. *American Journal of Ophthalmology*. 2012;153(6):1050-60.e1.
248. Craig JP, Muntz A, Wang MTM, Luensmann D, Tan J, Trave Huarte S, et al. Developing evidence-based guidance for the treatment of dry eye disease with artificial

tear supplements: A six-month multicentre, double-masked randomised controlled trial. *Ocul Surf.* 2021;20:62-9.

249. Geerling G, Tauber J, Baudouin C, Goto E, Matsumoto Y, O'Brien T, et al. The international workshop on meibomian gland dysfunction: Report of the subcommittee on management and treatment of meibomian gland dysfunction. *Investigative Ophthalmology and Visual Science.* 2011;52(4):2050-64.

250. Yin Y, Liu N, Gong L, Song N. Changes in the Meibomian Gland After Exposure to Intense Pulsed Light in Meibomian Gland Dysfunction (MGD) Patients. *Current Eye Research.* 2018;43(3):308-13.

251. Albietz JM, Schmid KL. Intense pulsed light treatment and meibomian gland expression for moderate to advanced meibomian gland dysfunction. *Clinical and Experimental Optometry.* 2018;101(1):23-33.

252. Dinnes J, Deeks JJ, Berhane S, Taylor M, Adriano A, Davenport C, et al. Rapid, point-of-care antigen and molecular-based tests for diagnosis of SARS-CoV-2 infection. *Cochrane Database of Systematic Reviews.* 2021(3).